ATLAS Internal Note
10 November 1998

ATLFAST 2.0

a fast simulation package for ATLAS

Elzbieta Richter-Was[1]

CERN, IT Division, 1211 Geneva 23, Switzerland;

Institute of Computer Science, Jagiellonian University,

Institute of Nuclear Physics, 30-059 Cracow, ul. Nawojki 26a, Poland

Daniel Froidevaux

CERN, PPE Division, 1211 Geneva 23, Switzerland

Luc Poggioli

LPNHE, Paris 6 and 7, Paris, France

Abstract

This paper documents the update of the ATLFAST program [6-1] for fast detector simulation and physics analysis. The algorithm is implemented as an independent package written in FORTRAN77 but exists also in an OO/C++ implementation. It can be used for fast event-simulation including the most crucial detector aspects: jet reconstruction in the calorimeters, momentum/energy smearing for leptons and photons, magnetic field effects and missing transverse energy. It provides, starting from the list of particles in the event, a list of reconstructed jets, isolated leptons and photons and the expected missing transverse energy. Optionally, the package provides also a list of reconstructed charged tracks. The package is completed by ATLFAST-B, a set of useful routines which simulate efficiencies/rejections for tagging of b-jets, c-jets and τ-jets. In most cases, the detector-dependent parameters are tuned to what is expected for the performance of the ATLAS detector from full simulation.

1. Work supported in part by Polish Government grants 2P03B00212, 2P03B14715; Polish-French Collaboration within IN2P3 and Polish-American Maria Sklodowska-Curie Joint Fund II in cooperation with PAA and DOE under project PAA/DOE-97-316.

VERSION SUMMARY *Title of the version of the program:* ATLFAST, version: 2.0

***Authors of the program**:* E. Richter-Was, D. Froidevaux, L. Poggioli.

***Computer**:* HP; *Installation:* CERN

***Operating system** (on which the version has been tested):* UNIX

***Programming language used**:* FORTRAN 77

***No. of bits in a word**:* 32

***External libraries**:* CERNLIB.

***Keywords**:* particle-level simulation.

***Nature of the problem**:* Particle-level simulation allows for fast analysis of the fully generated event in the *pp* collision including parametrisation of the most crucial detector aspects.

WWW home page: http://atlfastinfo.cern.ch/Atlas/GROUPS/PHYSICS/Physics.html

(entry: **Tools for physics simulation**)

***email**:* elzbieta.richter-was@cern.ch

Acknowledgements

The authors of the program are indebted to many colleagues who have contributed their own code:

- F. Gianotti for the parametrisation of the photon energy resolution
- M Virchaux, L. Chevalier and C. Guyot for the parametrisation of the muon p_T resolution
- E. Arik, S. Cetin and A. Mailov for preparing the routine for muon trigger efficiencies
- A. Reichold, R. Dankers and E.J. Buis for preparing and maintaining the routines for helix parameter resolutions of the Inner Detector
- G. F. Tartarelli for preparing the routine for helix parameter reconstruction
- G. F. Tartarelli and N. Labanca for preparing the parametrisation of low energy charged pions track resolutions
- S. Haywood for preparing the parametrisation of the electron track resolutions
- D. Cavalli and S. Resconi for the parametrisations of the τ-tagging performance
- E. Ros for the parametrisation of the b-tagging performance
- I. C. Park for providing the JetFinder library for reconstruction of QCD jets
- S. Klyukhin and J. Soderqvist for setting up the interfaces to the HERWIG and ISAJET event generators
- J. Soderqvist and M. Pearce for providing the calculation of circularity, thrust and oblateness
- M. Stavrianakou and I. Efthymiopoulos for setting up the ntuple format
- D. Rousseau for the implementation of the ATLFAST results into the standardised combined ntuples

E. Richter-Was acknowledges valuable discussions with D. Cavalli, M. Cobal, I. Efthymiopoulos, F. Gianotti, S. Haywood, E. Nagy, A. Nisati, J. Soderqvist, G. F. Tartarelli and thanks everybody who helped to debug the code particularly: A. Amorim, C. Biscarat, G. Eynard, S. Klyukhin, B. Lund-Jensen, S. Negroni, S. Resconi, H. Ruiz, L. Serin, J. Soderqvist, K. Strahl and T. Trefzer. Last but not least she thanks F. Dittus for assistance with FrameMaker.

1 Introduction

Particle-level simulation is a kind of intermediate step between simple parton-level analysis of the event topology and very sophisticated and CPU-consuming full detector simulation. It can be done in a more or less complex way but is *never* meant to replace the full simulation of the detector response. However, this kind of simulation is needed for quick and approximate estimates of signal and background rates for specific channels. In addition, fast simulation is the only practical tool for long-statistics studies of complex background processes at the LHC. In many cases, simpler parton-level simulations have been shown to give too optimistic and therefore misleading results.

The first version of this package [6-1] was used for systematic studies of MSSM Higgs discovery limits [6-2], SUSY particle searches [6-3], for some studies presented in the ATLAS Technical Design Reports [6-5], [6-6] and [6-7] and for monitoring the large ATLAS jet production [6-8]. The difference between parton-level and particle-level (called also sometimes jet-level) analyses was discussed already in some detail in [6-9].

This package attempts to reproduce as well as possible the expected ATLAS detector mass resolution for important physics signals, as obtained from full simulation. It does not attempt at present to reproduce accurately the expected efficiencies for lepton and photon isolation, but does attempt to do so for any jet reconstruction efficiency, especially for b-jets, and for the missing E_T resolution. However, for any specific channel, the ATLAS predictions in terms of resolution and reconstruction efficiency, should always be confirmed with full-simulation results. Such detailed comparisons have been done for the WH , $H\rightarrow b\bar{b}$ and $A\rightarrow \tau\tau$ channels [6-10], in terms of the selection cut acceptances, the jet reconstruction efficiencies and mass resolutions, and they have shown good agreement between fast and full simulations. Such comparison also has been performed for the jet-veto and forward jet-tagging efficiencies for the SM heavy Higgs channels

Not all detector effects can be readily parametrised in fast simulation and only the basic information of the detector geometry is used by the package. This basic information is for example: the η-coverage for precision physics and for the calorimetry, the size of the barrel/endcap transition region for the electromagnetic calorimeter, and the granularity of the calorimeters. No effects related for the detailed shapes of particle showers in the calorimeters, for the charged track multiplicity in jets, etc. are taken into account. In particular, energy isolation of leptons is only simulated in a crude way, and the results should always be replaced by those from more detailed simulations.

The main goal of the ATLFAST package is to simulate and analyse fully generated events and select isolated leptons and photons, reconstruct jets, label b-jets, c-jets and τ-jets and estimate the missing transverse energy. A more or less accurate parametrisation of photon, electron and muon momentum resolution is included, as well as a parametrisation of the hadronic calorimeter energy resolution and the effect of the ATLAS magnetic field on jet reconstruction. The reconstruction of helix track parameters in the Inner Detector is also provided with separate parametrisations of the resolutions for muon, electron and pion tracks.

From the point of view of convenience, it turns out that some properties of the detector are better simulated/analysed at the level of the ntuples created by ATLFAST. For this purpose ATLFAST-B was created, with routines randomly simulating b-, c- and τ-tagging and providing jet-energy recalibration. Therefore, the proposed procedure is to simulate events with ATLFAST and to analyse the results using the ATLFAST-B utilities whenever needed.

Below are summarised the main changes which have been implemented since version 1.0 [6-1] :

- ATLFAST-B utility package;
- Labelling of τ-jets (in ATLFAST);
- Parametrisation of b-tagging and τ–tagging performance, for low luminosity operation, consistent with full-simulation results (in ATLFAST-B);
- Parametrisation of the muon trigger efficiency (in ATLFAST and ATLFAST-B);
- Jet energy recalibration giving the correct mass scale for e.g. the reconstructed m_{jj} and $m_{b\bar{b}}$ distributions (in ATLFAST-B);
- Effect of pile-up on the jet energy resolution (in ATLFAST)
- Updated parametrisation of the muon momentum smearing (in ATLFAST);
- Jet reconstruction in cases of different ΔR for the barrel/end-cup and forward regions (jet reconstruction with two different cones in ΔR can also be invoked in ATLFAST);
- JetFinder library with several algorithms for jet cluster reconstruction;
- Track helix parameter reconstruction and parametrisation of Inner Detector resolution (in ATLFAST)
- Rearrangement of common blocks:

  The particle list is given in the /ATLFEVENT/ common block and not in /LUJETS/

  All jets are in one common block /JETALL/, (commons /BJET/ and /CJET/ have disappeared);

  In common blocks /ISOMUO/ and /NOISOMUX/ there is a new flag for the muon trigger

The outline of this note is as follows. Chapter 2 describes the physics issues of the algorithm used for the event analysis, and also compares the results from the package to those from the full simulation. Chapter 3 discusses in more detail the jet reconstruction, calibration and tagging. Chapter 4 discusses track reconstruction and conclusions are given in Chapter 5. Appendix A instructs the reader on how to use the program and Appendices B, C and D describe the structure of the program, the subroutines, commons blocks, and functions. Finally, Appendix E includes the listing of an output as an example.

2 Particle-level simulation

Fully or partially generated events, i.e. events generated including or not QED/QCD initial and final state radiation, fragmentation, hadronisation and decays of unstable particles can be analysed by the package. The list of generated particles should be rewritten (including their history) from the common blocks provided by the chosen event generator to the `/ATLFEVENT/` common block. From this common block, only the stable, final-state particles are treated by the ATLFAST algorithm, which selects and stores reconstructed isolated leptons and photons, hadronic jets and reconstructed tracks.

2.1 Calorimetric clusters

The transverse energies of all undecayed particles stored in `COMMON /ATLFEVENT/`, except for neutrinos, muons and the SUSY LSP, are summed up in calorimeter cells of a given granularity in $\eta \times \phi$ coordinates (default: 0.1×0.1 for $|\eta| < 3$ and 0.2×0.2 for $|\eta| > 3$) over the full calorimeter coverage (default: $|\eta|<5$). The effect of the solenoidal 2T magnetic field on the ϕ-position of charged particles with p_T above threshold (default: $p_T > 0.5$ GeV) is parametrised in `FUNCTION FLDPHI`. It is assumed that the contribution from charged particles with p_T below this threshold can be safely neglected.

All calorimeter cells with transverse energy greater than a given threshold (default: $E_T > 1.5$ GeV) are taken as possible initiators of clusters. These are scanned in order of decreasing E_T to verify whether the total E_T summed over all cells in a cone $\Delta R = \sqrt{\Delta^2\eta + \Delta^2\phi}$ exceeds the minimum required threshold for a reconstructed cluster (default: $E_T > 10$ GeV). The reconstruction cone is defined separately for the barrel/end-cup ($|\eta|<3$) and forward ($|\eta|>3$) part (default for barrel/end-cup and forward: $\Delta R=0.4$). It is possible to invoke also the algorithm for a second choice of the ΔR value, thus having each event analysed twice (default for barrel/end-cup and forward: $\Delta R=0.7$). Cells with a deposited transverse energy below threshold (default: 0 GeV) are not accounted for. As coordinates (η^{clu}, ϕ^{clu}) of the reconstructed clusters are taken the coordinates of the bary centres of the cones weighted by the cell E_T for all cells inside the cone around the initiator cell.

The $\Delta\eta$ and $\Delta\phi$ between the axis of the reconstructed clusters and the bary centres of all particles inside the reconstruction cone are shown in Figure 2-1 and Figure 2-2. The accuracy of the reconstruction is good (σ=0.022 rad) and the tails are small. The same quantities plotted for the difference between the position of the initial parton and the reconstructed cluster (Figure 2-3 and Figure 2-4) show much larger tails and worse resolutions. As can be seen from Figure 2-3 and Figure 2-4, the effect of the magnetic field is not very large for jets of E_T around $m_H/2$. This effect is to be expected since the direction of the initial parton does not always overlap with the direction of the final particles inside the cluster. The effect of the outcone energy loss is illustrated in Figure 2-5 and Figure 2-6, where $\Delta p_T/p_T$ between the reconstructed cluster and the initial parton is shown respectively for ΔR_{cone}=0.4 and 0.7. This effect can be mostly corrected for on average using the procedure of jet energy recalibration. As expected, for larger jet-cones, the efficiency for jet reconstruction is higher and the energy losses outside the jet-cone are smaller. The small tail at positive $\Delta p_T/p_T$ is caused by the effect of additional energy deposition inside the jet-cone coming from initial state radiation and the underlying event.

Reconstructed clusters are stored in COMMON /CLUSTER/ and the cell energy depositions in COMMON /CELLS/. Cells used for cluster reconstruction are labelled. Its is also possible to invoke an algorithm for the energy sharing of cells belonging to overlapping jets. No energy smearing is applied yet to these clusters, since some of them represent photon clusters or electron clusters. Appropriate energy smearing will be applied only after cluster identification. In addition to the default cone algorithm, several other algorithms for cluster reconstruction are available: Mulguisin algorithm, k_T-algorithm, sliding window algorithm, etc. Detailed descriptions of these algorithms is available in [6-4]

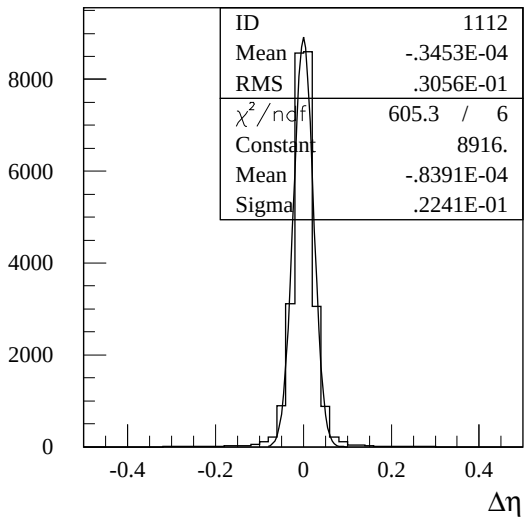

Figure 2-1 $\Delta\eta$ between reconstructed bary centre of particles and reconstructed cluster for the WH , $H\rightarrow u\bar{u}$ process with m_H=100 GeV (magnetic field included).

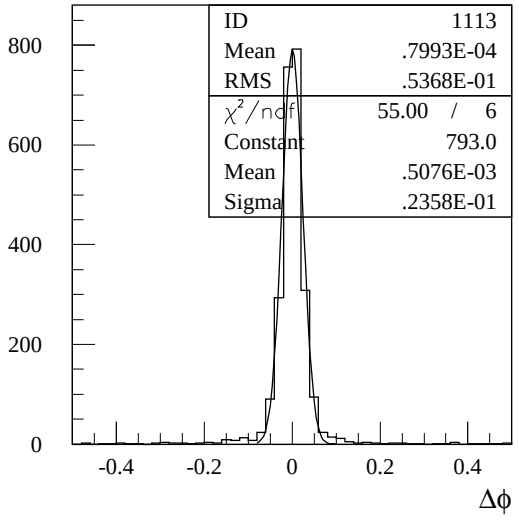

Figure 2-2 Same as Figure 2-1 for $\Delta\phi$.

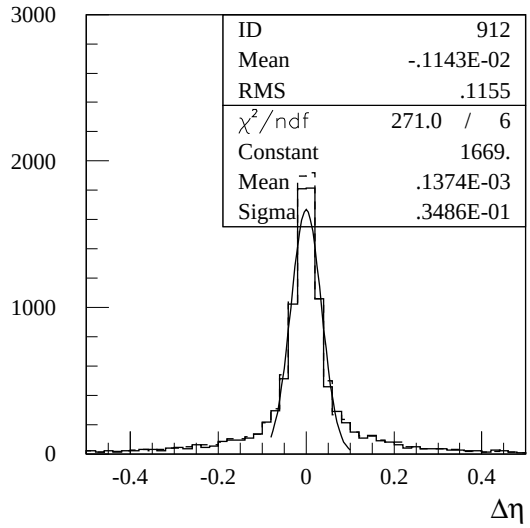

Figure 2-3 $\Delta\eta$ between initial parton and reconstructed cluster for the WH , $H\rightarrow u\bar{u}$ process with m_H = 100 GeV the solid (dashed) histogram is with (without) magnetic field.

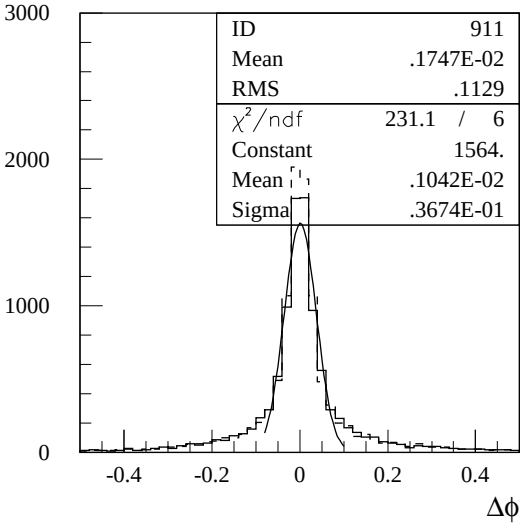

Figure 2-4 Same as Figure 2-3 for $\Delta\phi$.

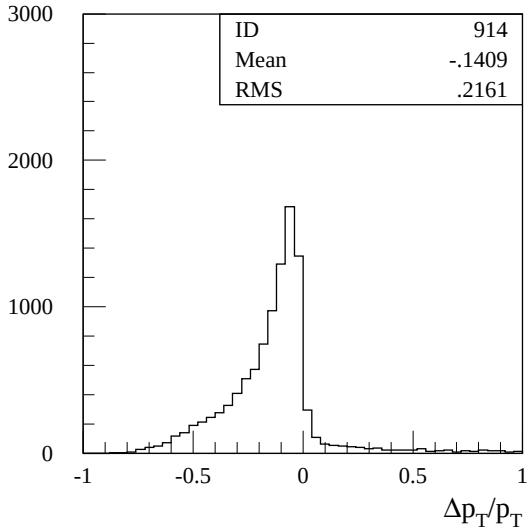

Figure 2-5 Relative difference in p_T, $\Delta p_T/p_T$ between the initial parton and the reconstructed cluster for the WH , $H \rightarrow u\bar{u}$ process with m_H = 100 GeV and for ΔR_{cone}=0.4.

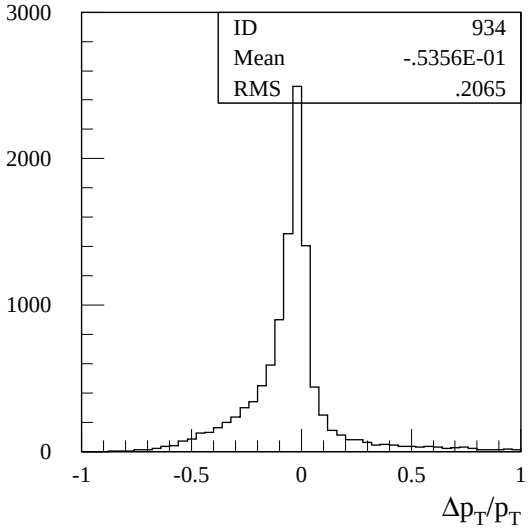

Figure 2-6 Same as Figure 2-5 for ΔR_{cone}=0.7.

2.2 Isolated photons

Isolated photon candidates are searched for in the particle `COMMON /ATLFEVENT/`. The polar angle of the photon is smeared with a Gaussian resolution parametrised in `FUNCTION RESTHE`. Then the photon 4-momentum is smeared according to a Gaussian energy resolution parametrised in `FUNCTION RESPHO`. Low and high luminosity options can be invoked.

For all photons which pass the selection criteria in p_T and $|\eta|$ (default: $p_T > 10$ GeV and $|\eta| < 2.5$), the associated reconstructed calorimeter cluster is identified (default: $\Delta R_{\gamma,\ cluster} < 0.1$). Photon isolation criteria, in terms of the distance from other clusters and of maximum transverse energy deposition in cells in a cone around the photon, are then applied (defaults: separation by $\Delta R > 0.4$ from other clusters and $E_T < 10$ GeV in a cone $\Delta R = 0.2$ around the photon). All photons passing the isolation criteria are stored in `COMMON /ISOPHO/` and the clusters associated with them are removed from `COMMON /CLUSTER/`. These default isolation criteria have a 97.5% efficiency for photons passing the kinematical selection cuts for $H \rightarrow \gamma\gamma$ searches. The same isolation criteria have also been studied in [6-14] for the photon bremsstrahlung background from quarks.

The reconstructed mass of the isolated photon pairs for a generated sample of $H \rightarrow \gamma\gamma$ events, after the standard kinematical cuts, $p_T^{\gamma} > 40$ and 25 GeV, is shown in Figure 2-7 and Figure 2-8 for low and high-luminosity respectively; and the expected mass resolutions are given in Table 2-1 . For comparison, results from full simulation of the Accordion calorimeter [6-5] are also given, showing reasonable agreement between the parametrisation used for the fast simulation and the expected performance from full simulation.

ATLFAST does not take into account efficiencies for identifying photons and/or misidentifying jets. Therefore, if needed, the estimated efficiencies, e.g. as given in [6-15], should be included by the user in the event analysis.

Table 2-1 Mass resolutions obtained for $H \rightarrow \gamma\gamma$ events with m_H = 100 GeV, after kinematical selection, for low and high luminosity. The results obtained from ATLFAST and from the full simulation of the ATLAS detector [6-5] are shown.

$H \rightarrow \gamma\gamma$ m_H=100 GeV	Low luminosity σ_m (GeV)	High luminosity σ_m (GeV)
ATLFAST	1.1	1.2
ATLAS	1.0	1.3

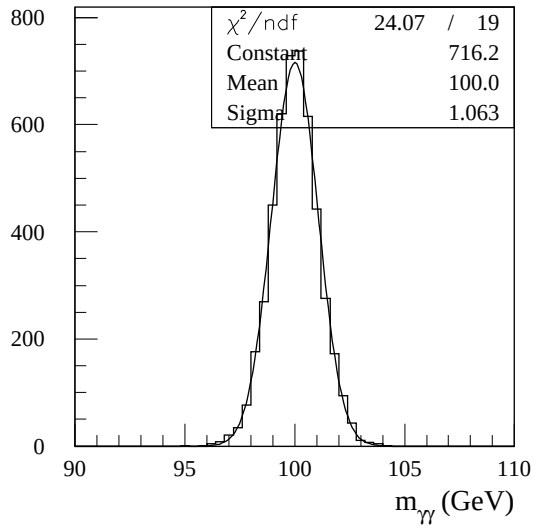

Figure 2-7 Reconstructed mass, $m_{\gamma\gamma}$, for $H \rightarrow \gamma\gamma$ events with m_H = 100 GeV and for low luminosity.

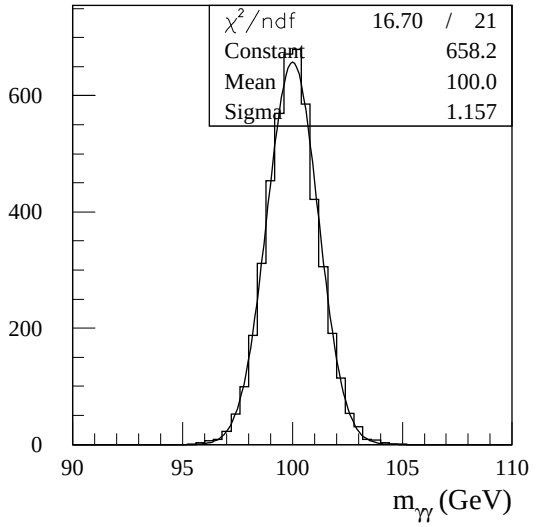

Figure 2-8 Same as Figure 2-7 for high luminosity.

2.3 Isolated electrons

Isolated electron candidates are searched for in the particle `COMMON /ATLFEVENT/`. Each electron momentum is smeared, according to a Gaussian energy resolution parametrised in `FUNCTION RESELE`. Low luminosity (`KEYLUM=1`) and high luminosity (`KEYLUM=2`) options can be invoked.

For all electrons which pass the selection criteria in p_T and $|\eta|$ (default: $p_T > 5$ GeV and $|\eta| < 2.5$), the associated reconstructed cluster is identified (default: $\Delta R_{e,\,cluster} < 0.1$). Electron isolation criteria, in terms of the distance from other clusters and of maximum transverse energy deposition in cells in a cone around the electron are then applied (defaults: separation by $\Delta R > 0.4$ from other clusters and $E_T < 10$ GeV in a cone $\Delta R = 0.2$ around the electron). These chosen default isolation criteria have a 95.3% efficiency for electrons passing the kinematical selection cuts for $H \rightarrow e^+e^-e^+e^-$ searches. All electrons passing the isolation criteria are stored in `COMMON /ISOELE/` and the clusters associated with them are removed from `COMMON /CLUSTER/`.

The mass resolution for electron pairs from a generated sample of $Z \rightarrow e^+e^-$ events is shown in Table 2-2 with and without subtraction of the natural Z width. The mass resolution for four electrons, from a generated sample of $H \rightarrow e^+e^-e^+e^-$ events with m_H = 130 GeV is also shown in Table 2-2, for low and high luminosities, and is in good agreement with results from the full

Table 2-2 Mass resolutions obtained for generated $Z \rightarrow e^+e^-$ and $H \rightarrow e^+e^-e^+e^-$ events (m_H=130 GeV), for low and high luminosity. For the $Z \rightarrow e^+e^-$ events, the results are given with and without subtraction of the natural Z width. The results obtained from ATLFAST and from the full simulation of the ATLAS detector [6-5],[6-6] are shown. The effect of QED inner bremsstrahlung is not included here.

	Low luminosity σ_m (GeV)	**High luminosity σ_m(GeV)**
	$Z \rightarrow e^+e^-$	**$Z \rightarrow e^+e^-$**
ATLFAST (Z width included)	1.94	2.00
ATLFAST (Z width subtracted)	1.16	1.31
	$H \rightarrow e^+e^-e^+e^-$	**$H \rightarrow e^+e^-e^+e^-$**
ATLFAST	1.36	1.63
ATLAS	1.48 ± 0.07	1.68 ± 0.07

simulation of the Accordion calorimeter [6-5], obtained without QED inner bremsstrahlung [6-18]. Figure 2-9 andFigure 2-10 show the mass distributions obtained for low and high luminosity respectively and for $H \rightarrow e^+e^-e^+e^-$ decays with m_H = 130 GeV.

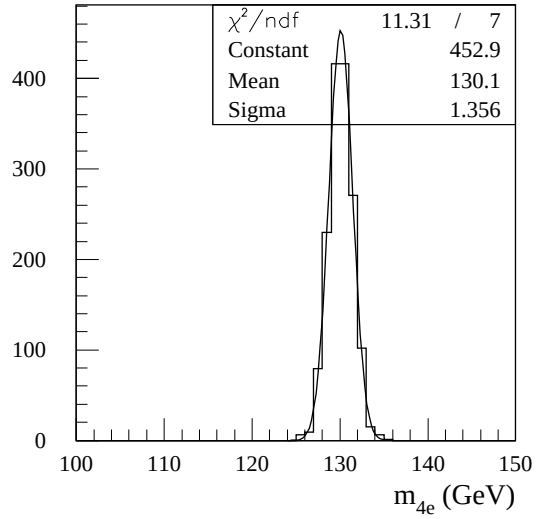

Figure 2-9 Reconstructed mass, m_{4e}, for $H \rightarrow e^+e^-e^+e^-$ events with m_H = 130 GeV and for low luminosity.

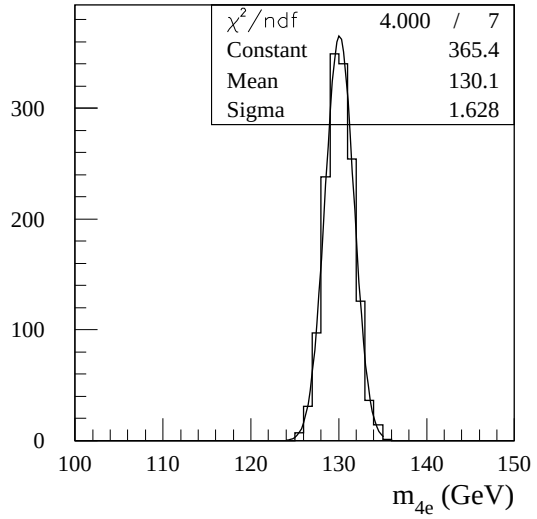

Figure 2-10 same as Figure 2-9 for high luminosity.

ATLFAST does not take into account efficiencies for identifying electrons and/or misidentifying jets. Therefore if needed, the estimated efficiencies should be included by the user in the event analysis.

2.4 Isolated muons

Isolated muon candidates are searched for in the particle `COMMON /ATLFEVENT/`. Each muon momentum is smeared according to a resolution which depends on the muon p_T, $|\eta|$ and ϕ.

Three options depending on which sub-detectors are assumed to be used for the muon measurement can be invoked: muon system stand-alone (approximate [6-20] or exact [6-20] parametrisation, default: exact), Inner Detector stand-alone (parametrisation from [6-21]) and combined (default: combined). The parametrisation of the momentum resolution is coded in `SUBROUTINE RESMUO`.

For all muons which pass the selection criteria in p_T and $|\eta|$ (default: $p_T > 6$ GeV and $|\eta| < 2.5$), isolation criteria, in terms of the distance from calorimeter clusters and of maximum transverse energy deposition in cells in a cone around the muon, are applied (default: separation by $\Delta R > 0.4$ from clusters and $E_T < 10$ GeV in a cone $\Delta R=0.2$ around the muon). These chosen default isolation criteria have a 97.8% efficiency for muons passing the kinematical selection cuts for $H \rightarrow \mu^+\mu^-\mu^+\mu^-$ searches. All muons passing the isolation criteria are stored in `COMMON /ISOMUO/` and the others are stored in `COMMON /NOISOMUO/`. Muons not passing the p_T or $|\eta|$ selection criteria are lost.

The mass resolution for muon pairs, obtained from a generated sample of $Z \rightarrow \mu^+\mu^-$ events is shown in Table 2-3, with and without subtraction of the natural Z width, for the three options for the muon momentum measurement. The mass resolution for four muons obtained, after kinematical selection from a generated sample of $H \rightarrow \mu^+\mu^-\mu^+\mu^-$ events is shown in Figure 2-11 -Figure 2-14 and in Table 2-3. The results obtained for the muon system and Inner Detector stand-alone resolutions are in good agreement between ATLFAST and the full simulation. The combined resolution still appears to be significantly better as obtained from ATLFAST, but it is expected that the ongoing work in the combined muon performance group will lead to better results from full simulation and reconstruction. The full simulation results quoted for $H \rightarrow \mu^+\mu^-\mu^+\mu^-$ decays were obtained for the ATLAS Technical Design Report muon system configuration [6-12].

ATLFAST does not take into account efficiencies for identifying muons. Therefore if needed, the estimated efficiencies should be included by the user in the event analysis. However, ATLFAST simulates muon triggering efficiencies, if required to, and isolated and non-isolated muons are flagged with an appropriate trigger flag.

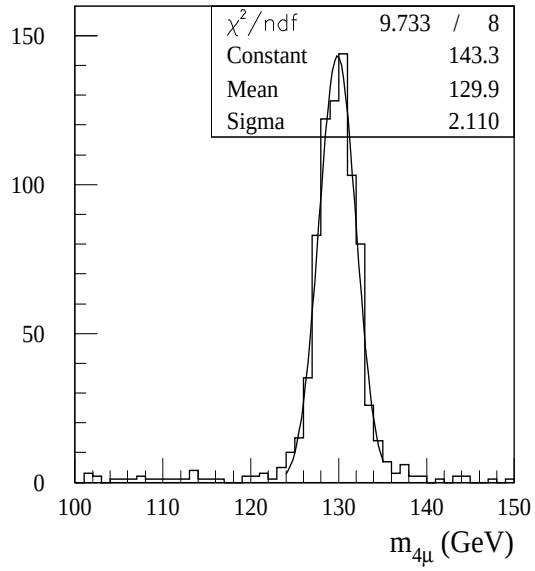

Figure 2-11 Reconstructed mass, $m_{4\mu}$, for $H \rightarrow \mu^+\mu^-\mu^+\mu^-$ events with m_H = 130 GeV and for the exact parametrization of the muon-system stand-alone momentum resolution from [6-19].

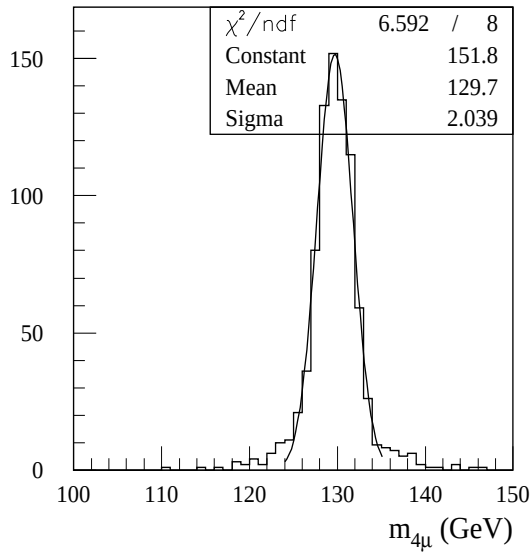

Figure 2-12 Same as Figure 2-11 for the approximate parametrization of the stand-alone muon-system momentum resolution resolution from [6-20].

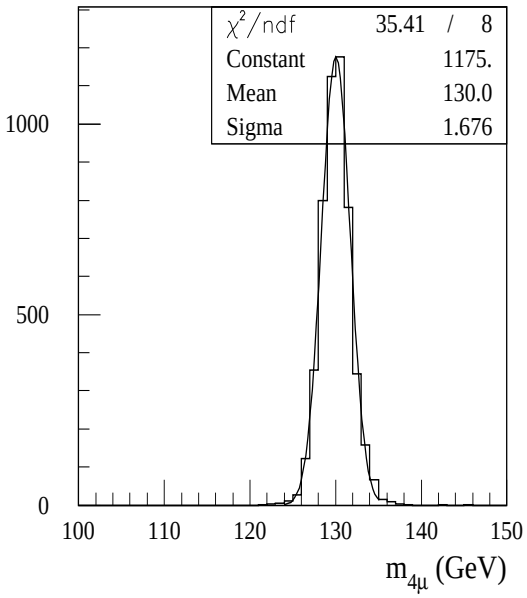

Figure 2-13 stand-alone momentum resolution.

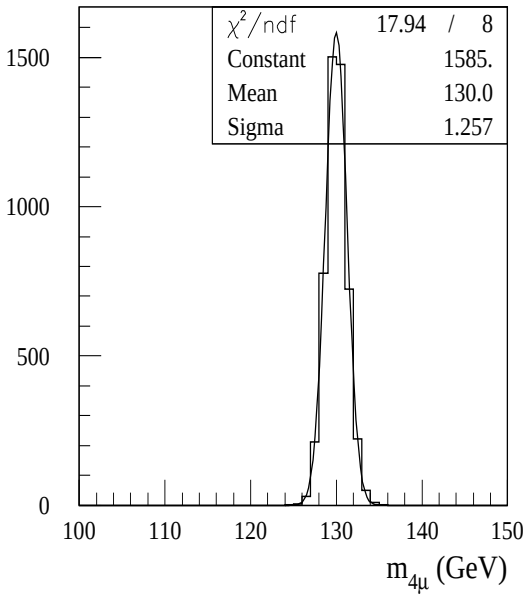

Figure 2-14 Same as Figure 2-3 for the combined muon momentum resolution.

Table 2-3 Mass resolutions obtained for generated $Z \rightarrow \mu^+\mu^-$ and $H \rightarrow \mu^+\mu^-\mu^+\mu^-$ events (m_H=130 GeV) for three cases of muon-momentum measurements: muon system stand-alone, Inner Detector stand-alone, and both combined. For the $Z \rightarrow \mu^+\mu^-$, events results are given with and without subtraction of the natural Z width. The results from full simulation of from ATLAS Muon System [6-12] and of the ATLAS Inner Detector ("Morges" layout) are also given. The combined result from full simulation is from an old study performed for the ATLAS Technical Proposal.

	Muon system σ_m (GeV)	**Inner Detector σ_m (GeV)**	**Combined σ_m (GeV)**
	$Z \rightarrow \mu^+\mu^-$	**$Z \rightarrow \mu^+\mu^-$**	**$Z \rightarrow \mu^+\mu^-$**
ATLFAST (Z width included)	2.16	2.29	1.85
ATLFAST (Z width subtracted)	1.56	1.63	1.14
	$H \rightarrow \mu^+\mu^-\mu^+\mu^-$	**$H \rightarrow \mu^+\mu^-\mu^+\mu^-$**	**$H \rightarrow \mu^+\mu^-\mu^+\mu^-$**
ATLFAST	2.04	1.68	1.26
ATLAS	1.95 ± 0.08	1.75 ± 0.07	1.6 ± 0.01

2.5 Jet reconstruction

2.5.1 Jet reconstruction at low luminosity.

Clustered cells are used for the jet reconstruction. The energies of clusters, which have not been selected as associated with isolated electrons or photons, are smeared according to a Gaussian energy resolution parametrised in `FUNCTION RESHAD`. Two options can be invoked: low luminosity and high luminosity. In the second case, the effect from pile-up is included in the parametrisation of the resolution. The energy of non-isolated muons which fall inside the cluster cone is added to the smeared cluster energy. The resulting jets with E_T greater than a given threshold (default: $E_T > 15$ GeV) are labelled as reconstructed jets, stored in `COMMON /JETALL/` and removed from `COMMON /CLUSTER/`.

Table 2-4 Effi ciency for jet reconstruction at low luminosity for different types of initial partons with $p_T^{parton} > 15$ GeV and $p_T^{jet} > 15$ GeV.

Parton type	**$\Delta R_{cone} = .4$ $\Delta R_{jet,\ parton} < 0.4$**
u-quark	83%
b-quark	76%
gluon	74%

The jet reconstruction efficiency and dijet mass resolution have been studied using events from WH production with $m_H = 100$ GeV and forcing the Higgs boson to decay into specific partons, namely $H \rightarrow u\bar{u}$, $H \rightarrow b\bar{b}$ and $H \rightarrow gg$. Only jets reconstructed within a cone $\Delta R < 0.4$ from a parton from Higgs decay are considered here. The relative difference in transverse energy between the initial parton and the reconstructed jet, as well as the mass distribution of the pairs of recosntructed jets are shown in Figure 2-16 - Figure 2-18 for $H \rightarrow u\bar{u}$, $H \rightarrow b\bar{b}$ and $H \rightarrow gg$ decays. The peaks of reconstructed mass are shifted to values significantly lower than the Higgs-boson mass, and this shift is larger for heavy quark and gluon jets. The width of the reconstructed peak and the non-gaussian tails at low values of the dijet mass are also larger for b-jets and gluon jets.

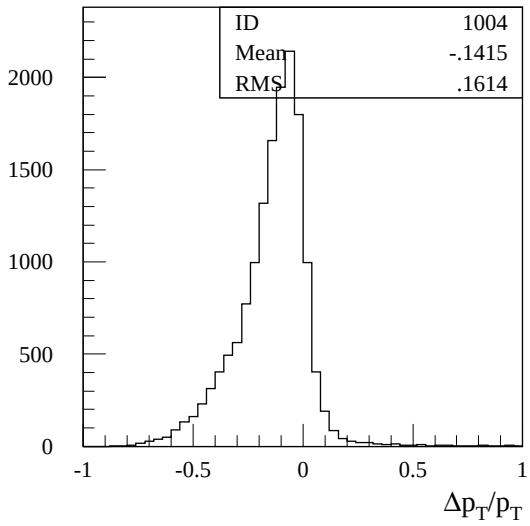

Figure 2-15 Relative difference in p_T, $\Delta p_T/p_T$ for initial parton and the reconstructed jet ($\Delta R_{jet,\ parton} < 0.4$) for WH , $H \rightarrow u\bar{u}$ events and for low luminosity (ΔR_{cone}=0.4).

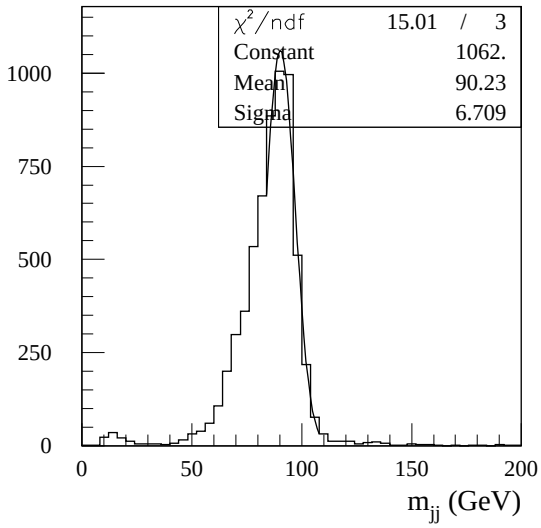

Figure 2-16 Distribution of m_{jj} for reconstructed jets from WH , $H \rightarrow u\bar{u}$ events for low luminosity (ΔR_{cone} = 0.4).

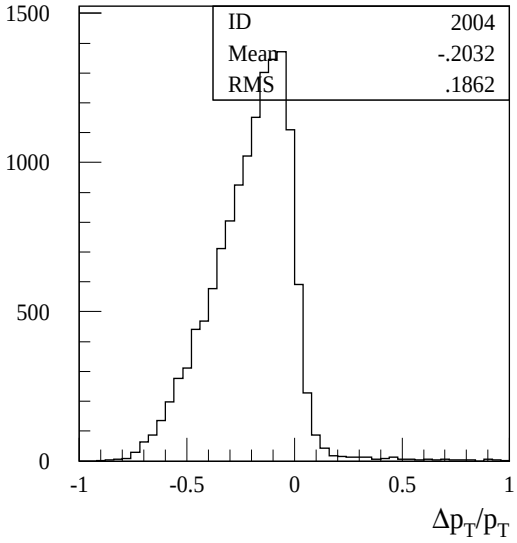

Figure 2-17 Same as Figure 2-15 for WH , $H \rightarrow b\bar{b}$ events.

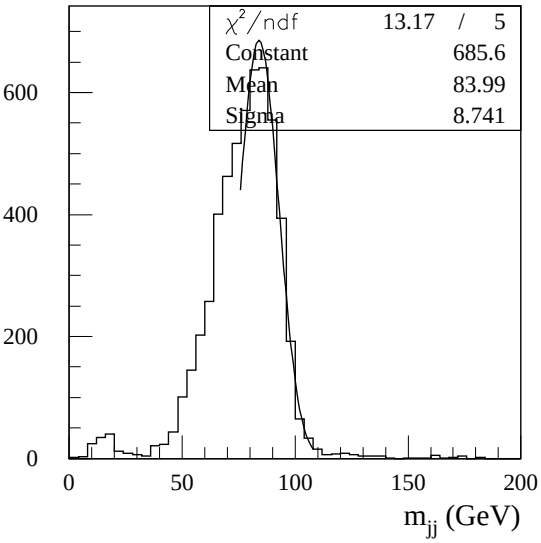

Figure 2-18 Same as Figure 2-16 for WH , $H \rightarrow b\bar{b}$ events.

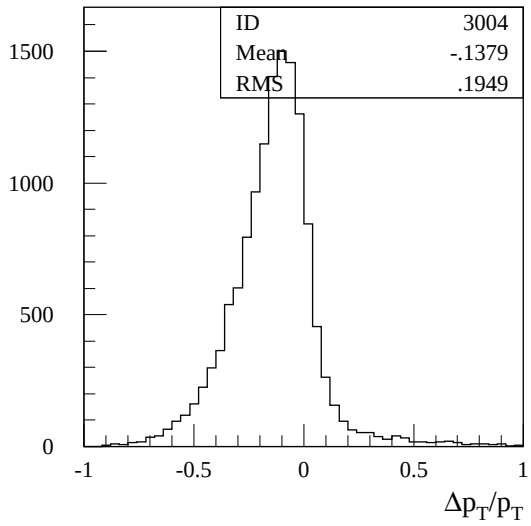

Figure 2-19 The same as Figure 2-15 but for WH , H→ gg process.

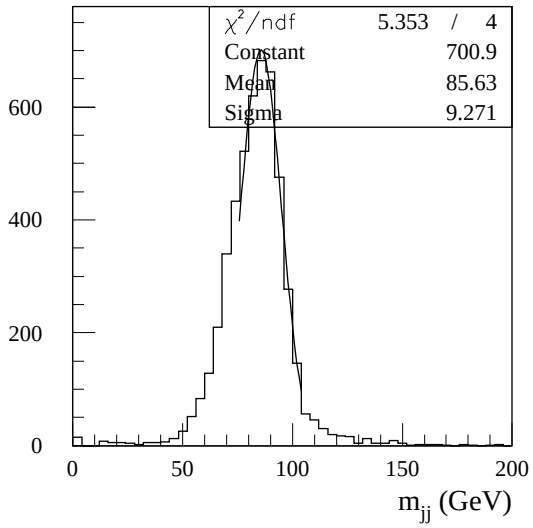

Figure 2-20 The same as Figure 2-16 but for WH , H→ gg process.

2.5.2 Jets labelled as b-jets and c-jets

Of special interest are jets originating from b-quarks (so-called b-jets) which can be identified using b-tagging techniques (vertex or soft-lepton tags). The package labels a jet as a b-jet, if a b-quark of $p_T > 5$ GeV (after FSR) is found in a cone of ΔR=0.2 around the reconstructed jet for jets with $|\eta| < 2.5$. These criteria have been discussed in more detail in [6-9]. These jets are labelled with `KJET(I, 2)=5`. The mass resolution of reconstructed $b\bar{b}$ pairs is of special interest and is shown in Figure 2-21, for events generated through WH production with $H \rightarrow b\bar{b}$ and for m_H = 100 GeV. The results are shown in three cases: a) no magnetic field and no smearing, b) magnetic field and no smearing and c) magnetic field and smearing. The dominant mass shift arises from final state radiation and hadronisation (-12.5 GeV), but a sizeable shift also originates from the magnetic field (-4.9 GeV). As shown by the Gaussian fits in Figures 2-21, the impacts of the fragmentation, solenoidal magnetic field and energy smearing are similar and contribute each ~ 5 GeV to the Gaussian part of the experimental resolution. The fraction of events within 82 ± 20 GeV decreases from 86.5% (Figure 2-21 a), to 84% (Figure 2-21 b) and to 83% (Figure 2-21 c). After jets energy recalibration (see Chapter 3), the position of the mass peak is shifted to nominal m_H mass, and the acceptance in the mass bin $m_H \pm 20$ GeV is of 85%.

Jets originating from c-quarks are labelled as c-jets (`KJET(I,2)=4`) if similar criteria are satisfied.

ATLFAST is not including efficiencies for b-jets tagging. For b-labelled jets efficiencies for tagging and inefficiencies for mistagging c-jets and other jets have been parametrised as p_T dependent functions [6-22] and are available in package ATLFAST-B.

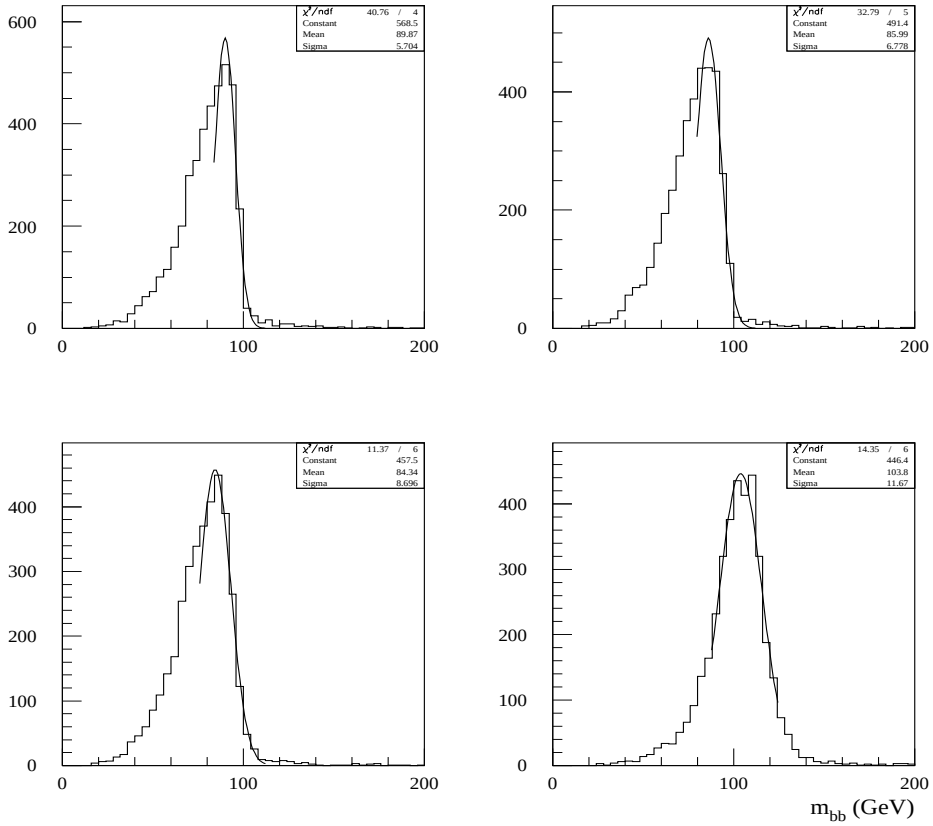

Figure 2-21 Reconstructed dijet mass $m_{b\bar{b}}$ distributions for b-labelled jets for no smearing and no B-fi eld, b) no smearing and with B-fi eld, c) with smearing and with B-fi eld, d) with jet energy recalibration from generated WH events with $H \rightarrow b\bar{b}$ and for m_H=100 GeV and for low luminosity performance and default cone algorithm.

2.5.3 Jets labelled as τ-jets

Of special interest are also jets originating from τ-decay (so called τ-jets), which can be identified in case of hadronic τ–decays. The systematic study of the ATLAS potential for τ-identification have been documented in ATLAS Technical Proposal [6-13] and was studied afterwards with new detector layout [6-23]. In case of ATLFAST simulation candidates to be identified as τ-jets are labelled. Required for hadronic τ-decay products is to be relatively hard (default: $p_T^{\tau\text{-had}} > 10$ GeV), inside tracking range ($|\eta| < 2.5$), dominate reconstructed jet (default: $p_T^{\tau\text{-had}}/p_T^{jet} > 0.9$) and within jet cone (default: $\Delta R_{jet,\,\tau\text{-had}} < 0.3$). The efficiency for τ-labelling is of 92% for τ-hadronic decays from $A \rightarrow \tau\tau$ and for $m_A = 300$ GeV.

ATLFAST is not correcting for efficiencies for τ-jet identification or other jets misidentification. For τ-labelled jets efficiencies for τ-tagging and mistagging have been parametrised [6-23] and are available in package ATLFAST-B.

2.5.4 Jet reconstruction at high luminosity

The effect of pile-up expected for high luminosity performance is included by invoking jets energy smearing with high luminosity option.

Figure 2-22 shows p_T resolutions for jets and for low (left-side) and high (right-side) luminosity performance. The simple parametrization of this effect affects clusters multiplicity for low p_T clusters and bias $p_T^{cluster}$ spectrum. The pile-up strongly degrades the resolution for jets with 40 < p_T < 50 GeV, whereas its impact on much higher-energy jets can be seen to be small. The jets energy resolutions obtained and shown in Figure 2-22 are in good agreement with the results from the full simulation[6-5].

Figure 2-23 shows $p_T^{cluster}$ distributions for simulated QCD di-jet events without (solid line) and with (dashed line) smearing for low (left-side) and high (right-side) luminosity performance. For jets transverse momenta below 40 to 50 GeV, the spectrum is clearly biased at high luminosity, whereas the low luminosity behaviour is more or less unbiased down to very low values of the jets transverse momenta.

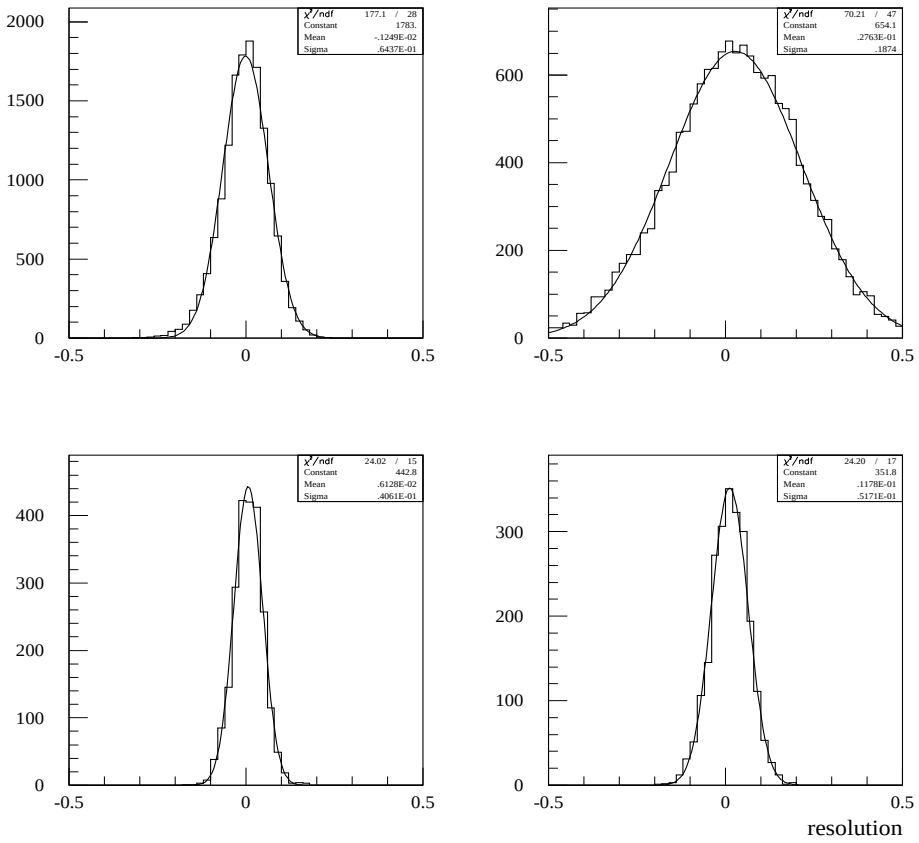

Figure 2-22 The p_T^{jet} resolution for reconstructed jets with 40 <p_T^{jet}< 50 GeV (top) and 200<p_T^{jet}<250 GeV (bottom) for low (left) and high (right) luminosity performance and default cone algorithm.

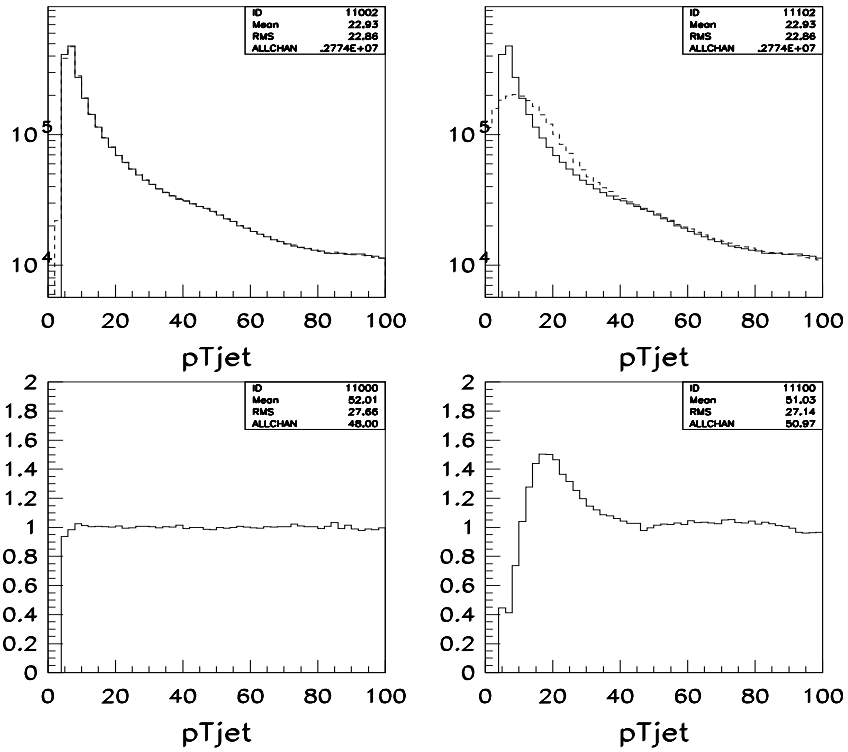

Figure 2-23 The p_T^{jet} distribution for reconstructed jets without (solid) and with (dashed) energy smearing included for low (left-side) and high (right-side) luminosity performance and the default cone algorithm. Respective ratios are shown on bottom plots. Events were fi ltered on 3 clusters with $p_T^{cluster}$ > 10 GeV (before energy smearing).

2.6 Tracks reconstruction

Optionally the tracks reconstruction is provided for charged, stable particles inside Inner Detector coverage ($|\eta|$<2.5) and for transverse momenta above threshold (default : $p_T^{particle} > 0.5$ GeV). Reconstructed tracks parameters (d_0, z_0, ϕ, cot(θ), q/p_T) are smeared with parametrization [6-24] as derived from the dedicated studies for Inner Detector TDR [6-6] and for [6-24] . Smeared and unsmeared tracks parameters are kept in *COMMON /TRACKS/* as well as information about the particle code, the position in event common block and the position and code of up to the 6-the mothers. Available is dedicated parametrization for muons, pions (including tails) and electrons (including bremsstrahlung) as well as reconstruction efficiency. All tracks fulfilling kinematical and geometrical criteria are reconstructed, but the corresponding efficiency is also calculated and this information is stored if needed for further analysis.

2.7 Missing transverse energy

The missing transverse energy E_T^{miss} is calculated by summing the transverse momenta of identified isolated photons, electrons and muons, of jets, b-jets and c-jets, of clusters not accepted as jets and of non-isolated muons not added to any jet cluster. Finally, the transverse energies deposited in cells not used for cluster reconstruction are also included in the total sum. Transverse energies deposited in unused cells are smeared with the same energy resolution function

as for jets, and cells with a deposited transverse energy below a given threshold (default: 0 GeV) are excluded from the sum. In case of high luminosity pile-up is included in cells as its hadronic part only. From the calculation of this total sum E_T^{obs} the missing transverse energy is obtained, $E_T^{miss} = E_T^{obs}$ as well as the missing transverse momentum components, $p_x^{miss}=-p_x^{obs}$, $p_x^{miss}=-p_y^{obs}$. The total calorimeter transverse energy, $\sum E_T^{calo}$ is calculated as the sum of all the above transverse energies except that of muons.

Figures 2-24 shows the p_T^{miss} distribution calculated using the above procedure, compared to the transverse energy distribution of particles escaping detection (muons outside the detector acceptance and neutrinos) for generated WH events with $W \rightarrow l\nu$ and $H \rightarrow b\bar{b}$ and for low luminosity performance. Figure 2-25 shows generated (solid) and reconstructed (dashed) W transverse mass for $W \rightarrow l\nu$ events and simple kinematical selections. The p_T^{miss} resolution, $\sigma_{miss}=\sigma(p_x^{miss})=\sigma(p_y^{miss})$, is given in Table 2-5 as a function of $\sum E_T^{calo}$, for three options: with and without magnetic field and energy smearing, and for the case of low luminosity. For low luminosity result of σ_{miss}=5.7 GeV is consistent with what is expected from the full simulation of the ATLAS detector [6-23]. For high luminosity as ATLFAST is not adding pile-up to cells empty after particle energy deposition the result of σ_{miss}=11.3 GeV represents rather the ultimate performance of the detector. The (p_x^{miss}- p_x^{obs}) resolution for di-jet events is shown on Figure 2-26 and Figure 2-27 for low and high luminosity performance. Results are very similar in the $A \rightarrow \tau\tau$ case, see Figure 2-28 and Figure 2-29.

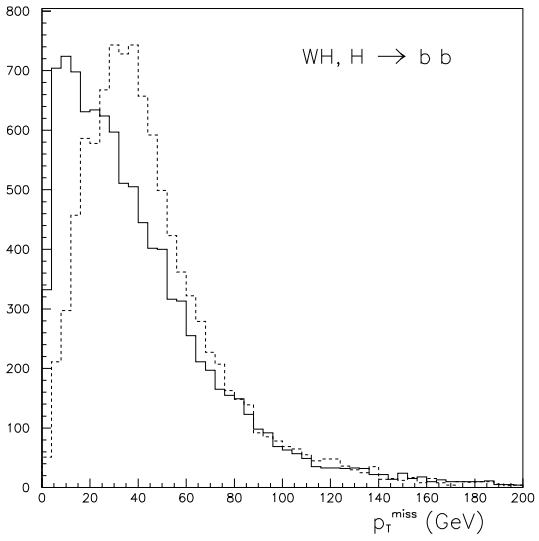

Figure 2-24 Reconstructed p_T^{miss} -distribution (solid line) from generated WH events with $H \rightarrow bb$ and $W \rightarrow l\nu$. The dashed line shows the transverse energy distribution of particles escaping detection (muons outside detector acceptance and neutrinos).

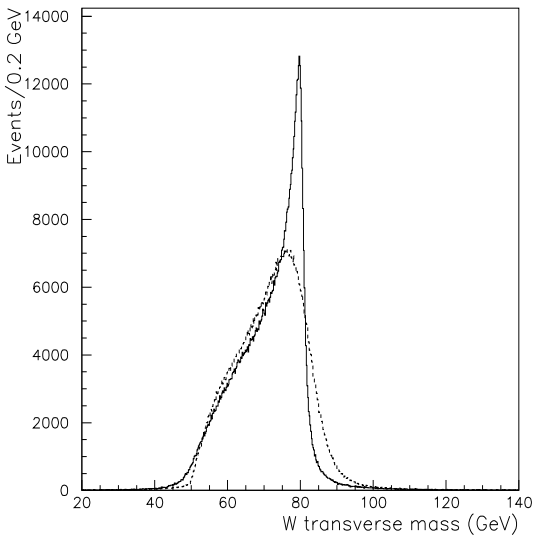

Figure 2-25 The generated (solid) and reconstructed (dashed) W transverse mass from $W \rightarrow l\nu$ events and after simple kinematical cuts. (Courtesy F. Gianotti)

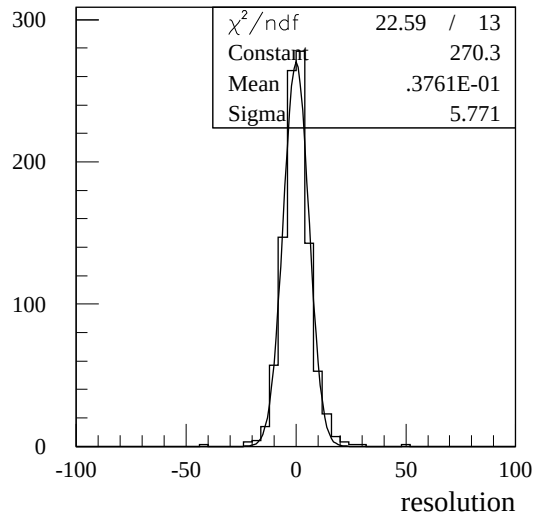

Figure 2-26 The (p_x^{miss}-p_x^{obs}) resolution for di-jet events generated with p_T^{hard} >17 GeV and low luminosity performance.

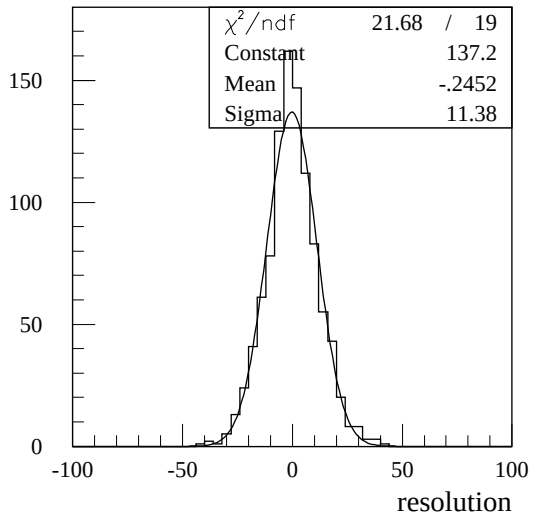

Figure 2-27 The same as Figure 2-26 but for high luminosity performance.

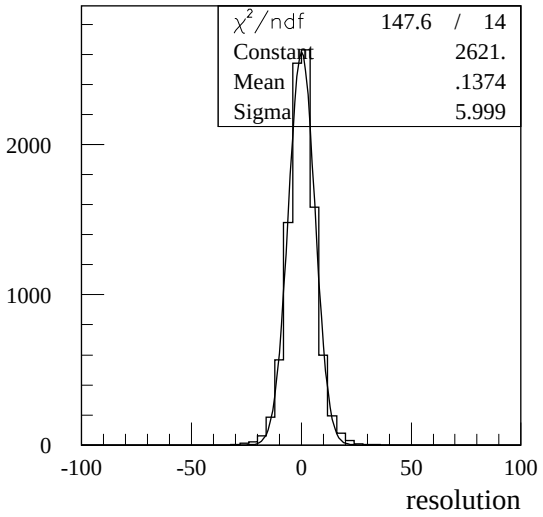

Figure 2-28 The (p_x^{miss}-p_x^{obs}) resolution for A→ ττ events with m_A=150 GeV and low luminosity performance.

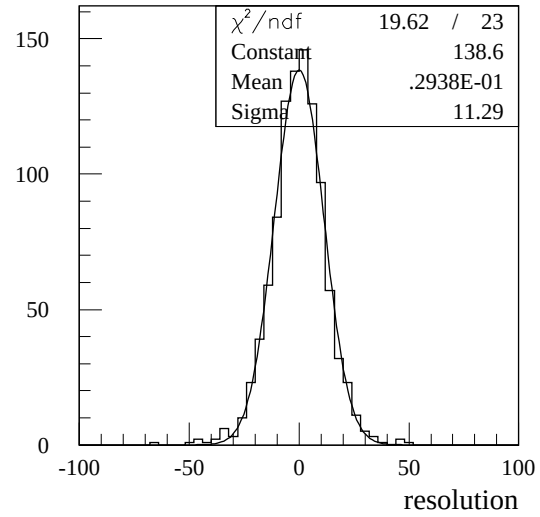

Figure 2-29 The same as Figure 2-28 but for high luminosity performance.

Table 2-5 Reconstructed E_T^{miss} -resolution with and without B-fi eld and/or smearing from generated WH events with H → bb and W → lν T

WH , H→ $b\bar{b}$	Without B-field Without smearing σ_m (GeV)	With B-field Without smearing σ_m (GeV)	With B-field With smearing σ_m (GeV)
25< $\sum E_T^{calo}$<50 GeV	2.36	2.57	2.94
50< $\sum E_T^{calo}$<100 GeV	2.46	2.68	3.72
100<$\sum E_T^{calo}$<200 GeV	3.22	3.54	4.89
200<$\sum E_T^{calo}$<300 GeV	5.41	5.49	6.84
300<$\sum E_T^{calo}$<400 GeV	6.89	7.52	9.26

2.8 Trigger selection

A primitive trigger routine to validate selected physics events can be invoked after each event has been analysed by the algorithm. This routine is not meant to cover all ATLAS trigger aspects and levels, but rather to eliminate events which have essentially no chance of passing the ATLAS level-1 and level-2 trigger as specified in trigger menu of [6-7]. It is more specifically dedicated to SUSY-particle searches, which will include many complex topologies of type n-jets + m-leptons + E_T^{miss}. The results from the ATLFAST analysis, i.e. the lists of isolated electrons, photons, isolated and non-isolated muons, and reconstructed jets are used for this trigger selection.

The proposed trigger selection is aimed at:

- compatibility with present LVL1 + LVL2 understanding; complete coverage of possible signatures;
- slightly lower thresholds than in the TP for some cases where it might turn out to be justified from the physics and where it is not clearly impossible to implement.

Three classes of trigger particles are used for low and high luminosity performance:

- isolated electrons and photons,
- muons
- jets.

For muons, parametrised trigger efficiency (as studied in [6-12]) is included, see Figure 2-30. Isolated and nonisolated muons are labelled with trigger flag (`KEYMUOTRG, KEYMUOXTRG`) and only the ones which passed high-p_T or low-p_T thresholds are considered by the trigger menu given in ATLFAST. For electrons/photons and jets 100% efficiency is assumed for the time being.

Please note, that for E_T^{miss} calculations all muons, which were classified as isolated or nonisolated contribute to visible energy, regardless trigger label.

The details of the default trigger criteria are given in Appendix B.18.

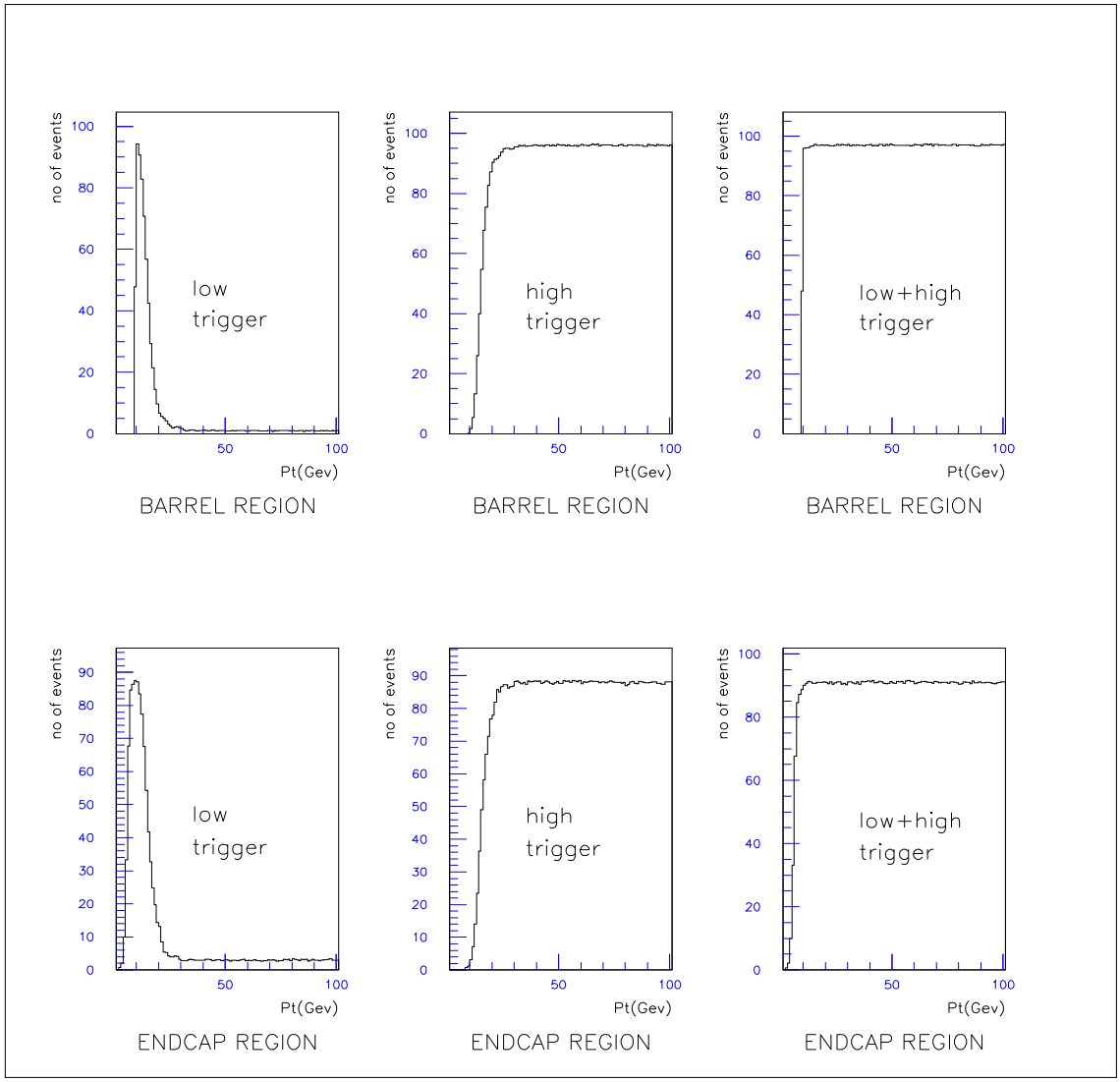

Figure 2-30 The parametrised effi ciency for muon trigger for low, high and low + high p_T-thresholds as a function of p_T^{μ} . The barrel and endcap regions are shown separately. Courtesy S. Cetin.

2.9 Miscellaneous

2.9.1 Electron/jet and photon/jet separation.

It is not parametrised neither in ATLFAST nor ATLFAST-B. The full simulation results were obtained for very particular and in some sense extreme requirements of the detector performance. For jets p_T of 20 GeV the rejection of 10 000 on the jets reconstructed by ATLFAST can be achieved but at the price of electron efficiency of 70% (estimated from [6-6]). The rejection of 5000-7500 could be obtained for jets against photons at the photon identification efficiency of 80% (see [6-15]).

For many physics analysis however that high jet rejection is not necessary. As the full simulation studies were not performed for such cases it is more informative to rather specify what rejection is needed to keep the reducible background at the level of 10-20% of signal+bgd for given sample than to use some crude number in the fast simulation analysis.

2.9.2 Electron, muon, photon isolation

This issue was not studied with the full simulation. ATLFAST uses a rather crude estimation, asking for $E_{dep} < 10$ GeV in $R_{cone} = 0.2$ and a separation from other jets with $R_{cone} > 0.4$.

2.9.3 Electron/photon separation

Not treated by ATLFAST.

For electrons of p_T=40 GeV the electron veto efficiency above 99.8% can be achieved while retaining an efficiency above 96% for photons (not including calorimeter identification criteria) even at high luminosity [6-16].

2.9.4 Charge misidentification

Not treated by ATLFAST.

Electrons are sufficiently delicate that this issue should be studied with full reconstruction . For muons it is relevant only for very high energies and it is reasonably parametrised by the smearing routine for track helix parameters.

3 More about jets: reconstruction, calibration and tagging

3.1 Comparison to parton-level simulation for b-jets

Parton-level simulation, where selection criteria are applied to quarks and gluons, often leads to too optimistic results. In [6-9], the parton-level simulation was compared to the particle-level simulation (called there jet-level simulation), and large differences were observed for the reconstruction of b-jets and of invariant $b\bar{b}$ masses and their source was identified. The main points of this discussion are recalled below:

- **Efficiency for b-jet reconstruction $\varepsilon_{\text{b-jet}}^{\text{recon}}$.**

The probability, that a b-quark produced in the hard scattering process, of $p_T^{\text{b-quark}} > p_T^{\text{thr}}$ leads to a reconstructed jet with $p_T^{\text{b-jet}} > p_T^{\text{thr}}$, labelled as a b-jet was studied carefully. This probability is close to 100%, if only hard-scattering process (HP) is generated and remains unchanged, if initial-state radiation (ISR) is included. However, if final-state radiation (FSR) and hadronisation (HD) are included also, this probability, called subsequently the efficiency for b-jet reconstruction $\varepsilon_{\text{b-jet}}^{\text{recon}}$, drops [1] to ~ 80% for p_T^{thr}>15 GeV and ΔR_{cone}=0.4 and for the WH , H$\rightarrow b\bar{b}$ process with m_H =100 GeV. This loss in efficiency depends on the b-quark p_T- distribution and therefore depends on the process considered.

- **Reconstruction of the invariant mass of two b-jets.**

Due to FSR and HD, a large shift in the peak position of the reconstructed mass, $m_{b\bar{b}}$, of two b-jets is observed. Additional important effects are the degradation of the mass-resolution and large asymmetric tails in the mass distribution (see Figure 2-21). All these effects lead to a significant degradation of the acceptance in a mass window of ± 20 GeV (around the nominal Higgs boson mass), where the size of the mass bin was chosen as that needed in ATLAS. Figure 3-1 and Table 3-1, similar to Fig.1 and Table 5 of [6-9], illustrate these effects, as obtained from the ATLFAST package, including solenoidal magnetic field. All these effects depend only weakly on the parameters used for the jet-finding algorithm.

Table 3-1 Main characteristic of the reconstruction of the H $\rightarrow b\bar{b}$ mass peak at particle level, as a function of the ingredients used in the event generation, for the WH, H $\rightarrow b\bar{b}$ signal at LHC and for m_H=100 GeV

Event generation	Peak position <m> in GeV	Resolution σ_m GeV	Effi ciency for $m_{b\bar{b}}$ within < m > ± 20 GeV
HP	99.0	5.0	98.5%
HP + ISR	100.0	6.0	98.5%
HP + ISR + FSR	92.0	9.0	84.0%
HP + ISR + FSR+HD	82.0	9.5	83.0%

1. The values quoted here are slightly different from these in [6-9], due to the different algorithm used for the jet reconstruction. More accurate values should always be supplied by the full simulation results.

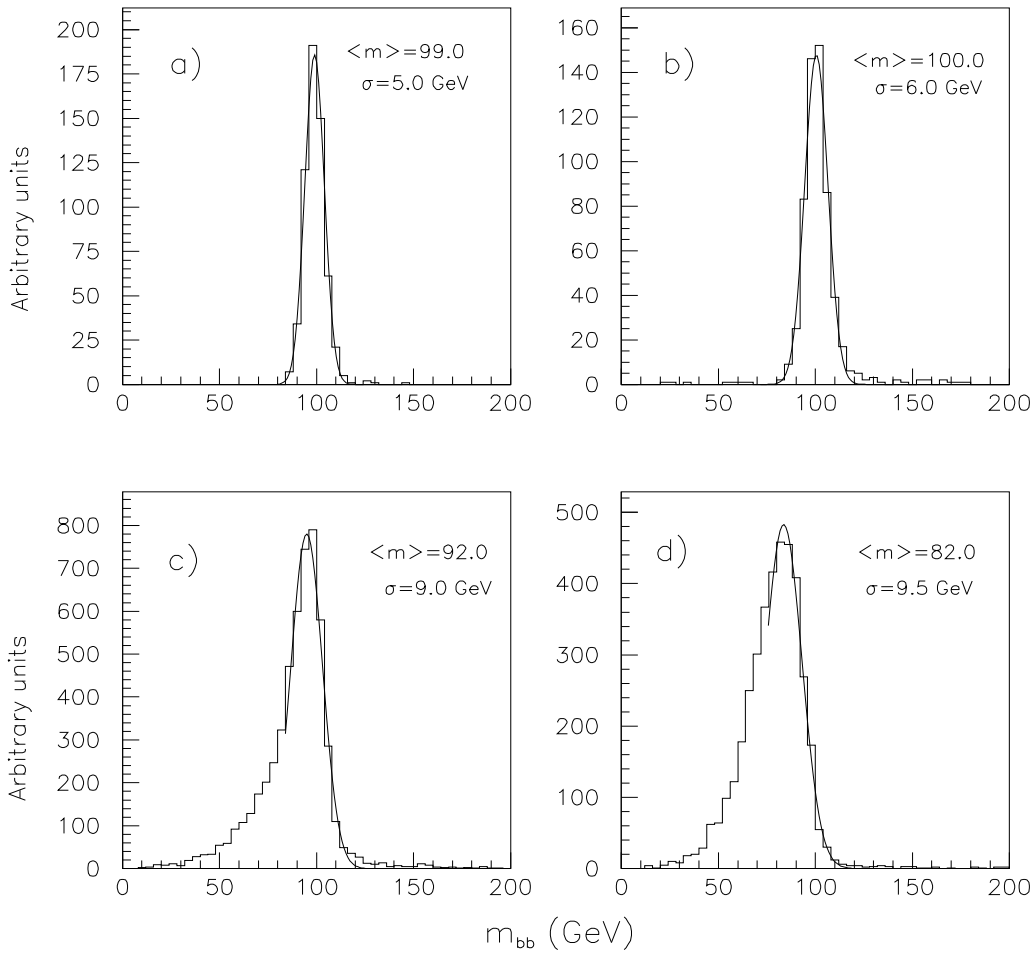

Figure 3-1 Reconstruction of the invariant mass distribution of the two b-jets from Higgs boson decay for m_H = 100 GeV and WH production with $H \rightarrow b\bar{b}$ at the LHC, as a function of the ingredients used in the event generation: (a) hard scattering process, (b) initial state radiation, (c) fi nal state radiation and (d) hadronisation/decays.

- **The effect of the B-field.**

Table 3-3 shows the average ratio $<p_T^{\text{b-jet}}/p_T^{\text{b-quark}}>$, the efficiency for b-jet reconstruction $\varepsilon_{\text{b-jet}}^{\text{recon}}$ and the fitted position of the mass peak $<m_{b\bar{b}}>$ for WH production with $H \rightarrow b\bar{b}$ and m_H =100 GeV. Three options with and without B-field and smearing are shown. The magnetic field reduces the efficiency for b-jet reconstruction by 3% and shifts the position of the $m_{b\bar{b}}$ peak by -5 GeV. The average value $<p_T^{\text{b-jet}}/p_T^{\text{b-quark}}>$ is also reduced by 3% due to the magnetic field.

Table 3-2 Average ratio $<p_T^{b\text{-jet}}/p_T^{b\text{-quark}}>$, effi ciency for b-jet reconstruction $\varepsilon_{b\text{-jet}}^{recon}$, and fi tted position of the $)m_{b\bar{b}}$ peak and acceptance ε_{bin} in a mass bin $<m_{b\bar{b}}> \pm 20$ GeV, for WH production with $H \rightarrow b\bar{b}$ and m_H=100 GeV. The expected results with B-fi eld being on and off are shown without smearing as well as the results with B-fi eld and smearing.

WH , $H \rightarrow b\bar{b}$	Without B-fi eld Without smearing	With B-fi eld Without smearing	With B-fi eld With smearing
$<p_T^{b\text{-jet}}/p_T^{b\text{-quark}}>$	0.83	0.80	0.80
$\varepsilon_{b\text{-jet}}^{recon}$	83%	80%	81%
$<m_{b\bar{b}}>$	87.5 GeV	82.6 GeV	82.0 GeV
ε_{bin} = 82 ± 20 GeV	86.5%	84%	83%

3.2 Jet energy calibration (in ATLFAST-B)

The possibility to recalibrate the peak position for the dijet mass has been studied for samples of u-jets, gluon-jets and b-jets obtained from WH production with respectively $H \rightarrow u\bar{u}$, $H \rightarrow gg$ and $H \rightarrow b\bar{b}$ decays. The jet momenta are recalibrated by a calibration factor $K_{jet}=p_T^{parton}/p_T^{jet}$. Here, p_T^{parton} denotes the transverse momentum of the parton which initiated the jet (before FSR). Figure 3-2 shows these calibration factors as a function of p_T^{jet} for the three jet flavour initiators and Figure 3-3 as a function of ΔR_{cone}. For p_T^{jet} >50 GeV, the distributions become asymptotically flat at a value $K_{jet} \sim 1.2$ independent of the jet flavour. For p_T^{jet}<50 GeV, K_{jet} is closer to unity for u-jets than for g-jets and b-jets. The values of $K_{b\text{-jet}}$ and $K_{g\text{-jet}}$ are the same within errors over the whole range of $p_T^{cluster}$.

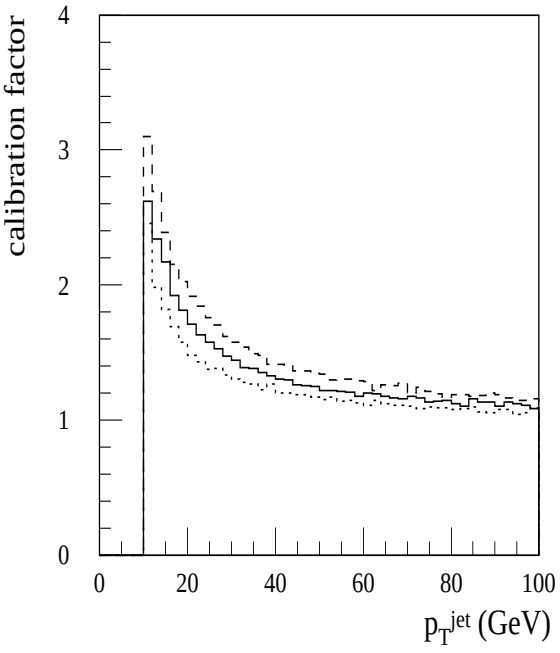

Figure 3-2 Calibration factor, $K_{jet}=p_T^{parton}/p_T^{jet}$, as a function of the reconstructed jet transverse momentum, p_T^{jet}, for b-jets (solid line), gluon-jets (dashed line) and light-quark jets (dots)

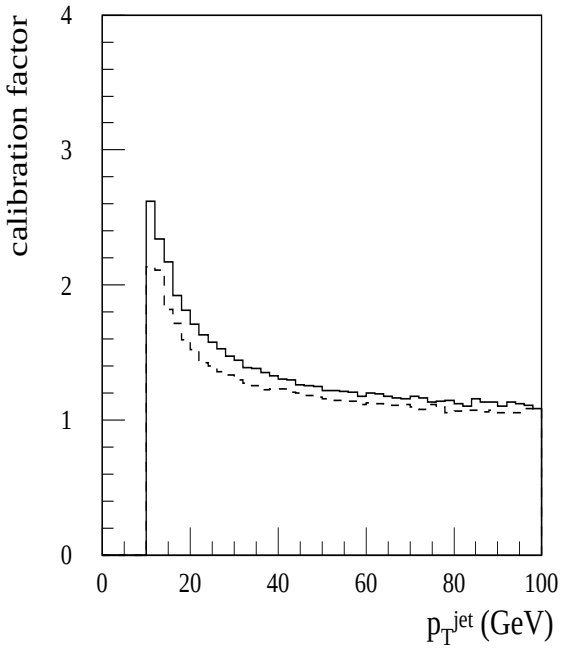

Figure 3-3 Calibration factor, $K_{b\text{-jet}}=p_T^{b\text{-quark}}/p_T^{b\text{-jet}}$, as a function of the reconstructed jet transverse momentum, $p_T^{b\text{-jet}}$, for jets reconstructed in ΔR_{cone}=0.4 (solid line) and ΔR_{cone}=0.7.

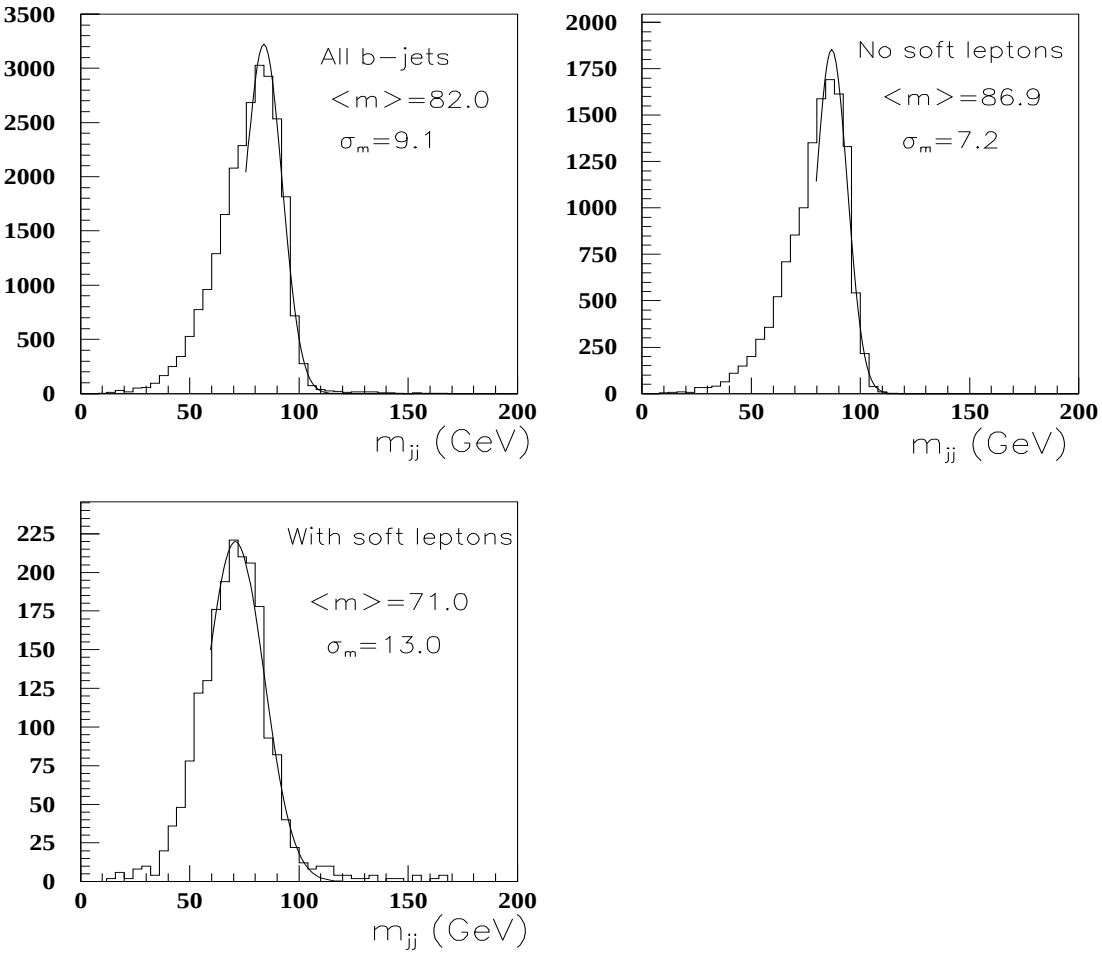

Figure 3-4 Uncorrected $m_{b\bar{b}}$ distributions for WH events with $H \rightarrow b\bar{b}$ and m_H =100 GeV. Shown are the distributions for all b-jet pairs (top left), for b-jet pairs not containing any identifiable soft lepton (top right), and for b-jet pairs where both b-jets contain at least one identifiable soft lepton (bottom left). The B-field effects and smearing are included.

Table 3-3 Average ratio $\langle p_T^{\text{b-jet}}/p_T^{\text{b-quark}}\rangle$, efficiency for b-jet reconstruction $\varepsilon_{\text{b-jet}}^{\text{recon}}$, and fitted position of the $m_{b\bar{b}}$ peak and acceptance ε_{bin} in a mass bin $\langle m_{b\bar{b}}\rangle \pm 20$ GeV, for WH production with $H \rightarrow b\bar{b}$ and m_H=100 GeV. The expected results with B-field being on and off are shown without smearing as well as the results with B-field and smearing.

WH , H→ bb̄	**Without B-field Without smearing**	**With B-field Without smearing**	**With B-field With smearing**
$\langle p_T^{\text{b-jet}}/p_T^{\text{b-quark}}\rangle$	0.83	0.80	0.80
$\varepsilon_{\text{b-jet}}^{\text{recon}}$	83%	80%	81%
$\langle m_{b\bar{b}}\rangle$	87.5 GeV	82.6 GeV	82.0 GeV
ε_{bin} = 82 ± 20 GeV	86.5%	84%	83%

In fact, it is well known by now that the properties of b-jets and gluon jets are very similar, whereas they differ noticeably from these of the light-quark jets [6-25]. The case of b-jets was studied further for b-jets containing at least one identifiable lepton (electron or muon with p_T>1 GeV inside the jet cone), for which the calibration factor $K_{b\text{-jet}}^{lepton}$ was calculated separately. Figure 3-5 compares the two calibration factors: $K_{b\text{-jet}}^{aver}$ and $K_{b\text{-jet}}^{lepton}$. It was observed that $K_{b\text{-jet}}^{lepton}$ is systematically higher. This can be qualitatively explained by the effect of missing neutrino(s) in b-jets with soft leptons. No strong dependency on the p_T of the soft lepton was found for $K_{b\text{-jet}}^{lepton}$, however this dependence is visible as a function of the transverse momenta of neutrinos in the final state. This calibration gives (as shown bellow) proper mass energy scale however is not giving the proper jet energy scale. Figures 3-4 shows the reconstructed $m_{b\bar{b}}$ distribution (without calibration) for all b-jets for pairs with two non-leptonic b-jets (52% of the sample) and for pairs with two leptonic b-jets (8% of the sample). It can be seen that the pairs of non-leptonic b-jets give a distribution for $m_{b\bar{b}}$ similar to that for pairs of u-jets (compare to Figure 2-15) while the pairs of leptonic b-jets give a much larger shift in the peak position and width than the average b-jets. Figure 3-6 shows the m_{jj} distributions for WH events with $H \rightarrow gg$ and $H \rightarrow u\bar{u}$. The difference between correcting p_T of these jets by using the b-jet calibration factor $K_{b\text{-jet}}$ (left side of Figures 3-6) or by using the calibration factors, $K_{g\text{-jet}}$ and $K_{u\text{-jet}}$, determined for each appropriate jet flavour (right side of Figure 3-6), is noticeably only for $H \rightarrow u\bar{u}$ decays. The position of the reconstructed mass peak and the acceptance in the mass window after calibrations using calibration factors $K_{g\text{-jet}}$ and $K_{u\text{-jet}}$ or using calibration factor $K_{b\text{-jet}}$ is shown in Table 3-4 .

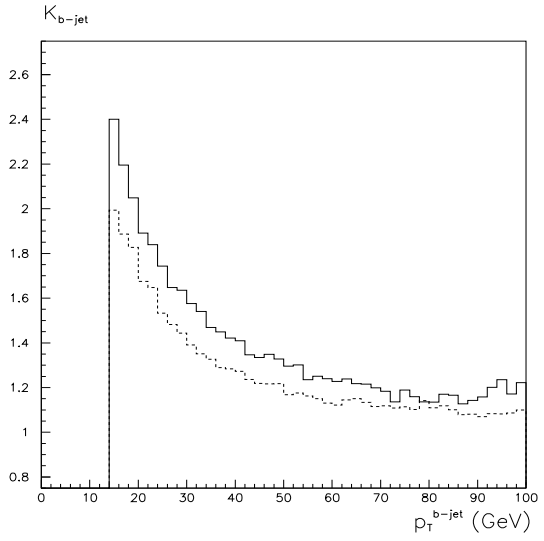

Figure 3-5 Calibration factor, $K_{b\text{-jet}}=p_T^{b\text{-quark}}/p_T^{b\text{-jet}}$, as a function of $p_T^{b\text{-jet}}$, shown separately for b-jets containing at least one identifi able soft lepton (solid line) and for all b-jets (dashed line).

One should be however aware that the above calibration gives the proper mass energy scale but is not giving proper jet energy scale, as illustrated on Figure 3-7.

The calibration factors can be apply with facilities of the ATLFAST-B package.

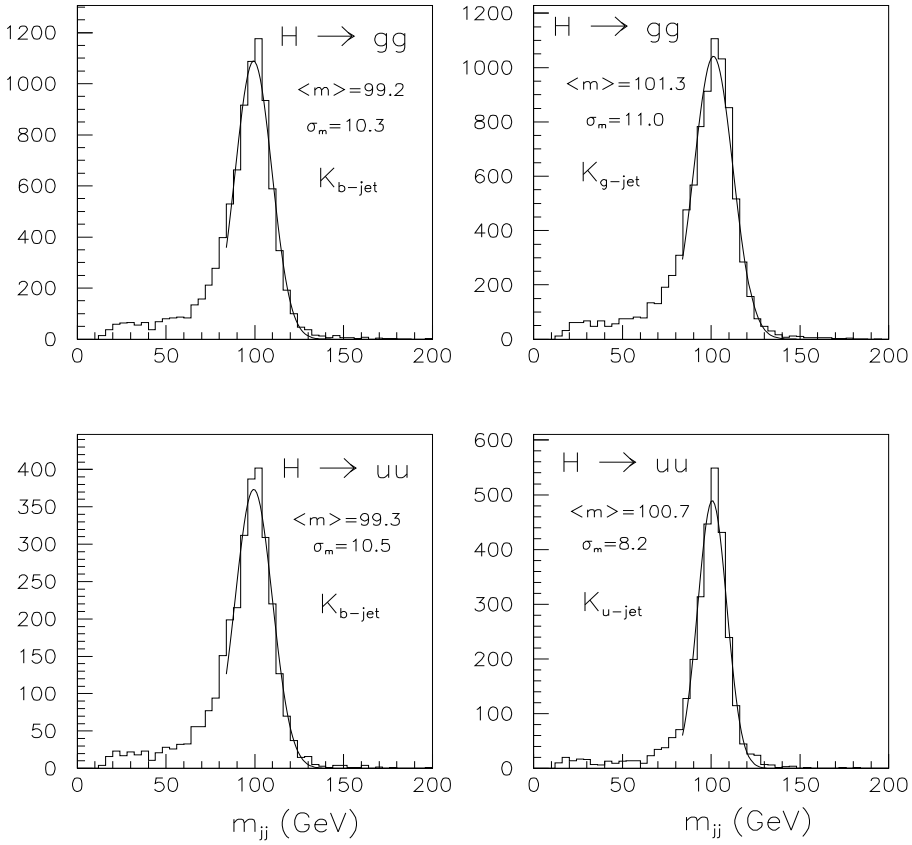

Figure 3-6 Corrected m_{jj} distributions for WH events with m_H =100 GeV and $H \rightarrow gg$ decays (top) and $H \rightarrow u\bar{u}$ decays (bottom). The calibration factors applied were those for b-jets (left) and those obtained for gluon jets and u-quark jets respectively (right)

Table 3-4 The fitted peak position $<m_{jj}>$ for generated WH events with $H \rightarrow gg$ and $H \rightarrow u\bar{u}$ decays with and without jet calibration by the $K_{b\text{-}jet}$ factor. The acceptance in a given mass window is also shown for the corrected sample.

calibration		**$H \rightarrow gg$**	**$H \rightarrow u\bar{u}$**
$K_{b\text{-}jet}$	$<m_{b\bar{b}}^{calib}>$ ε_{bin}=100 ± 20 GeV	99.2 GeV 78%	99.3 GeV 77%
$K_{u\text{-}jet}$, $K_{g\text{-}jet}$	$<m_{jj}^{calib}>$ ε_{bin}=100 ± 20 GeV	101.3 79%	100.7 GeV 86%

Table 3-5 he fitted $<m_{b\bar{b}}^{calib}>$ peak position for corrected sample of b-jets and acceptance in the mass window is given for WH process with $H \rightarrow b\bar{b}$ and m_H =100 GeV. The option with B-field on/off is shown without smearing as well as option with B-field and smearing.

WH , $H \rightarrow b\bar{b}$	**no B-field no smearing**	**with B-field no smearing**	**with B-field with smearing**
$<m_{b\bar{b}}^{calib}>$	102.5 GeV	102.4 GeV	102.4 GeV
ε_{bin}= 100 ± 20 GeV	85.6%	85.4%	84.6%

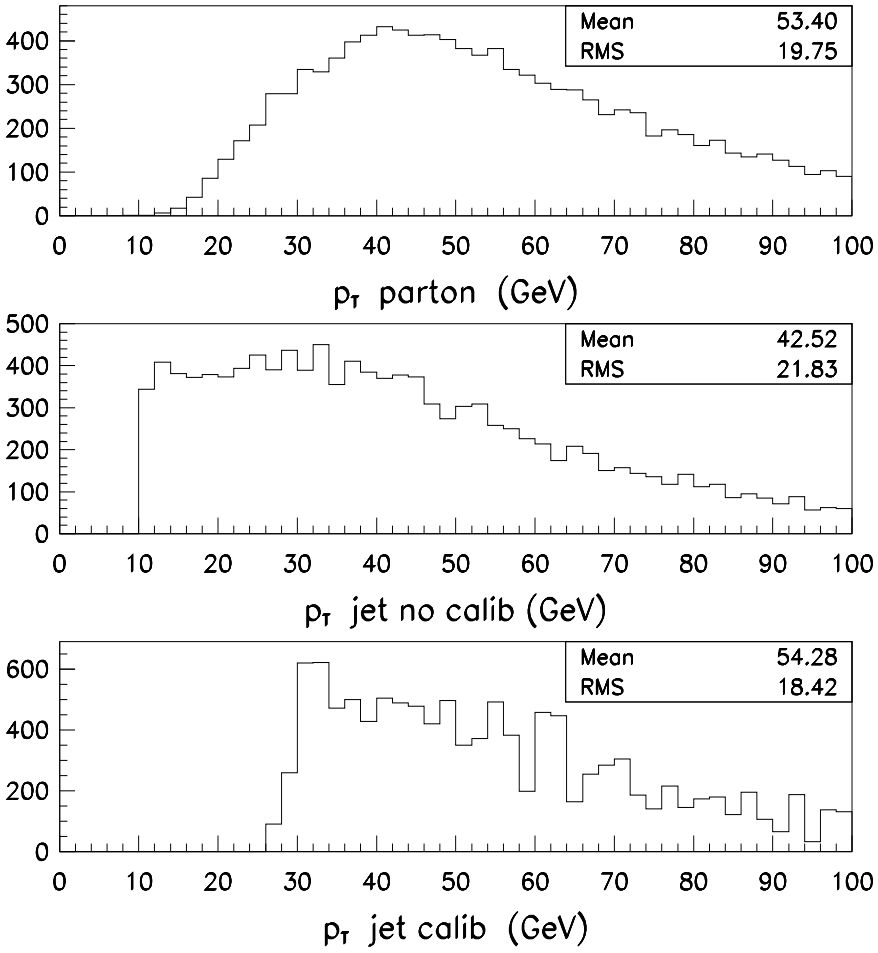

Figure 3-7 The p_T distribution for hard-process b-quarks (top), reconstructed b-labelled jets (middle) and calibrated b-labelled jets (bottom) for WH , $H \rightarrow b\bar{b}$ process and low luminosity operation.

3.3 Jets reconstruction with Jet Finder library

The Jet Finder library [6-4] which contains different algorithms for clusters reconstruction was interfaced to ATLFAST. This provides flexible possibility to combine/cross-check full and fast simulation analyses. Detailed description on available algorithms and comparison of mass resolution and calibration coefficients can be found in [6-4]. The JetFinder Library can be activated with `KEYJF=1` (for `KEYJF=0` the default cone algorithm is used). Choice of the required algorithm and its parameters have to be specified. For description see [6-4] .

The same version of the jetFinder Library is used also by the full simulation DICE+ATRECON package.

3.4 b-tagging algorithm (in ATLFAST-B)

The fraction of p_T of the b-labelled jet carried by the B-hadron is on average ~ 95% for a cone size of ΔR=0.4. The b-jet itself, however, carries only on average ~80% of the p_T of produced b-quark. These numbers illustrate well some of the large differences between parton-level and particle-level simulations of b-quark reconstruction and of the b-tagging in a real experiment. In order to explore the expected Inner Detector environment, when attempting to tag b-jets, the expected numbers of charged particles found within the b-jet cone was studied in [6-9]. It was shown that a cone size of ΔR_{cone}=0.4 is sufficient to measure more than 90% of the charged particles from the B-hadron decay. For a realistic threshold of $p_T^{particle} > 1$ GeV and uncalibrated jets, this cone size includes on average ~ 4.8 charged tracks from B-hadron decay, ~ 2.4 charged tracks from the b-quark fragmentation and from the underlying event, and a negligible number (<0.2) from minimum bias pile-up at low luminosity. This average (for charged tracks from B-hadron) increases to ~ 5.2 for b-labelled uncalibrated jets. For calibrated jets it becomes respectively ~ 4.5 for any and ~ 5.1 for b-labelled jets.

Table 3-6 The average $<n_{track}>$ multiplicity from B-hadrons for different values of ΔR_{cone} and for $p_T^{track} > 1$GeV and for WH , $H \rightarrow b\bar{b}$ events.

$<n_{track}$	ΔR_{cone} around hard-b	ΔR_{cone} around jet axis	ΔR_{cone} around b-jet axis
ΔR_{cone}=0.4, uncalibrat.	4.21	4.77	5.18
ΔR_{cone}=0.4, calibrat.	4.21	4.46	5.06
ΔR_{cone}=0.7 calibrat.	4.23	4.45	5.08

The much more detailed understanding of the b-tagging performance achieved through the studies of [6-6] has permitted the implementation of a realistic parametrisation of the b-tagging performance into the fast simulation used for the study of the signal from WH , $H \rightarrow b\bar{b}$ associated production. This parametrisation has been implemented in the following way [6-22]. The results from Section 6.7.6 of [6-6] for m_H = 100 GeV have been adapted to account for the different methods used for labelling jet flavour in the full-simulation studies and in the fast simulation program (the latter has to treat many background sources with varying jet multiplicities and flavours). ATLFAST is labelling jets as b-jets and c-jets on the criteria that in the distance of ΔR_{cone}=0.2 from the jet axis the heavy flavour quark after FSR with $p_T > 5$ GeV was found. On the other hand algorithm which has been used in full simulation for defining the true b-jet bases on the charged track from B-hadron decay of p_T> 1GeV found around hard-b quark which initiated a jet [6-6]. In Table 3-7 matching between both algorithms is illustrated. b-quarks from hard process (hard-b), jets and b-labelled jets, without and with energy calibration (cluster were reconstructed down to $p_T^{cluster}$>10 GeV and after energy smearing accepted down to $p_T^{jet} > 15$ GeV) were accepted for $p_T^{jet} > 15$ GeV and B-hadron charged tracks with $p_T^{track} > 1.0$ GeV. Only in 0.3 -0.4 % of cases a jet was labelled as a b-jet in absence of a charged track from the B-hadron inside the jet cone. However asking for charged track inside the jet cone would give a better acceptance (89.7 % instead of 82.7 %) for the b-labelling of reconstructed jets (80.4 % instead of 75.7 % for non-calibrated jets). The direction of hard-b quark does not always coincide with the jet direction (as seen already on Figure 2-3 and Figure 2-4) and the efficiency for combination jet+track+hard-b to match inside $\Delta R_{cone} < 0.4$ is of 82.9 % for the cone around jet-axis and of 81.1% for the cone around hard-b. In Table 3-8 these efficiencies are compared for calibrated jets and two sizes of ΔR_{cone} and for b-quark and gluon originated jets.

Table 3-7 The matching between hard partons, charged tracks from B-hadrons, jets and b-labelled jets in the cone DR<0.4 for calibrated (uncalibrated) jets. Normalized to the hard-process b-quark with pT>15 GeV, |h|<2.5. ISR switched off.

generated: WH , H→ $b\bar{b}$	**all jets**	**b-labelled jets**
ΔR_{cone} around hard-b	ΔR_{cone} around hard-b	ΔR_{cone} around hard-b
1. hard-b 100 %		
2. hard-b + track 91.4 %		
3. hard-b + jet	83.7 % (77.6 %)	78 % (73.4 %)
4. hard-b + jet + track	81.1 % (75.7%)	77.7 % (73.0 %)
5. hard-b + jet + no-track	2.4 % (1.9 %)	0.5 % (0.4 %)
6. hard-b + no-jet + track	10.3 % (15.6 %)	13.7 % (18.3 %)
7. hard-b + no-jet + no-track	6.2 % (6.8 %)	8.1 % (8.2 %)
ΔR_{cone} around jet	ΔR_{cone} around jet	ΔR_{cone} around jet
1. jet	99.9 % (87.1 %)	**82.7 % (76.5 %)**
2. jet + track	**89.7 % (80..0 %)**	82.5 % (76.2 %)
3. jet + hard-b	86.2 % (79.1 %)	77.9% (73.3 %)
4. jet + hard-b + track	82.9 % (76.2 %)	77.7 % (73.0 %)
5. jet + hard-b + no-track	3.8 % (2.9 %)	0.4 % (0.3 %)
6. jet + no hard-b + track	6.0 % (3.8 %)	4.7 % (3.2 %)
7. jet + no hard-b + no-track	7.1 % (4.2 %)	0.04% (0.02 %)

Table 3-8 The same as Table 3-7 but for calibrated jets. The matching between calibrated jets, b-labelled jets and charged tracks from B-hadrons, in cone ΔR_{cone}<0.4 (in cone ΔR_{cone}=0.7). Normalized to hard-process partons with p_T>15 GeV, |η|<2.5. ISR was switched off.

generated:	**all jets**	**b-labelled jets**
WH , H→ $b\bar{b}$		
1. jet	99.9 % (100 %)	**82.7 % (84.4 %)**
2. jet + track	**89.7 % (91.4 %)**	82.5 % (84.2 %)
WH , H→ gg		
1. jet	99.9 % (100 %)	1.4 % (1.5 %)
2. jet + track	**2.4 % (2.5 %)**	1.4 % (1.5 %

The expected b-tagging performance was parametrised consistently with algorithm for jet-labelling. Table 3-9 and Table 3-10 shows efficiencies for jets from u, d, s, g (not containing c-quarks nor b-quarks in the final parton shower process) and from charm, respectively and for vertexing alone. The rejections averaged over η and p_T are shown in the second column as a function of the b-tagging efficiency and the other columns show the correction factors applied to these values to account for the p_T-dependence discussed in Section 6.7.6 of [6-6]; These num-

bers are implemented in ATLFAST-B package and can be used for randomly tagging on jets labelled as b-jets, c-jets and other jets.

Table 3-9 For calibrated jets from Higgs-boson decay with m_H = 100 GeV not containing any heavy flavour component from charm or bottom, rejections achieved by vertexing alone as a function of the jet p_T and of the chosen effi ciency for tagging b-jets. Table 6-24 from [6-6].

Jets from u,d,s,g	Global rejection	Correction: 15< p_T<30	Correction: 30< p_T<45	Correction: 45< p_T<60	Correction: 60< p_T<100	Correction: p_T > 100
ε_b = 33%	1400±400	0.11	0.35	1.80	1.80	1.80
ε_b = 43%	220 ±30	0.28	0.49	2.16	2.16	1.58
ε_b = 53%	91±7	0.24	0.51	1.75	2.10	1.95
ε_b = 64%	32±2	0.18	0.59	1.50	2.11	1.94

Table 3-10 For calibrated c-jets from Higgs-boson decay with m_H = 100 GeV, rejections achieved by vertexing alone as a function of the jet p_T and of the chosen effi ciency for tagging b-jets. Table 6-25 from [6-6].

Jets from charm	Global rejection	Correction: 15< p_T<30	Correction: 30< p_T<45	Correction: 45< p_T<60	Correction: 60< p_T<100	Correction: p_T > 100
ε_b = 33%	22.9 ±2.0	0.44	0.68	1.10	1.57	2.17
ε_b = 43%	10.8 ±0.6	0.58	0.66	1.23	1.59	1.13
ε_b = 53%	6.7 ±0.3	0.58	0.75	1.40	1.54	1.40
ε_b = 64%	4.2 ±0.1	0.60	0.82	1.22	1.29	1.28

3.5 τ-tagging algorithm (in ATLFAST-B)

The expected detector performance for identifying hadronic τ–jets was studied extensively with full simulation in [6-23]. In ATLFAST the consistent criteria for labelling jets as τ-jets candidates were incorporated. This parametrization, obtained with the full simulation of A→ ττ events [6-23], specifies p_T and $|\eta|$ dependent jets rejection for required efficiency for τ–jets identification and for low luminosity performance. Parametrization is given for three ranges of pseudorapidity: $|\eta|<0.7$, $0.7 < |\eta| < 1.5$ and $|\eta| < 1.5$ and for $15 < p_T^{jet} < 150$ GeV. On Figure 3-8 and Figure 3-9 is shown parametrised non-tau jet rejection for fixed tau-tagging efficiency.

The tau-veto can be useful for rejection of backgrounds containing taus. A more detailed study for tau-veto was done on A to tau-tau events and on the large-jets production events, as presented in [6-23] using cutoffs on electromagnetic radius and number of associated tracks with p_T^{track}>1 GeV. For $p_T^{cluster}$ > 60 GeV the $\varepsilon^{veto,jet}$=90% with $\varepsilon^{veto,tau}$=5% can be achieved. For $p_T^{cluster}$<60 GeV, with fixed $\varepsilon^{veto,tau}$ = 5% the $\varepsilon^{veto,jet}$ < 90% and is decreasing with decreasing $p_T^{cluster}$. Also for $p_T^{cluster}$<60 GeV and fixed $\varepsilon^{veto,jet}$ = 90% the $\varepsilon^{veto,tau}$ > 5 % and is increasing with $p_T^{cluster}$.

The parametrization for τ–tagging efficiency of jets labeled as τ–jets is provided by ATLFAST-B. This package provides as well parametrisation for the non-tau jet veto.

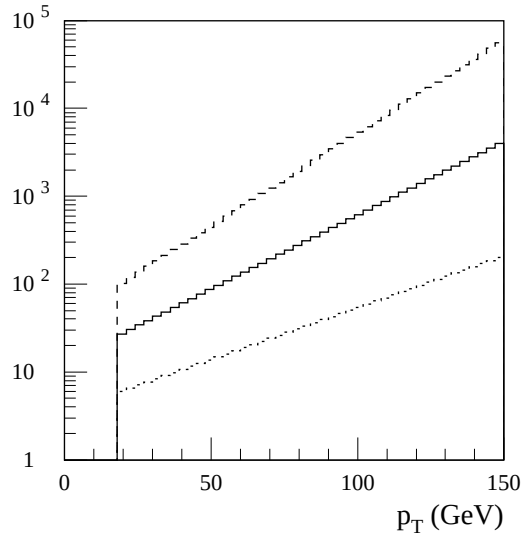

Figure 3-8 Parametrisation for non-tau jet rejection for fi xed value of tau-tagging effi ciency (from top to bottom) 30%, 50%, 70% and central rapidity range |η| < 0.7.

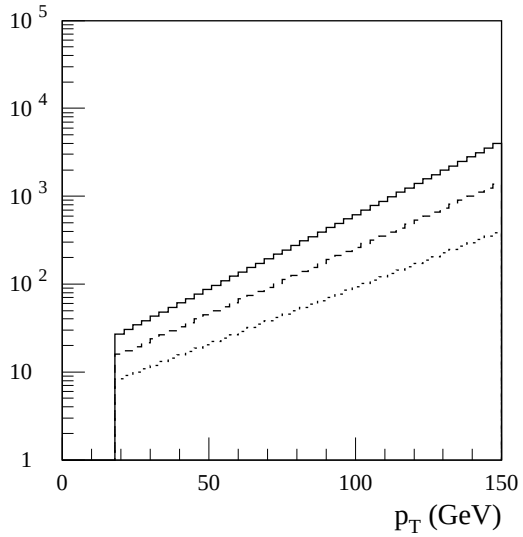

Figure 3-9 Parametrisation for non-tau jet rejection for fi xed value of tau-tagging effi ciency of 50% and for (from top to bottom) |η|<0.7, 0.7<|η| <1.4 and 1.4 |η| < 2.5

4 More about tracks helix parameters reconstruction.

Main motivation for including helix parameters reconstruction for charged tracks in the fast simulation is its possible applicability to the B-physics studies.

For a given set of tracks parameters a smeared set is calculated with a good approximation to the current best estimate of the Inner Detector performance. Smearing is done according to the particle type. The three distinguished particle types are: electrons, muons and pions. All other charged particles are treated as pions.

The detailed description of the parametrisation for tracks resolution and reconstruction efficiency can be found in [6-24] . Resolution for muon tracks derived from the full simulation results is considered to have no tails within precision aimed for the fast parametrisation. Tracks of electrons are smeared initially as for muons but then their tracks parameters are altered by adding a parametrised effect of the bremsstrahlung process. Smearing for pions is described by the sum of two Gaussian contributions representing the core and the tail.

The tracks finding efficiency is also parametrised. All tracks which pass kinematical and geometrical selection are reconstructed with 100% efficiency by the ATLFAST but the expected reconstruction efficiency is however calculated and stored in the ntuple together with the tracks parameters.

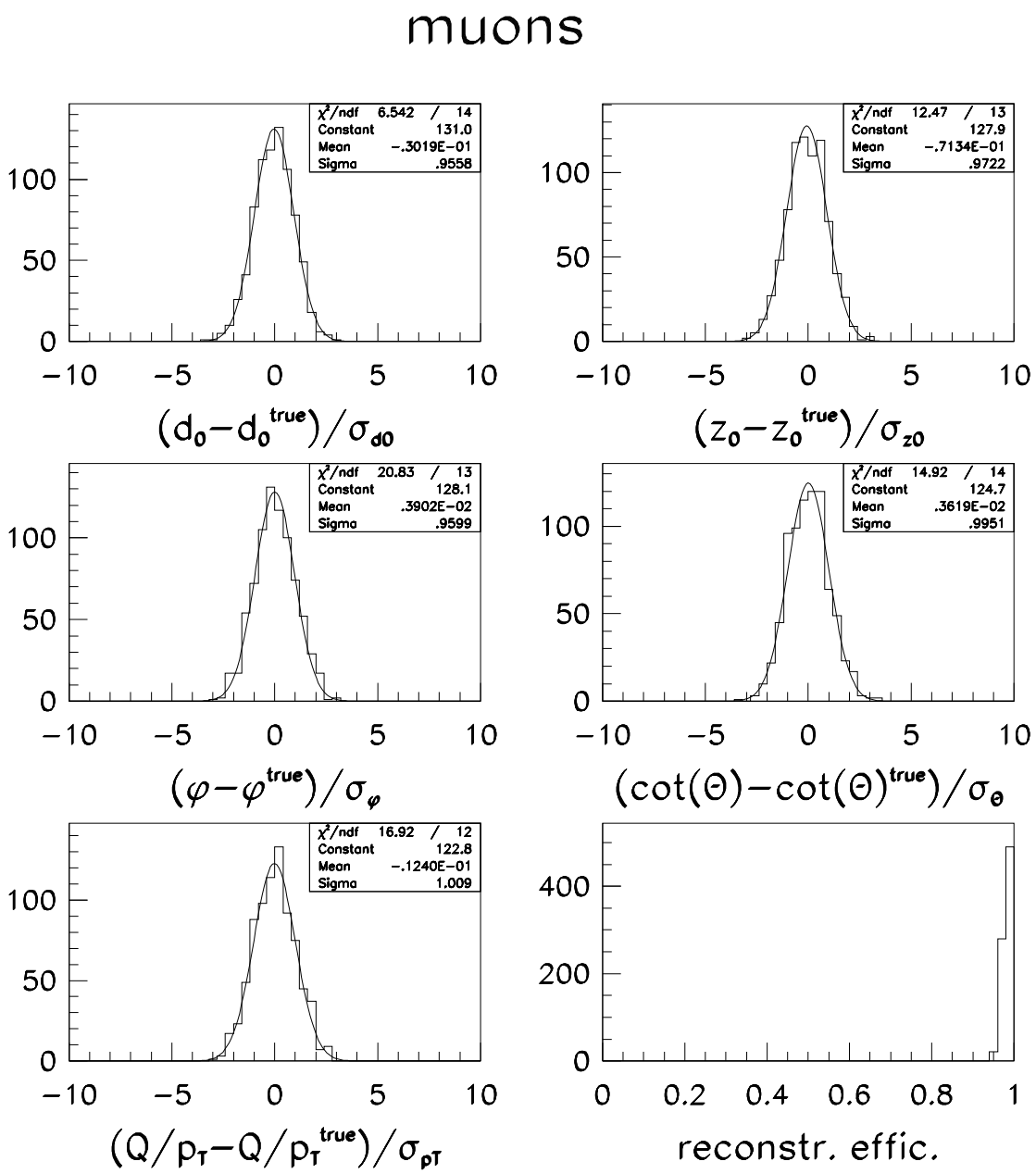

Figure 4-1 Normalised resolution for helix parameters and reconstruction track efficiency for muons. (WH, $H \rightarrow b\bar{b}$ sample was generated).

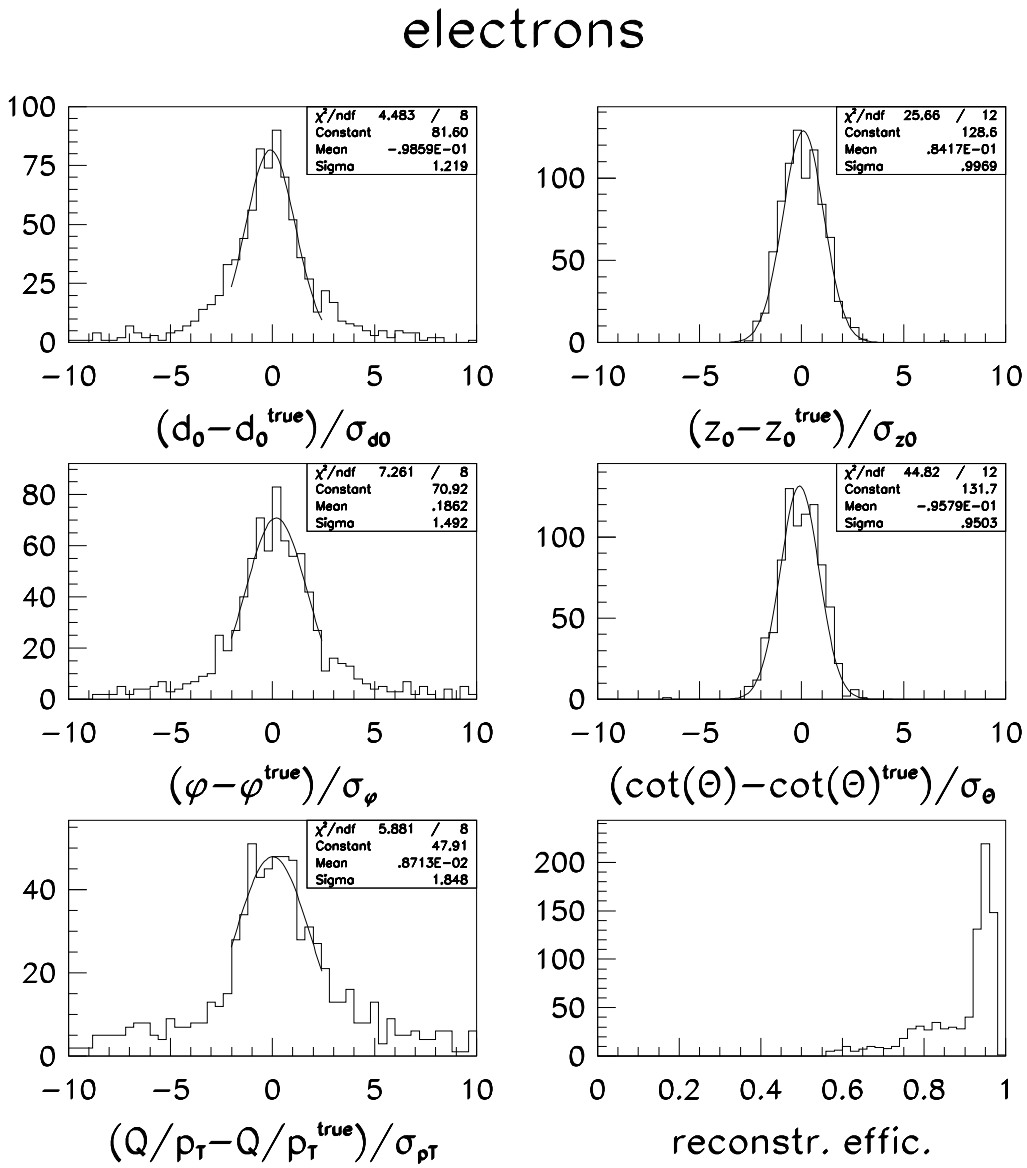

Figure 4-2 Normalised resolution for helix parameters and reconstruction track efficiency for electrons. (WH, H → $b\bar{b}$ sample was generated)

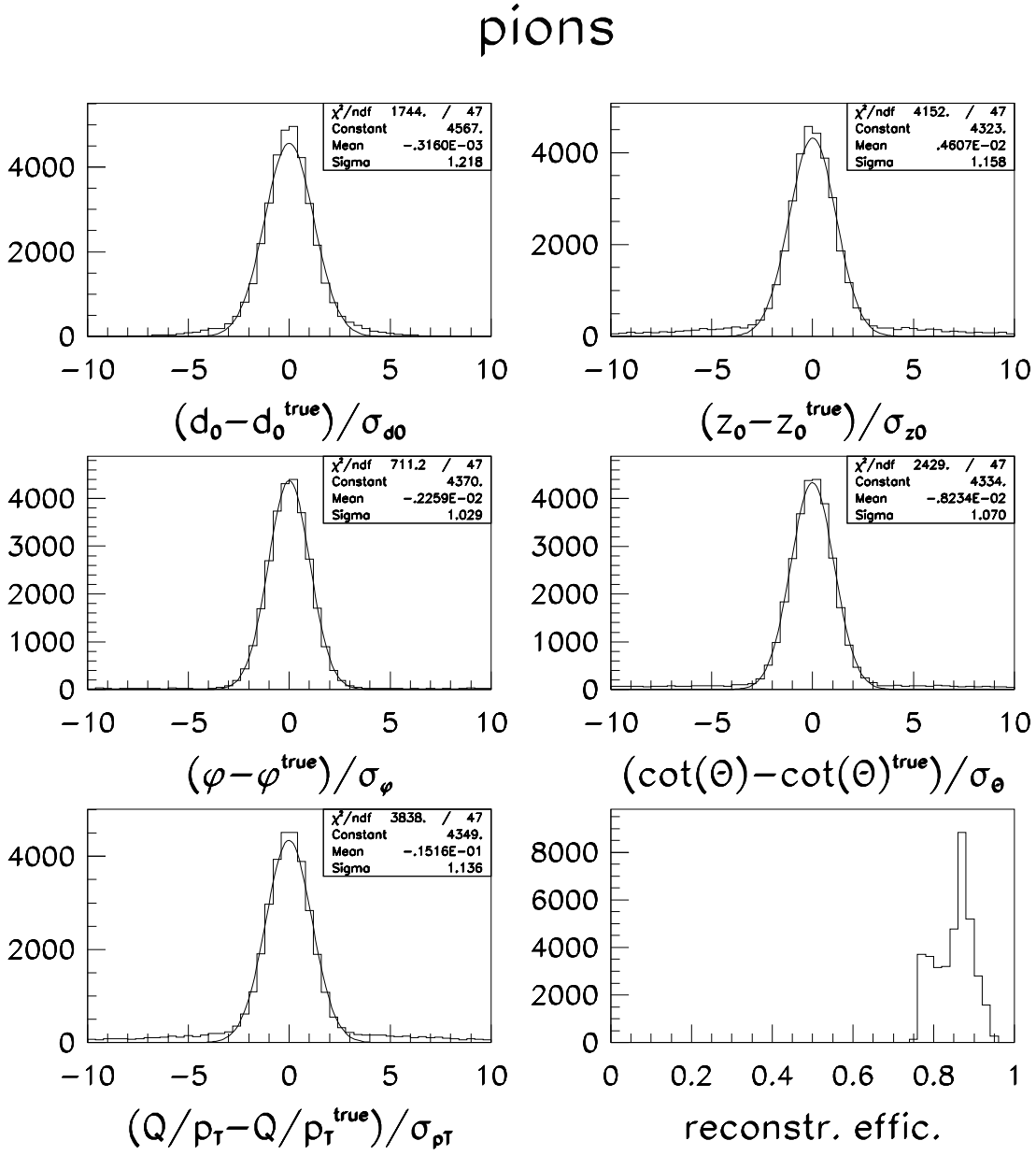

Figure 4-3 Normalised resolution for helix parameters and reconstruction track efficiency for pions. (WH, H $\rightarrow b\bar{b}$ sample was generated)

5 Outlook

This second version of a somewhat elaborate particle-level simulation program, which incorporates most of the ATLAS detector global performance parameters, can be used for many studies, where the details of the ATLAS detector performance (non-Gaussian tails, cracks, etc...) are not of crucial importance. Till now it has been used for many physics studies performed inside Physics Working Groups of ATLAS Collaboration. Hopefully in the present version this package inadequate for many studies foreseen with the fast simulation for the Overall Performance Physics TDR.

The ATLFAST can be used as "stand-alone" but is also implemented into the ATGEN package [6-29] with the aim to have a complete tool for physics studies at the particle level abnd into the Combined Ntuple framework (CBNT) [6-32]of ATLAS reconstruction packages.

6 Reference

6-1 E. Richter-Was, D. Froidevaux and L. Poggioli, ATLAS Internal Note, PHYS-No-079 (1996)

6-2 E. Richter-Was, D. Froidevaux, F. Gianotti, L. Poggioli, D. Cavalli and S. Resconi , ATLAS Internal Note, PHYS-No-074 (1996).

6-3 ATLAS presentation on LHCC SUSY workshop, CERN, October 1996.

6-4 M. Bosman, I.C. Park , M. Cobal, D. Costanzo, S. Lami, R. Paoletti, G. Azuelos, K. Strahl, ATLAS Internal Note, ATL-SOFT-98-038 (1998) ;

6-5 ATLAS Collaboration, Calorimeter Performance Technical Design Report, CERN/LHCC/97-1, 15 January 1997.

6-6 ATLAS Collaboration, Inner Detector Technical Design Report, CERN/LHCC/97-16, ATLAS TDR 4, 30 April 1997.

6-7 ATLAS Collaboration, ATLAS Trigger Performance Status Report, CERN/LHCC/98-15, 30 June 1998.

6-8 A. DellAcqua et al, ATLAS Internal Note PHYS-No-102 (30 July 1997).

6-9 D. Froidevaux, E. Richter-Was, ATLAS Internal Note, PHYS-No-043 (1994);

6-10 D. Cavalli and S. Resconi, ATLAS Internal Note PHYS-No-100 (1996)

6-11 P. Savard and G. Azuelos, ATLAS Internal Note, ATL-PHYS-98-128 (1998).

6-12 ATLAS Collaboration Muon Spectrometer Technical Design Report, CERN/LHCC/97-22, ATLAS TDR 10, 31 May 1997.

6-13 ATLAS Technical Proposal, CERN/LHCC/94-43, 15 December 1994.

6-14 D. Froidevaux and E. Richter-Was, *The $H \to \gamma\gamma$ channel in association with high E_T/E jets*, unpublished;

6-15 E. Richter-Was, D. Froidevaux, F. Gianotti, L. Poggioli, D. Cavalli and S. Resconi , ATLAS Internal Note, PHYS-No-048 (1995).
F. Gianotti and I. Vichou, ATLAS Internal Note PHYS-No-78 (1996).

6-16 D. Rousseau, ATLAS Internal Note , INDET-N0-198, Phys-N0-119 (1998)

6-17 L. Poggioli, ATLAS physics meeting, Trest, 1995.

6-18 O. Linossier and L. Poggioli, ATLAS Internal Note, PHYS-No-075 (1995) and PHYS-No-101 (1997).

6-19 C. Guyot, private communication, July 1997.

6-20 M.Virchaux and L.Chevalier, private communication, July 1997.

6-21 L. Poggioli, D. Froidevaux and C. Guyot, ATLAS Internal Note, Phys-No-076 (1995).

6-22 E. Ross private commun. and [6-6].

6-23 D. Cavalli and S. Resconi, ATLAS Internal Note , ATLAS Phys-No-118 (1998).

6-24 E.J.Buis, R. Dankers, S. Haywood, A. Reichold. ATLAS Internal Note, INDET-No-195, December 1997; E.J.Buis, R. Dankers, A. Reichold, S. Haywood, F.G. Tartarelli, and N. labanca, ATLAS Internal Note, ATL-INDET-98-215 (1998).

6-25 OPAL Collaboration, CERN preprint CERN-PPE/95-126.

6-26 See transparencies from ATLAS Physics Workshop on SUSY Particles, Stockholm 18-19 January 1996 (Sweden).

6-27 T. Sjostrand, “High-Energy-Physics Event Generation with PYTHIA 5.7 and JETSET 7.4”, CERN preprint CERN-TH.7111/93 and CERN-TH.7112/93.

6-28 G. Marchesini et al., Comput. Phys. Commun. **67** (1992) 465.

6-29 A. Amorim, “ATGEN-Monte Carlo interface using GENZ”, ATLAS Internal Note, SOFT-No-010 (1995).

6-30 F. E. Paige and S. D. Protopopescu, Manual ISAJET 7.13.

6-31 The demonstration deck was preapared and tested by S. Klyukhin, email: klyukhin@mx.ihep.su

6-32 D. Rousseau, Combined Ntuple from ATLAS reconstruction packages, http://atlasinfo.cern.ch/Atlas/GROUPS/PHYSICS/physics.html

A General comments about ATLFAST and ATLFAST-B

The simulation algorithm is run by a call to the routine ATLFAST.

The analysed events should be stored in COMMON /ATLFEVENT/.

```
      INTEGER N, K                                              Event content
       REAL P, V
       COMMON/ATLFEVENT/N,K(10000,5),P(10000,5),V(10000,5)
```

The conventions for the particle status, mother-daughter relations, particle codes etc. as in common block /LUJETS/ from PYTHIA generator should be assured by the user. Please, follow the manual [6-27]. Vertex position should be given in mm!.

The input/output logical identifiers should be defined in COMMON /ATLNOUT/

```
       INTEGER ATLNINP, ATLNOUT                                  Input/output
       COMMON/ATLNOUT/ ATLNINP, ATLNOUT
```

The package uses one input data file, which contains the parameters for event analysis and triggering.

A.1 Subroutine ATLFAST

This is the main routine called by the user to run the ATLFAST package. The following modes are implemented:

- MODE=-1 — initialising, which should be called before the first event is analysed;
- MODE= 0 — simulating, which should be called event by event;
- MODE= 1 — closing, which should be called after the last event has been analysed.
- also it is possible to invoke additional modes for special purposes:
- MODE= 2 — simulating event with a second set of values of the jet-cone reconstruction. In this case the algorithm is repeated and ATLFAST common blocks are overwritten;

This routine calls other routines: MAKIOU, MAKFMT, MAKINF, MAKINI, MAKDMP, MAKCLU, MAKELE, MAKMUO, MAKPHO, MAKJET, MAKBJE, MAKCJE, MAKTAU, MAKTRA, MAKMIS, MAKMSC, MAKTRG, MAKUSE.

A.2 Interface to event generators

The information on the simulated event is based on particle COMMON /ATLFEVENT/ with the conventions for particle codes and inheritance as in the PYTHIA [6-27] generator. The examples of using PYTHIA, HERWIG[6-28], and ISAJET [6-30] as generators for simulated events are prepared as well as an example of reading events from GENZ tape [6-26]. ATLFAST is also interfaced to the ATGEN package [6-29] for ATLAS event generation and to the Combined Ntuple (CBNT) [6-32] from ATLAS recosntruction packages.

A.3 Structure of the output from ATLFAST

The output of the algorithm consists of lists arranged in order of decreasing p_T, of selected isolated electrons COMMON /ISOELE/, isolated muons COMMON /ISOMUO/, non-isolated muons COMMON /NOISOMUO/, isolated photons COMMON /ISOPHO/, of reconstructed jets COMMON /JETALL/, and of the reconstructed p_T^{miss} COMMON /PTMISS/. Each event is passed through a primitive trigger routine and the logical output from this routine is contained in the COMMON /TRIGER/. For specific studies one can also use the COMMON /CLUSTER/, where all hadronic clusters are kept, and the COMMON /CELLS/, which contains all cell-energy depositions.

In addition, some standard histograms are also filled, to give more information about the analysed sample. These histograms monitor multiplicity of isolated leptons, photons and jet multiplicities, the average shifts in E, p_T, η and ϕ due to energy smearing, the mass distributions for lepton and jet pairs, etc. Another set of histograms keeps track of the differences between parton-level and particle-level analyses, by monitoring the kinematical variables of the original partons. These histograms should however be treated with some caution, since some of them are only correctly filled for certain physics processes, or certain option of the event generation.

SUBROUTINE ATLFNTUP (in file atlfastntup.f) can be used for ntuples storage.

A.4 User analysis with ATLFAST

The algorithm invokes the dummy routine SUBROUTINE MAKUSE where the user analysis can be implemented. This routine is called by the algorithm in the initialization, running and closing mode. In the running mode, it is called after each event is analysed by the algorithm.

A.5 User analysis with ATLFAST-B

This set of routines is meant to facilitate user analysis of events simulated with ATLFAST and also provides parametrization for jet recalibration and b-tagging and τ-tagging efficiencies. Event stored in CWNtuple (SUBROUTINE ATLFNTUP in atlfastntup.f file) can be processed through the chain of routines ATLFEVE, ATLFPHO, ATLFLEP, ATLFBJE, ATLFTAU, ATLFTRG (ATFPHO, ATLFLEP still dummy) in atlfast-b.f file to complete the simulation by ATLFAST of randomly applied efficiencies for tagging and identification. The output structure (incorporated in common blocks) is very similar to the ATLFAST one and provides the user with CRUDE (after ATLFAST) and DETECTED (after ATLFAST + ATLFAST-B) events. In SUBROUTINE ATLFASTB, in loops over already existing ntuple, the user should build sequence of calls to ATLFXXX routines specific to his analysis (e.g. there is no point to identify τ-jets if they are of no interest) and supply the ATLFUSE routine which provides crude and detected events.

A.6 Structure of the distributed version

ATLFAST is written in FORTRAN77, and its source code is splitted into several files and the input data are in one data file (for ATLFAST steering) and dedicated data files for muon resolution calculations, tracks parameter smearing and jetfider library. The distributed ver-

sion contains a set of UNIX subdirectories:

- **lib** - contains main source code of ATLFAST in files: **atlfast.f , atlfastmuo.f atlfastind.f atlfastmsc.f atlfastntup.f and subdirectories: lib/id_atlfast, lib/jet_atlfast and lib/mu_atlfast**
- **data** - contains the input parameters set-up by the user in one single file **atlfast.dat** and as well as subdirectories with data files for JetFinder Library and used by smearing procedures: **mu_dat, id_dat, jet_dat.**
- **demo-pythia57**, **demo-pythia61, demo-pythia6103-isasusy**- are a demonstration directories for running with the PYTHIA generator
- **demo-isajet** - is a demonstration directory for running with the ISAJET generator
- **demo-herwig** - is a demonstration directory for running with the HERWIG generator
- **demo-genz** - is a demonstration directory for running with events stored on GENZ format tapes.
- **demo-atlfast-b** - contains source code of **ATLFAST-B** in one single file **atlfast-b.f** and and example how to use it.

Directory **atlfast**

```
-rw-r-----   1 erichter zzmn      553287 Aut  7 14:57 NOTE-ATLFAST-2.0.ps
drwxr-x---   2 erichter zzmn        1024 Aut  7 13:40 data
drwxr-x---   2 erichter zzmn        1024 Aut  7 15:39 demo-atlfast-b
drwxr-x---   2 erichter zzmn        1024 Aut  7 15:39 demo-genz
drwxr-x---   3 erichter zzmn        1024 Aut  7 14:57 demo-isajet
drwxr-x---   3 erichter zzmn        1024 Aut  8 09:11 demo-herwig
drwxr-x---   3 erichter zzmn        1024 Aut  8 09:11 demo-pythia57
drwxr-x---   3 erichter zzmn        1024 Aut  8 09:11 demo-pythia61
drwxr-xr-x   6 erichter  zp        2048 Jul 29 16:10 demo-pythia6103-isasusy
drwxr-x---   2 erichter zzmn        1024 Aut  8 08:58 lib
-rw-r-----   1 erichter zzmn         192 Aut  6 17:33 makefile
```

Directory **atlfast/lib**

```
-rw-r-----   1 erichter zzmn      132569 Aut  8 08:58 atlfast.f
-rw-r-----   1 erichter zzmn      132569 Aut  8 08:58 atlfastind.f
-rw-r-----   1 erichter zzmn      132569 Aut  8 08:58 atlfastmsc.f
-rw-r-----   1 erichter zzmn      132569 Aut  8 08:58 atlfastmuo.f
-rw-r-----   1 erichter zzmn      132569 Aut  8 08:58 atlfastntup.f
drwxr-xr-x   6 erichter   zp        2048 Jul 31 06:18 id_atlfast
drwxr-xr-x   2 erichter   zp        2048 Jul 29 12:36 jet_atlfast
-rw-r--r--   1 erichter   zp      573948 Aug  4 15:43 libatlfast.a
drwxr-xr-x   2 erichter   zp        2048 Jul 29 12:33 mu_atlfast
-rw-r-----   1 erichter zzmn         383 Aut  8 09:51 makefile
```

Directory **atlfast/data**

```
-rw-r--r--   1 erichter   zp            6395 Mar  1 19:19 atlfast.dat
lrwxr-xr-x   1 erichter   zp              22 Mar  7 14:55 id_data
lrwxr-xr-x   1 erichter   zp              22 Mar  7 14:55 jetdata
lrwxr-xr-x   1 erichter   zp              22 Mar  7 14:55 mu_data
```

Each subdirectory is equipped with a **makefile**. The user can thus execute the commands **make** and **make run** issued from the **demo-...** subdirectories. The first command compiles the program and the latter executes with an example data file.

A.6.1 demo-pythia57

This directory contains a demonstration program **demo.f**. This program generates a sample of events using the PYTHIA generator and analyses them using ATLFAST. The input data are read from the file **atlfast.dat** in subdirectory **data** and the outputs of the program are written to the subdirectory **demo-pythia/prod** in the file **demo.out** and the stored histograms and ntuple in the file **demo.hbook** and ntuple in the file **atlfast.ntup**.

In this demonstration program, the generation of the following hard processes can be invoked by changing in the **demo.f** code the value of the parameter **KEYPRO**:
KEYPRO= 1 — $H \to \gamma\gamma$, m_H =100 GeV
KEYPRO= 2 — $Z \to e^+e^-$,
KEYPRO= 3 — $Z \to \mu^+\mu^-$,
KEYPRO= 4 — $H \to ZZ^* \to 4e$, m_H=130 GeV
KEYPRO= 5 — $H \to e^+e^-\mu^+\mu^-$, m_H =130 GeV
KEYPRO= 6 — $H \to \mu^+\mu^-\mu^+\mu^-$, m_H =130 GeV
KEYPRO= 7 — WH , $H \to b\bar{b}$, $W \to l\nu$, m_H =100 GeV
KEYPRO= 8 — WH, $H \to g\underline{g}$, m_H =100 GeV
KEYPRO= 9 — WH, $H \to u\underline{u}$, $W \to l\nu$, m_H =100 GeV
KEYPRO=10 — $b\bar{b}A$, $A \to \tau\tau$, m_A=300 GeV

The user can also easily select various options for the event generation by changing the parameter KEYHAD in the code of **demo.f**:
KEYHAD=0 — HP,
KEYHAD=1 — HP + ISR,
KEYHAD=2 — HP + ISR + FSR,
KEYHAD=3 — HP + ISR + FSR + HD (default),
KEYHAD=4 — HP + ISR + HD,
KEYHAD=5 — HP + FSR + HD,

Directory **atlfast/demo-pythia57**

```
-rw-r-----   1 erichter zzmn       13564 Aut   8 09:11 demo.f
-rw-r-----   1 erichter zzmn         746 Aut   1 11:06 makefile
drwxr-x---   2 erichter zzmn        1024 Aut   8 08:56 prod
```

Directory **atlfast/demo-pythia57/prod**

```
-rw-r--r--   1 erichter zzmn     5143360 Aut   7 15:43 atlfast.ntup
-r--r-----   1 erichter zzmn          75 Aut   7 15:43 core
-rw-r--r--   1 erichter zzmn      143360 Aut   7 15:43 data--> ../../data
-rw-r--r--   1 erichter zzmn      143360 Aut   7 15:43 demo.hbook
-rw-r--r--   1 erichter zzmn      221835 Aut   6 17:20 demo.out
-rw-r-----   1 erichter zzmn          64 Aut   6 17:20 go
```

A.6.2 demo-herwig

This directory contains a demonstration program for generation with HERWIG. The main program is **herwgen.f**. There is a **makefile** for building an executable. First the pointers to external libraries and datafiles on your favourite computer need to be defined in the makefile. The distribution should include:

-rw-r--r-- 1 jesper zp 2173 Nov 19 16:49 README.txt

-rwxr--r-- 1 jesper zp 45 Nov 19 12:19 go

-rw-r--r-- 1 jesper zp 7894 Nov 17 18:42 herwgen.f

-rw-r--r-- 1 jesper zp 127303 Nov 17 16:06 hwudat.f

-rw-r--r-- 1 jesper zp 1954 Nov 19 12:20 makefi le

-rw-r--r-- 1 jesper zp 338 Nov 19 11:09 test.datacard

To compile type **make** and to install type **make install**. To cleanup and remove all directories do make superclean if you need to reinstall. The directories created and their contents are (after you have executed the makefile).

./prod

drwxr-xr-x 2 jesper zp 2048 Nov 21 16:03 data

-rwxr--r-- 1 jesper zp 45 Nov 21 16:03 go

lrwxr-xr-x 1 jesper zp 15 Nov 21 16:03 herw.par -> ./test.datacard

-rwxr-xr-x 1 jesper zp 3121632 Nov 21 16:04 herwgen.x

-rw-r--r-- 1 jesper zp 338 Nov 21 16:03 test.datacard

./prod/data/atlfast.dat -- the ATLFAST data fi les copied from atlfast/data

Parameters are set in the test.datacard file that either needs to be linked or copied to herw.par which is the file that herwgen.x reads. After installation herw.par is linked to test.datacard. The following HERWIG parameters are read from the datacard file herw.par: IPROC, MAXEV, IPRINT, MAXPR, NRN(1), NRN(2), PTMIN, PTMAX, NSTRU. The colliding beams and their momenta are hardwired in herwgen.f. All other HERWIG parameters are set to their default value. Consult the HERWIG manual. All parameters can in principle be set in the datacard file, but then you need to include those parameters in **SUBROUTINE HERWCARD, which is using the FFREAD package**. (If you do so note that HERWIG real variables are defined to be double precision).

HERWIG stores the particles in HEPEVT format. It is converted with calls to the following routines:

HERW2LU -- converts HEPEVT to LUJET format (included in herwgen.f)

ATLPYTHIA57 -- converts LUJET to ATLFEVENT format (part of ATLFAST distribution, but is included in herwgen.f)

The output files of the sample job are written to the prod directory.

The file fort.88 is the Sudakov table generated by HERWIG (see manual).

To run:

Go to directory prod and:

herwgen.x > test.log& or use script **go**

--> the normal atlfast output is written to this directory

To remove atlfast output one can use: **make cleanprod**

A.6.3 demo-isajet

This directory contains a demonstration program for generation with ISAJET. The main program is isagene.f. There is a **makefile** for building an executable. First the pointers to external libraries and datafiles on your favourite computer need to be defined in the makefile. The distribution include:

```
-rw-r-----   1 jesper     zp          2127 Nov 19 22:19 README.txt
-rwxr--r--   1 jesper     zp            47 Nov 19 12:23 go
-rw-r--r--   1 jesper     zp          4837 Nov 20 09:20 isagene.f
-rw-r--r--   1 jesper     zp          2194 Nov 19 14:35 makefi le
-rw-r--r--   1 jesper     zp           169 Nov 20 08:57 test.datacard
```

To compile type **make** and to install type **make install**.

To cleanup and remove all directories do make superclean if you need

to reinstall. The directories created and their contents are

(after you have executed the make install):

/prod/

```
drwxr-xr-x   2 jesper     zp           2048 Nov 21 16:08 data
-rwxr--r--   1 jesper     zp             47 Nov 21 16:08 go
drwxr-xr-x   2 jesper     zp           2048 Nov 21 16:08 isadata
-rwxr-xr-x   1 jesper     zp       12007448 Nov 21 16:09 isagene.x
lrwxr-xr-x   1 jesper     zp             15 Nov 21 16:08 isajet.par -> ./test.datacard
-rw-r--r--   1 jesper     zp           169 Nov 21 16:08 test.datacard
```

/prod/data/atlfast.dat -- atlfast settings

You need change the LSP code to be 67

./prod/isadata/isadecay.dat -- the ISAJET decaytable

All parameters for ISAJET generation are read from the datacard file **isajet.par**. All parameters can be set in the datacard file. For the parameter descriptions consult the ISAJET manual. The LSP particle code need to be set in the atlfast.dat - **SPYTHIA uses particle code 66 for the LSP** and **ISAJET particle code 67**. Before generation copy or link your datacard file to **isajet.par**. After installation **isajet.par** is linked to **test.datacard**

The output files for the sample job will be written to the prod directory.

ISAJET stores the particles in its own event format. It is converted with calls to the following routines:

ISAHEP(1) -- converts from ISAJET to HEPEVT format (part of ISAJET distribution)

HEP2LU -- converts HEPEVT to LUJET format (included in isagene.f)

ATLPYTHIA57 -- converts LUJET to ATLFEVENT format (part of ATLFAST distribution, but is included in isagene.f)

The output files of the sample job are written to the prod directory.

To run:

Go to directory prod and:

herwgen.x > test.log& or use script go

--> the normal atlfast output is written to this directory

To remove atlfast output one can use: **make cleanprod**

A.6.4 demo-genz

This directory contains a demonstration program **demo.f**, which simulates events stored onto the tape in GENZ format. The event is read form the file ZEBRA.P (the modified version of routines `READJOB` and `GNZOPEN` by R. DeWolf are used), stored in the `COMMON /ATLFEVE/` and analysed by ATLFAST algorithm. The input data are read from the file **atlfast.dat** in subdirectory **data** and the outputs of the program are written to the subdirectory **demo-genz/prod** in a file **demo.out** and ntuple in a file **atlfast.ntup**.

Directory **atlfast/demo-genz**

```
lrwxr-xr-x   1 erichter zp           39 Aut  4 14:30 ZEBRA.P->.....
-rw-r--r--   1 erichter zp        13265 Aut  4 15:49 demo.f
-rw-r-----   1 erichter zp       268764 Aut  8 12:11 libgenz.a
-rw-r-----   1 erichter zp          831 Aut  4 15:58 makefile
drwxr-x---   2 erichter zp         2048 Aut  4 15:56 prod
```

The user should however check if the *`COMMON /ATLFEVENT/`* is correctly filled (correct status of particles and particle code) if the event stored on tape were generated by generator other then PYTHIA generator.

A.6.5 demo-atlfast-b

This directory contains the source code of ATLFAST-B in **atlfast-b.f** file, the histograms used for jets recalibration in **atlf_calibration.hbook**, and in **atlf_analiza.kumac** with example of analysis done with ATLFAST-B on ntuple **atlfast.ntup** with simulated WH , $H \rightarrow b\bar{b}$ events **.** The **atlf_histos.kumac** defines histograms and **atlf_nice.kumac** gives nice graphics. The **atlf_analiza.hbook** contains stored histograms of the results of analysis.

The main ingredients of **atlfast-b.f** are routines: **ATLFCAL**, **ATLFBJE, ATLFTAU** for jets energy calibration, b-tagging and τ-tagging simulations.

Directory **atlfast/demo-atlfast-b**

```
drwxr-xr-x   2 erichter  zp    2048 Aug  1 16:47 .
drwxr-x---  10 erichter  zp    2048 Jul 22 14:41 ..
-rw-r--r--   1 erichter  zp   16384 Jul 22 11:15 atlf_anal.hbook
-rw-r-----   1 erichter  zp   14265 Aug  1 16:47 atlf_analiza.f
-rw-r-----   1 erichter  zp     282 Jul 22 11:01 atlf_analiza.kumac
-rw-r--r--  1 erichter   zp   16384 Jul 18 16:41 atlf_calibration.hbook
-rw-r-----   1 erichter  zp     471 Jul 22 11:14 atlf_histos.kumac
-rw-r-----   1 erichter  zp     287 Jul 18 18:07 atlf_nice.kumac
-rw-r--r--   1 erichter   zp 4411392 Jul 18 16:27 atlfast.ntup
```

B Subroutines in the ATLFAST package

B.1 Subroutine MAKUSE

The dummy user routine for the event analysis.

B.2 Subroutine MAKIOU

This routine defines the input/output logical identifies for the ATLFAST package. It transfers them from `COMMON /ATLNOUT/` to `COMMON /MAKNOUT/`.

B.3 Subroutine MAKFMT

This routine defines nice and flexible formats for printing outputs. These formats are stored in the `COMMON /BX/` and `COMMON /DX/`.

B.4 Subroutine MAKINF

This routine prints out information about the package version.

B.5 Subroutine MAKDMP

This routine prints out the contents of output commons.

B.6 Subroutine MAKINI

This routine reads from the input data file the values of all parameters which can be set by the user and which are subsequently used for the event analysis. These parameters are sent to other routines via the arrays `LPAR (99)`, `YPAR(999)` and `TPAR(99,2)`. The lists of these parameters and of their default values are given in Table B-1 and Table B-2 .

Table B-1 List of parameters read by the SUBROUTINE MAKINI from atlfast.dat. Parameters for the event analysis. The default values are quoted in front of each parameter's name and defi nition.

------ Flags and switches ----------	
1	--- LPAR(1) ....Id for histograms
1	--- LPAR(2) ....Luminosity option low=1, high=2
1	--- LPAR(3) ....B-field on=1, off=0

Table B-1 List of parameters read by the SUBROUTINE MAKINI from atlfast.dat. Parameters for the event analysis. The default values are quoted in front of each parameter's name and defi nition.

1	--- LPAR(4) ....Smearing on=1, off=0
3	--- LPAR(5) ....Smear for muons: muon=1, track=2, combin=3
2	--- LPAR(15) ....Smear for muons: exact=1, approxim =2
66	--- LPAR(6) ....Code for SUSY LSP particle
10	--- LPAR(7) ....Number of events to be printed
0	--- LPAR(11) ....track/finding on=1, off=0
011	--- LPAR(12) ....ID config.: 011=B-layer, no vertex constr, uniform B-field
2	--- LPAR(112) ....ID reconstr cuts: 1=btag cuts; 2=btag+TR cuts
0	--- LPAR(13) ....JetFinder switch: 0= cone algorithm; 1=JetFinder algorithms
0	--- LPAR(14) ....muon trigger labelling: off=0, on=1
C------ Parameters for MAKCLU ----------	
10.000	--- YPAR(10) ....Minimum E_T for calo cluster
0.400	--- YPAR(11) ....Cone Delta R for barrel set 1
0.400	--- YPAR(16) ....Cone Delta R for forward set 1
0.700	--- YPAR(111) ....Cone Delta R for barrel set 2
0.700	--- YPAR(116) ....Cone Delta R for forward set 2
5.000	--- YPAR(12) ....Rapidity coverage for calorimeter
1.500	--- YPAR(13) ....Min E_T for cluster initiator
0.500	--- YPAR(14) ....Min p_T for B-field
0.000	--- YPAR(15) ....Min E_T for cell
3.000	--- YPAR(17) ....Barrel/fwd transition in eta in CALO
0.100	--- YPAR(18) ....Granularity in eta (barrel), 2x in fwd
0.100	--- YPAR(19) ....Granularity in phi (barrel), 2x in fwd
0	--- LPAR(10) ....Cells energy sharing in clusters on/off
C------ Parameters for MAKMUO ----------	
6.000	--- YPAR(20) ....Minimum muon momentum
2.500	--- YPAR(21) ....Maximum muon eta
0.400	--- YPAR(27) ....Min cone R separation from clusters for muon isol.
0.200	--- YPAR(28) ....Delta R cone for energy deposition
10.000	--- YPAR(29) ....Max energy deposition for isolation
C------ Parameters for MAKPHO ----------	
5.000	--- YPAR(30) ....Minimum photon momentum
2.500	--- YPAR(31) ....Maximum photon eta

Table B-1 List of parameters read by the SUBROUTINE MAKINI from atlfast.dat. Parameters for the event analysis. The default values are quoted in front of each parameter's name and defi nition.

0.100	--- YPAR(35) ....Delta R for photon matching to cluster
0.400	--- YPAR(37) ....Min cone R separation from clusters for photon isolation
0.200	--- YPAR(38) ....R_cone for energy deposition
10.000	--- YPAR(39) ....Max energy deposition for isolation
C------ Parameters for MAKELE ----------	
5.000	--- YPAR(40) ....Minimum electron momenta
2.500	--- YPAR(41) ....Maximum electron eta
0.100	--- YPAR(45) ....Delta R for electron matching to cluster
0.400	--- YPAR(47) ....Min cone R separation from clusters for electron isolation
0.200	--- YPAR(48) ....R_cone for energy deposition
10.000	--- YPAR(49) ....Max energy deposition for isolation
C------ Parameters for MAKJET ----------	
15.000	--- YPAR(51) ....Minimum E_T for jet
5.000	--- YPAR(52) ....Rapidity coverage for jets
C------ Parameters for MAKBJE ----------	
5.000	--- YPAR(60) ....Minimum b-quark p_T(after FSR) for b-jet matching
2.500	--- YPAR(61) ....Maximum b-quark eta for b-jet matching
0.200	--- YPAR(62) ....Delta R for b-jet matching to b-quark
C------ Parameters for MAKCJE ----------	
5.000	--- YPAR(70) ....Minimum c-quark p_T(after FSR) for c-jet matching
2.500	--- YPAR(71) ....Maximum c-quark eta for c-jet matching
0.200	--- YPAR(72) ....Delta R for c-jet matching to c-quark
C------ Parameters for MAKMIS ----------	
0.000	--- YPAR(80) ....Minimum E_T for unused cells
C------ parameters for MAKTAU ----------	
10.000	--- YPAR(90) ....minimum tau-had pt for tau-jet label
2.500	--- YPAR(91) ....maximum tau-eta for tau-jet label
0.300	--- YPAR(92) ....max R_tauj for tau-jet
0.900	--- YPAR(93) ....min ratio for tau-hadron/jet momentum
C------ parameters for MAKTRA ----------	
0.500	--- YPAR(100) ....minimum pt for track
2.500	--- YPAR(101) ....maximum eta for track

Table B-2 CList of parameters read by SUBROUTINE MAKINI from atlfast.dat. Parameters for the event trigger. The default values are quoted in front of each parameters name and defi nition.

```
C------ parameters for MAKTRG ----------
C ..... isolated electron/photon trigger.....
   2.5      ---  TPAR( 9,1) ... eta-coverage for electrons/photons
  20.0      ---  TPAR( 1,1) ... Minimum p_T for 1 electron  low lumi
  30.0      ---  TPAR( 1,2) ...                  high lumi
  40.0      ---  TPAR( 2,1) ... Minimum p_T for 1 photon    low lumi
  60.0      ---  TPAR( 2,2) ...                  high lumi
  15.0      ---  TPAR( 3,1) ... Minimum p_T for 2  ele/phot low lumi
  20.0      ---  TPAR( 3,2) ...                  high lumi
C ..... muon  trigger.....
   2.4      ---  TPAR(19,1) ... eta-coverage for muons
   6.0      ---  TPAR(11,1) ... Minimum p_T for 1 iso. muon   low lumi
  20.0      ---  TPAR(11,2) ...                   high lumi
  15.0      ---  TPAR(12,1) ... Minimum p_T for 1      muon   low lumi
  30.0      ---  TPAR(12,2) ...                   high lumi
   6.0      ---  TPAR(13,1) ... Minimum p_T for 2      muons  low lumi
  10.0      ---  TPAR(13,2) ...                   high lumi
   6.0      ---  TPAR(14,1) ... Minimum p_T for 2 iso. muons high lumi
C ..... electron/muon   trigger.....
   2.5      ---  TPAR(28,1) ... eta-coverage for electrons
   2.4      ---  TPAR(29,1) ... eta-coverage for muons
   5.0      ---  TPAR(21,1) ... Minimum p_T for iso. ele   low lumi
  15.0      ---  TPAR(21,2) ...                   high lumi
   6.0      ---  TPAR(22,1) ... Minimum p_T for muon       low lumi
   6.0      ---  TPAR(22,2) ...                   high lumi
C ..... jet   trigger.....
   3.2      ---  TPAR(39,1) ... eta-coverage for jets
 300.0      ---  TPAR(31,1) ... Minimum p_T for 1 jet   low lumi
 300.0      ---  TPAR(31,2) ...                   high lumi
  80.0      ---  TPAR(32,1) ... Minimum p_T for 3 jets  low lumi
 100.0      ---  TPAR(32,2) ...                   high lumi
  30.0      ---  TPAR(33,1) ... Minimum p_T for 4 jets  low lumi
  50.0      ---  TPAR(33,2) ...                  high lumi
```

B.7 Subroutine MAKCLU

This routine deposits the transverse energies of undecayed particles (i.e. those with `0 < K(I,1) < 10` in `COMMON /ATLFEVENT/`, (except neutrinos, muons and SUSY LSP) in $\eta \times \phi$ cells with default granularity: 0.1×0.1 for $|\eta|<3$ and 0.2×0.2 for $|\eta|>3$. This granularity can be modified, but with the limitation that the granularity of cells beyond the barrel/forward transition ($|\eta| = 3$) is twice as large as inside. The algorithm then groups these cells into clusters of cone ΔR stored in `COMMON /CLUSTER/` if sum of their transverse energy is above a threshold value. The ΔR is set separately for barrel and forward parts. The same event can be also analysed with two different sets for the ΔR.

The energies deposited in the cells are stored also in a cell map in `COMMON /CELLS/`. Cells used for cluster reconstruction are flagged (`KCELL(I,5)=0`). The effect of the solenoidal magnetic field is only parametrised as a shift in the ϕ-position of charged particles, which is calculated by the `FUNCTION FLDPHI`. Charged particles with p_T below the default threshold of 0.5 GeV are not stored if the magnetic field is on.

For `KEYJF=0` default cone algorithm is executed for clusters recosntruction. There is the possibility to activate the energy sharing of cells belonging to overlapping jets (default: no sharing). In that case the corresponding cell energy is shared according to the relative energies of each overlapping jet.

For `KEYJF=1` the JetFinder library is called and the algorithm requested in **jetfinder.dat** datacard is activated.

The common block filled by this routine is:

```
      INTEGER NCLU, KCLU                for reconstructed clusters
      REAL PCLU
      COMMON/CLUSTER/NCLU,KCLU(100,5),PCLU(100,5)
      INTEGER NCMIN, NCMAX, KCELL       for energy deposition in cells
      REAL PCELL
      COMMON /CELLS/ NCMIN, NCMAX, KCELL(4000,5),PCELL(4000,5),
```

where the vector `PCLU(I,5)=(`η^{init}, ϕ^{init}, η^{clu}, ϕ^{clu}, E_T^{clu}`)` contains the coordinates of reconstructed cluster `I` . The variables η^{init}, ϕ^{init} denote the position of the cluster initiator cell (geometrical centre of the cluster) and the variables η^{clu}, ϕ^{clu} denote the position of the E_T-weighted centre of the cluster (centre-of-gravity of the cluster). The variable E_T^{clu} is the transverse energy of the cluster. The variable `NCLU` is the number of reconstructed clusters. The array `KCLU` contains `KCLU(I,1)=I`, `KCLU(I,2)=98`, `KCLU(I,3)` the number of cells used for the reconstruction of cluster I, , `KCLU(I,4)` the number of particles assigned to cluster I, and `KCLU(I,5)=1`. If the cluster is accepted as a jet by routine `MAKJET`, then `KCLU(I,5)=0`. Clusters are arranged in order of decreasing E_T.

The vector `PCELL(I,5)=(`η^{cell}, ϕ^{cell}, η^{cell}, ϕ^{cell}, E_T^{cell}`)` contains the coordinates of all cells; `NCMIN` and `NCMAX` are the minimum and maximum indices of the cells and `KCELL(I,5)` is set to 0 for cells belonging to reconstructed clusters.

B.8 Subroutine MAKMUO

This routine searches for muons, by scanning through the COMMON /ATLFEVENT/. If a muon is found, its momentum is smeared using FUNCTION RESMUO. Three options for muon-momentum smearing are available: stand-alone Muon System (KEYMUO=1), Inner Detector alone (KEYMUO=2) and combined (KEYMUO=3). The parametrization for the momentum smearing is coded in FUNCTION RESMUO (exact and approximate parametrization are available for resolution from Muon System). Isolated muons are stored in COMMON /ISOMUO/. Non-isolated muons are stored in COMMON /NOISOMUO/. Muons outside the η-coverage or below the p_T-threshold are lost.

```
 INTEGER NMUO, KMUO KMUOTRG                for isolated muons
REAL PMUO
COMMON/ISOMUO/NMUO,KMUO(100,5),PMUO(100,5),KMUOTRG(100)
INTEGER NMUOX, KMUOX,KMUOXTRG             for non-isolated muons
REAL PMUOX
COMMON/NOISOMUO/NMUOX,KMUOX(100,5),PMUOX(100,5),KMUOXTRG(100)
```

where the vector PMUO(I,5)=(η^{μ}, ϕ^{μ}, η^{μ}, ϕ^{μ}, p_T^{μ}) contains the coordinates of the isolated muon I. The variable NMUO denotes the number of isolated muons and the array KMUO contains KMUO(I,1)=I, KMUO(I,2) the muon KF-code, KMUO(I,3) the position of the muon in COMMON /ATLFEVENT/, KMUO(I,4) the muon-mother KF-code and KMUO(I,5)=1. COMMON/NOISOMUO/ is analogous (respective variables are called NMUOX, KMUOX) for non-isolated muons. If a non-isolated muon is added to a calorimeter cluster in SUBROUTINE MAKJET, it is flagged by setting KMUOX(I,5)=0.

KMUOTRG and KMUOXTRG gives muon trigger flag which is filled in routine MAKTRG.

B.9 Subroutine MAKELE

This routine searches for isolated electrons, by scanning through the COMMON /ATLFEVENT/. If an electron is found, its energy is smeared using FUNCTION RESELE. Different energy-smearing for low luminosity (KEYLUM=1) and high luminosity (KEYLUM=2) can be invoked. Isolated electrons are stored in COMMON /ISOELE/ and the energy clusters associated with them are removed from COMMON /CLUSTER/. Non-isolated electrons remains clasified as cluster-type energy deposition.

```
INTEGER NELE, KELE                for isolated electrons
REAL PELE
COMMON/ISOELE/NELE,KELE(100,5),PELE(100,5),
```

where the vector PELE(I,5)=(η^{e}, ϕ^{e}, η^{e}, ϕ^{e}, p_T^{e}) contains the coordinates of isolated electron I. The variable NELE denotes the number of isolated electrons and the array KELE(I,1) contains KELE(I,1)=I, KELE(I,2) the electron KF-code, KELE(I,3) the position of the electron in COMMON /ATLFEVENT/, KELE(I,4) the electron-mother KF-code and KELE(I,5)=1.

B.10 Subroutine MAKPHO

This routine searches for isolated photons, by scanning through the COMMON /ATLFEVENT/. If a photon is found, its energy is smeared using FUNCTION RESPHO and its polar angle using FUNCTION RESTHE. Different energy smearings for low luminosity (KEYLUM=1) and high luminosity (KEYLUM=2) can be invoked. Isolated photons are stored in the COMMON /ISOPHO/ and the energy clusters associated with them are removed from the COMMON /CLUSTER/. Non-isolated photons are not considered further.

```
INTEGER NPHO, KPHO        for isolated electrons
REAL PPHO
COMMON/ISOPHO/NPHO,KPHO(100,5),PPHO(100,5),
```

where the vector PPHO(I,5)=(η^{γ}, ϕ^{γ}, η^{γ}, ϕ^{γ}, $p_T{}^{\gamma}$) denotes coordinates of the isolated photon I. The NPHO denotes number of isolated photons and the array KPHO contains KPHO(I,1)=I, KPHO(I,2) the photon KF code, KPHO(I,3) the position of the photon in COMMON /ATLFEVENT/, KPHO(I,4) the photon-mother KF-code and KPHO(I,5)=1.

B.11 Subroutine MAKJET

This routine scans through the clusters remaining in COMMON /CLUSTER/ after the isolated leptons and photons have been identified. The cluster energies are smeared using FUNCTION RESHAD. The non-isolated muons from the COMMON /NOISOMUO/, if falling into a given cluster cone, are included in the cluster energy and such muons are flagged with KMUOX(I,5)=0. The clusters passing the acceptance criteria for jets are copied to COMMON /JETALL/ and such clusters are flagged with KCLU(I,5)=0.

```
INTEGER NJET, KJET                    for jets
 REAL PJET
 COMMON/JETALL/NJET,KJET(100,5),PJET(100,5),
```

where the vector PJET(I,5)=(η^{init}, ϕ^{init}, η^{jet}, ϕ^{jet}, $p_T{}^{jet}$) contains the coordinates of jet I. The variable NJET denotes the number of the reconstructed jets, and the array KJET contains KJET(I,1)=I, KJET(I,2)=98, KJET(I,3) the number of cells used for reconstruction, KJET(I,4) the number of particles assigned to jet I, and KJET(I,5)=1.

B.12 Subroutine MAKBJE

This routine selects jets which can be associated to b-quarks, by scanning through COMMON /ATLFEVENT/. b-quarks (after FSR), which pass the acceptance cuts in p_T and η are identified. For each of these b-quarks, a reconstructed jet associated with it is searched for. These jets are labelled as b-jets if certain acceptance criteria are fulfilled, and KJET(I,2) is the KF-code of the b-quark which is matched to b-jet I.

B.13 Subroutine MAKCJE

This routine selects jets which can be associated to c-quarks, by scanning through the COMMON /ATLFEVENT/. c-quarks (after FSR), which pass the acceptance cuts in p_T and η are identified. For each of these c-quarks, a reconstructed jet associated with it is searched for. These jets are labelled as c-jets if certain acceptance criteria are fulfilled, and KJET(I,2) is the KF-code of the c-quark which is matched to c-jet I.

B.14 Subroutine MAKTAU

This routine select jets which can be associated with τ–leptons decaying hadronically. The COMMON /ATLFEVENT/ is scanned for hadronic decays of τ-leptons and if they pass the acceptance criteria and associated jet is found, such jet is labelled with KJET(I,2) equal to the KF code of the τ-leptons.

B.15 Subroutine MAKTRA

This routine reconstructs charged tracks and stores in the COMMON /TRACKS/ the information-about particle position in the /ATLFEVENT/ common block, the particle code, the tracks parameters (a_0, z_0, ϕ, cot(θ), q/p_T) before and after smearing and calculates 15 correlation coefficients.

```
      COMMON /TRACKS/ NTRA,KPTRA(500),KFTRA(500),
     +          KPM1TRA(500),KFM1TRA(500),KPM2TRA(500),KFM2TRA(500),
     +          KPM3TRA(500),KFM3TRA(500),KPM4TRA(500),KFM4TRA(500),
     +          KPM5TRA(500),KFM5TRA(500), KPM6TRA(500),KFM6TRA(500),
     +          D0TRACRU(500),Z0TRACRU(500), PHITRACRU(500),
     +          COTTRACRU(500),PTINVTRACRU(500),
     +          D0TRA(500), Z0TRA(500),PHITRA(500), COTTRA(500),PTINVTRA(500),
     +          CORR11(500), CORR21(500),CORR31(500), CORR41(500),CORR51(500),CORR22(500),
     +          CORR32(500),CORR42(500),CORR52(500), CORR33(500),CORR43(500),CORR53(500),
     +          CORR44(500),CORR54(500),CORR55(500), EFFTRA(200), ISTATRA(200)
```

NTRA denotes number of tracks, KPTRA - particle position in /ATLFEVENT/, KFTRA-particle code, KPM1TRA, KFM1TRA- position and code of the first mother, and respectively up to the 6-th mother, AOTRA, Z0TRA, PHITRA, COTTRA, PTINVTRA- values of tracks parameters (a_0, z_0, ϕ, cot(θ), q/p_T) after smearing, and with extension CRU before smearing. In case smearing is not activated (KEYSME=0) smeared and unsmeared values are identical. CORR11...CORR55 denote correlations coefficients. EFFTRA denotes the efficiency for track reconstruction which is calculated but not applied. ISTATRA denotes the status of the track: ISTATRA=0 for correctly reconstructed tracks, ISTATRA=1 if reconstruction fails. In this case the values for CORRxx and xxTRA are put to zero.

B.16 Subroutine MAKMIS

This routine calculates the total missing transverse energy in the event. The transverse energies of cells not used for cluster reconstruction are smeared using FUNCTION RESHAD. The total measured transverse momenta p_x^{obs} and p_y^{obs} are obtained by summing over jets, isolated

leptons and photons, non-isolated muons which were not added to clusters, unused clusters, unused cells. The total missing transverse momenta p_x^{miss}, p_y^{miss} are calculated as $p_x^{miss} = - p_x^{obs}$ and $p_y^{miss} = - p_y^{obs}$, and finally $E_T^{miss} = \sqrt{\langle p_x^{miss} \rangle^2 + \langle p_y^{miss} \rangle^2}$. The sum of the momenta of all particles escaping detection is also calculated in this routine.

```
REAL PXMISS,PYMISS,PXNU, PYNU                for missing energy
 COMMON /PTMISS/ PXMISS,PYMISS,PXNU,PYNU,
```

where `PXMISS,PYMISS` denote the reconstructed missing transverse energy components and `PXNU,PYNU` denote the sum of momenta components of particles escaping detection (muons outside detector acceptance, neutrinos and SUSY LSP).

B.17 Subroutine MAKMSC

This routine provides miscellaneous information about event itself: circularity, trust and oblateness:

REAL CIRCJET, CIRCEVE, THRUST, OBL
COMMON /MISCELAUS/CIRCEVE, THRUST, OBL

Where `CIRCEVE` denotes the circularity calculated respectively from jets and from cells. `THRUST` and `OBL` represent respectively the thrust axis and the oblateness of the event.

B.18 Subroutine MAKTRG

This routine apply muon trigger efficiency to isolate and nonisolated muons. The flag `KTRGMUO=0(KEYTRGMUOX=0)` in common blocks `/ISOMUO/` and `/NOISOMUO/` is given for not triggered muons while this flag is put to 1 for triggered with low p_T-threshold and put to 2 for triggered muons with high p_T-threshold (as parametrised in [6-8]). Please note, that first high-p_T threshold is checked and only if it is failed the low-p_T threshold is checked.

Further the primitive trigger routine provides nine types of trigger selection:

- one isolated electron `TRGEM1`
- one isolated photon `TRGPH1`
- two isolated electrons/photons `TRGEM2`
- one muon `TRGMU1`
- two muons `TRGMU2`
- electron-muon pairs `TRGMUE`
- one jet `TRGJT1`
- three jets `TRGJT3`
- four jets `TRGJT4`

```
      LOGICAL TRGEM1, TRGPH1, TRGPH2
      LOGICAL TRGMU1, TRGMU2
      LOGICAL TRGEMU                                        for trigger
      LOGICAL TRGJT1, TRGJT3, TRGJT4
      LOGICAL TRGALL
      COMMON /TRIGER/ TRGALL,TRGEM1,TRGPH1,TRGEM2, TRGMI1, TRGMU1
     #                TRGMI2,TRGMU2,TRGEMU,TRGJT1,TRGJT3,TRGJT4
```

where the logical values for `TRGEM1`, `TRGPH1`, `TRGEM2`, `TRGMU1`, `TRGMU2`, `TRGEMU`, `TRGJT1`, `TRGJT3`, `TRGJT4` can be `true/false` depending on whether the event passed the trigger selection criteria. If any of above listed logical variables is true then `TRGALL=true`. The default trigger selection criteria are given in Table B-3 and the efficiency for muon trigger (function `TRIGMUO`) is included.

Table B-3 Trigger criteria used in SUBROUTINE MAKTRG

Name	Type	High lumi	Low lumi
TRGEM1	Isolated electrons and photon $\|\eta\| < 2.5$	One isol. electron with $p_T > 30$ GeV	One isol. electron with $p_T > 20$ GeV
TRGPH1		One isol. photon with $p_T > 60$ GeV	One isol. photon with $p_T > 40$ GeV
TRGEM2		Two isol. /electrons/photons with $p_T > 20$ GeV	Two isol. electrons/photons with $p_T > 15$ GeV
TRGMU1	muons $\|\eta\| < 2.4$	One isolated muon with $p_T > 20$ GeV	One muon with $p_T > 20$ GeV
TRGMU2		Two muons with $p_T > 10$ GeV	Two muons with $p_T > 6$ GeV
TRGMEU	electron-muon pair $\|\eta^e\| < 2.5$ and $\|\eta^\mu\| < 2.4$	One isolated electron with $p_T > 15$GeV and One isolated muon with $p_T > 10$ GeV	One isolated electron with $p_T > 15$ GeV and One isolated muon with p > 6 GeV
TRGJT1	Jets $\|\eta\| < 3.2$	One jet with $p_T > 290$ GeV	One jet with $p_T > 180$ GeV
TRGJT3		Three jets with $p_T > 130$ GeV	Three jets with $p_T > 75$ GeV
TRGJT4		Four jets with $p_T > 90$ GeV	Four jets with $p_T > 55$ GeV

B.19 Subroutine ATLFNTUP

ATLFAST package (file **atlfastntup.f**) provides routine for ntuple storage which can facility usage of the ATLFAST-B routines. The provided a CWN format takes e.g. ~0.66 MB for 1000 events $H \rightarrow \mu^+\mu^-\mu^+\mu^-$ (with `/PTRACKS/` and `/BPHYSICS/` empty, means executed with KEYTRA=0), or almost 1.2 MB for 1000 events WH , $H \rightarrow b\bar{b}$ with stored information from `/PTRACKS/` and `/BPHYSICS/.`

Not full information contained in common blocks `/ISOPHO/, /ISOMUO/, /JETALL/` etc. is stored into ntuple and it is up to the user to modify format of CWNtuple if more information is needed for his analysis.

C Parametrization for the energy/momenta resolution, B-field effect and muon trigger efficiency

When available, the most detailed parametrization of the detector response has been used. Sometimes a cruder parametrization has been adapted to reproduce full simulation results. The expressions used here are straightforward to update, and will evolve with the better understanding and defining of the various parts of the detector.

C.1 Subroutine RESMUO

The parametrization for the muon momentum resolution derived from [6-19]-[6-24] is used. Three options for these parametrization are possible:

- The stand-alone Muon System momentum resolution σ_μ is parametrised as a function of the p_T the azimuth ϕ and pseudorapidity $|\eta|$, taking into account the effect of the toroidal magnetic field. Two options are available: approximation [6-19] (KEYFUN=1) (default) and [6-20] fast calculation which make use of the field map and the layout data base (KEYFUN =2) . Both of them correspond to the spectrometer layout as in the [6-8] and give similar mass resolutions e.g.. for $H \rightarrow \mu^+\mu^-\mu^+\mu^-$.
- $$p^{\mu}_{smeared} = \frac{p^{\mu}_{true}}{(1+\sigma)}$$
- The Inner Detector resolution is parametrised as described in [6-21] .
- The combined measurement of the muon 4-momenta are evaluated combining with the weighted technique the expected resolution from Inner Detector stand-alone and muon-system stand-alone.

C.2 Function RESPHO

The parametrization of the photon energy resolution is taken from the LARG group. The parametrization is given for low and high luminosity performance, in the second case the effect from pile-up is included also. These formulae are a good approximation but not fully correct, specially when treating independently the electronic noise and pile-up contributions.

$$\frac{\delta E_\gamma}{E_\gamma} = \frac{0.10}{\sqrt{E_\gamma}} \oplus \frac{0.245}{E^T_\gamma} \oplus 0.007$$

$$\frac{\delta E_\gamma}{E_\gamma} = \frac{0.10}{\sqrt{E_\gamma}} \oplus \frac{\sigma_{electronic}}{E_\gamma^T} \oplus \frac{\sigma_{pile-up}}{E_\gamma^T} \oplus 0.007$$

The upper formula is for low luminosity and the bottom formula for high luminosity operation of the detector. The pile-up coefficient $\sigma_{pile\text{-}up}$ and the coefficient for electronic noise $\sigma_{electronic}$ are parametrised as in the ATLAS Technical Proposal (TP).

C.3 Function RESTHE

The photon position Θ is smeared according to the Gaussian resolution function depending on $|\eta|$ position:

$$\sigma(\Theta_\gamma) = \frac{0.065}{\sqrt{E_\gamma}} \quad \text{for} \quad |\eta| < 0.8$$

$$\sigma(\Theta_\gamma) = \frac{0.050}{\sqrt{E_\gamma}} \quad \text{for} \quad 0.8 < |\eta| < 1.4$$

$$\sigma(\Theta_\gamma) = \frac{0.40}{\sqrt{E_\gamma}} \quad \text{for} \quad 1.4 < |\eta| < 2.5$$

C.4 Function RESELE

The parametrization of electron energy resolution is taken from LARG group. It is an extrapolation of the full simulation results to reproduce properly the mass spectra resolution. The low and high luminosity cases are treated separately, in the latest case the effect from pile-up is included also. This formula are a good approximation but not fully correct, specially when treat-

ing independently the electronic noise and pile-up contributions. For the electrons the Θ angle is well measured using the Inner Detector information.

$$\frac{\delta E_e}{E_e} = \frac{0.12}{\sqrt{E_e}} \oplus \frac{0.245}{E_e^T} \oplus 0.007$$

$$\frac{\delta E_e}{E_e} = \frac{0.12}{\sqrt{E_e}} \oplus \frac{\sigma_{lectronic}}{E_\gamma^T} \oplus \frac{\sigma_{pile-up}}{E_e^T} \oplus 0.007$$

The upper formula is for low lumi and the bottom formula for high lumi operation of the detec tor.The pile-up coefficient $\sigma_{pile\text{-}up}$ and coefficient for electronic noise $\sigma_{electronic}$ are parametrised as in the TP.

C.5 Function RESHAD

The formula used for the energy smearing for hadronic jets and cells is given below:

• for $|\eta| < 3$ and $\Delta\eta \times \Delta\phi = 0.1 \times 0.1$ cells

$$\frac{\delta E}{E} = \frac{0.50}{\sqrt{E}} \oplus 0.03$$

• for $|\eta| > 3$ and $\Delta\eta \times \Delta\phi = 0.2 \times 0.2$ cells

$$\frac{\delta E}{E} = \frac{1.0}{\sqrt{E}} \oplus 0.07$$

For high luminosity case additional term of is added in quadrature, interpolated according to used core for reconstruction between values of $\sigma_{pile\text{-}up}$= 7.5 GeVE_T for $\Delta R_{cone} = 0.4$, $\sigma_{pile\text{-}up}$ = 12 GeV ET for $\Delta R_{cone} = 0.5$ and $\sigma_{pile\text{-}up}$ = 18 GeV E_T for $\Delta R_{cone} = 0.7$. For cells which were not used for clusters reconstruction but were hit the expected resolution for hadronic cells of 0.4 GeV E_T is used only.

C.6 Function FFLDPHI

The effect of the field parametrised as a shift in the ϕ position of the particle is calculated ac-

cording to the following formula:

$$|\delta\phi|(\text{radians}) = (-150)\frac{0.006}{2p_T(\text{GeV})} \qquad \text{for} \qquad |\eta| < 1.4$$

$$|\delta\phi|(\text{radians}) = (-350)\tan\Theta\frac{0.006}{2p_T(\text{GeV})} \qquad \text{for} \qquad |\eta| > 1.4$$

The sign of the $\delta\phi$ is the same as the sign of the particle charge.

C.7 Function TRIGMUO

This function parametrises efficiency for muon triggering for low and high p_T thresholds in both barrel and endcap regions using the data points from [6-8]. Cubic Spline method is used for parametrization of the efficiencies between each data point pair (Figure 6-1). The function input is the $|\eta|$ and p_T of the muon and output is the trigger value (trigger=1 for low p_T trigger, 2 for highp_T trigger, 0 for no trigger) which is calculated by comparing the corresponding parametrised efficiency with a uniformly generated random number.

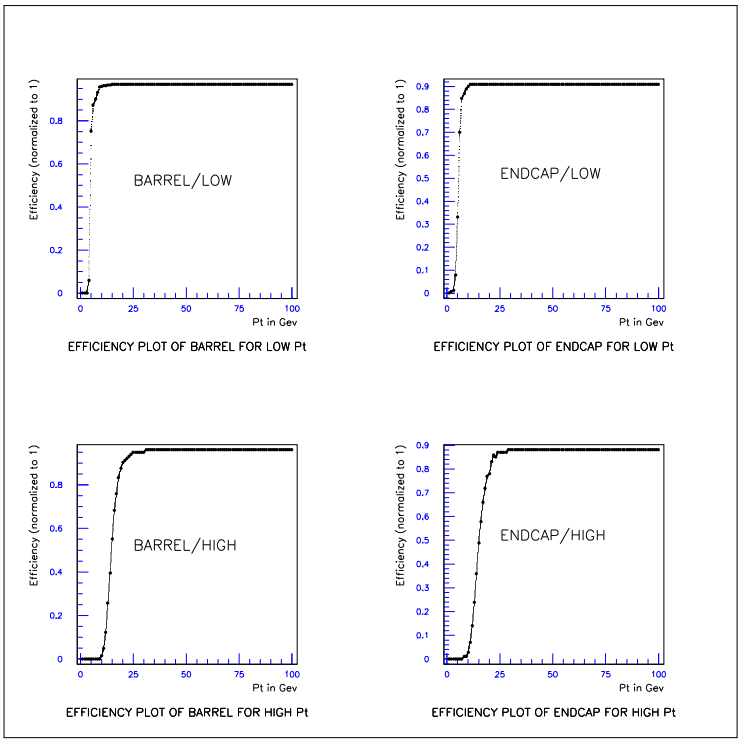

Figure 6-1 Parametrised muon trigger effi ciency and data points [6-8]. Courtesy S. Cetin.

D Subroutines in ATLFAST-B package

The ATLFAST-B package facilitaties the analysis of ntuples produced by ATLFAST. It provides parametrization of efficiencies for b- and τ- tagging of b-, c- and τ- labelled jets.

D.1 Subroutine ATLFEVE

This subroutine read the current event from ntuple and organizes into few common blocks:
COMMON/INFO/ISUB
COMMON/PTMISS/ PXMISS, PYMISS
COMMON/LEPTON/ NLEP, KLEP(12),PLEP(12,4)
COMMON/PHOTON/ NPHO, KPHO(12),PPHO(12,4)
COMMON/JET/ NJET, KJET(20),PJET(20,4)
COMMON/PARTON/ NPAR, KPAR(40),PPAR(40,4)

COMMON/LEPTON_CRU/ NLEPCRU,KLEPCRU(12),PLEPCRU(12,4)
COMMON/PHOTON_CRU/ NPHOCRU,KPHOCRU(12),PPHOCRU(12,4)
COMMON/JET_CRU/ NJETCRU,KJETCRU(20),PJETCRU(20,4)

Variables with extension `CRU` will be kept untouched, while this without extension will be overwritten after energy calibration, random b-tagging and τ-tagging is applied.

D.2 Subroutine ATLFCAL

Energy calibration factor is applied to four-momenta of each jet in `COMMON /JETS/`. The calibration factor is read from histogram id=`IDHISTJJ, IDHISTBB` (arguments of the subroutine) and jets four-momenta are overwritten. b-tagged jets are recalibrated with Kb-jet factor stored in histo `IDHISTBB` and non tagged jets are recalibrated with K_{jet} factor stored in histo `IDHISTJJ`. Prepared parametrisation assumes that above p_T^{jet}=100 GeV the calibration factor is constant and on the level of 1.2 . It may not be applicable to all studies, so one is advised to produce individual calibration histogram for studied sample.

input: parameter `IDHISTJJ, IDHISTBB`

D.3 Subroutine ATLFPHO

Still empty, supposed to deal with efficiencies for photon/jet and electron/jet identification and charge identification.

D.4 Subroutine ATLFLEP

Still empty, supposed to deal with efficiencies for electron/jet identification and charge identification.

D.5 Subroutine ATLFBJE

This subroutine applies random b-tagging on jets from `COMMON /JET/.` One can choose one out of four sets of provided tagging/mistagging parametrisations (`NSET=1,..4`) consistent with the full simulation results and consistent with algorithm for jet labelling with ATLFAST (see Table 3-9 and Table 3-10). They represent the expected performance for vertexing alone and low luminosity operation. The b-tagging procedure overwrites `KJET` flag setting `KJET=5` for all b-tagged jets and `KJET=98` for non-b-tagged. (Note, that there should be no jets with `KJET=4` afterwards). The τ–labelled and non-b-tagged jets stay labelled with `KJET=15`. The parametrised efficiencies are p_T dependent so it is applied for the would-be recalibrated p_T of a given jet.

input: parameter NSET, IDHISTBB

D.6 Subroutine ATLFTAU

This subroutine applies random τ-tagging/mistagging efficiencies. For required efficiency for τ-tagging (`EPSITAU`) respective mistagging efficiency is calculated. The τ-tagging procedure overwrites `KJET` flag setting `KJET=15` for τ-tagged jets (τ-labelled but not-tagged jets receive flag `KJET=98`), and leaves unchanged `KJET` flag otherwise.

input: parameter `EPSITAU`

D.7 Subroutine ATLFVETO

This subroutine apply random τ-veto efficiencies. For `IND=1` tau-background fixed to 5%, for `IND=2` jet-efficiency fixed at 90%. The τ-veto procedure overwrites `KJET` flag setting `KJET=15` for τ-tagged jets (τ-labelled but not-tagged jets receive flag `KJET=98`), and leaves unchanged `KJET` flag otherwise.

input: parameter `IND`

D.8 Subroutine ATLFTRG

Parametrization for muon trigger is randomly applied on isolated and non-isolated muon (in fact the same procedure was already performed in `MAKTRG`, so if you use this information don't apply it second time). Triggered muons got the flag `MUOTRG=2` (for high p_T threshold), `MUOTRG=1` (for low p_T threshold) and `MUOTRG=0` if both triggers have failed.

D.9 Subroutine ATLFUSE

This subroutine provides common blocks with **crude** and **detected** photons, leptons, jets and shows example of the $m_{b\bar{b}}$ mass reconstruction for WH , H→ $b\bar{b}$ analysis.

E Output from ATLFAST demontration deck

file demo-pythia/prod/demo.out

```
 ************************************************************************
 ************************************************************************
  *                                                                      *
 *                    *************************                         *
 *                      ATLFAST, version:2.20                            *
 *                      Released at: 10/11/98                           *
 *                    *************************                         *
 *                                                                      *
 *                Analyses event on particle level                      *
 *                                                                      *
 *                        Simulation package by:                        *
 *          E. Richter-Was, D. Froidevaux, L. Poggioli                  *
 *                                                                      *
 *  Contributed code:                                                   *
  *  # L. Chevalier, M. Virchaux, C. Guyot -->                          *
 *           muon pT  resolution (in ATLFAST)                           *
 *  # E. Arik, S. Cetin and A. Mailov     -->                          *
 *           muon trigger efficiency (in ATLFAST and ATLFAST-B)         *
 *  # G. F. Tartarelli,                   -->                          *
 *           helix parameters reconstruction (in ATLFAST)               *
 *  # A. Reichold, R. Dankers, E.J.Buis  -->                           *
 *           helix parameters resolution for muons (in ATLFAST)         *
 *  # G. F. Tartarelli, N. Labanca       -->                          *
 *           helix parameters  resolution for pions (in ATLFAST)        *
 *  # D. Cavalli and S. Resconi          -->                          *
 *           tau-tagging efficiency (in ATLFAST-B)                      *
 *  # E. Ross                            -->                          *
 *           b-tagging efficiency (in ATLFAST-B)                        *
 *  # I.C. Park                           -->                         *
 *           JetFinder library (in ATLFAST)                             *
 *  # S. Klyukhin, J. Soderqvist         -->                          *
 *           interface to HERWIG and ISAJET (in ATLFAST)                *
 *  # J. Soderqvist, M. Pearce            -->                         *
 *           trust,oblateness,circularity calc.(in ATLFAST)             *
 *  # M. Stravrianakou, I. Efthymiopoulos              -->              *
 *           ntuples format (in ATLFAST)                                *
*  # D. Rousseau for implementation into standarised ntuple             '
  ************************************************************************
   ***********************************************************************
 *               *********************************                      *
 *               *     ****************          *                      *
 *               *     ***  MAKCLU   ***          *                      *
 *               *     ****************          *                      *
 *               *********************************                      *
  *              clustering option used ....                              *
 *                0                cone algorithm            KEYJF      X1 *
 *                 clusters definition ....                               *
 *         10.00000                 E_T_min cluster           ETCLU      X1 *
 *           .00000                 E_T_min cell thresh       ETTHR      X1 *
 *          1.50000                 E_T_min cell initia       ETINI      X1 *
 *           .40000                 R cone                    RCONE      X1 *
 *          5.00000                 eta coverage clust        ETACLU     X1 *
 *          3.00000                 eta transit in CALO       CALOTH     X1 *
 *           .10000                 gran in eta (barrel)      DBETA      X1 *
 *           .10000                 gran in phi (barrel)      DBPHI      X1 *
```

```
*                B field apply ....                                      *
*               1                          on/off           KEYFLD     X1 *
*           .50000               p_T min for shift         PTMIN      X1 *
*                cells energy sharing ....                               *
*               0                          on/off           KEYSHR     X1 *
*************************************************************************
*************************************************************************
*               *********************************                       *
*               *     *****************         *                       *
*               *     ***   MAKMUO   ***         *                       *
*               *     *****************         *                       *
*               *********************************                       *
*                clusters definition ....                                *
*         10.00000               E_T_clust                ETCLU       X1 *
*           .40000               R cone                   RCONE       X1 *
*                muon isolation ....                                     *
*          6.00000               min. muon p_T            PTMUMIN     X1 *
*          2.50000               max. muon eta            ETAMAX      X1 *
*           .40000               min R_lj for isolat.     RISOLJ      X1 *
*           .20000               R for energy deposit     RDEP        X1 *
*         10.00000               max E_dep for isolat     EDMAX       X1 *
*               1                smearing on/off          KEYSME      X1 *
*               3                option for muon smea     KEYMUO      X1 *
*               2                option for muon smea     KEYFUN      X1 *
*              11                detec. config.           KEYIDC      X1 *
*************************************************************************
*************************************************************************
*               *********************************                       *
*               *     *****************         *                       *
*               *     ***   MAKELE    ***         *                       *
*               *     *****************         *                       *
*               *********************************                       *
*                clusters definition ....                                *
*         10.00000               E_T_clust                ETCLU       X1 *
*           .40000               R cone                   RCONE       X1 *
*                electron isolation ....                                 *
*          5.00000               min. lepton p_T          PTLMIN      X1 *
*          2.50000               max. lepton eta          ETAMAX      X1 *
*           .10000               max R_ej for ele-clu     RJE         X1 *
*           .40000               min R_lj for isolat.     RISOLJ      X1 *
*           .20000               R for energy deposit     RDEP        X1 *
*         10.00000               max E_dep for isolat     EDMAX       X1 *
*               1                smearing on/off          KEYSME      X1 *
*               1                low/high lumi            KEYLUM      X1 *
*************************************************************************
*************************************************************************
*               *********************************                       *
*               *     *****************         *                       *
*               *     ***   MAKPHO    ***         *                       *
*               *     *****************         *                       *
*               *********************************                       *
*                clusters definition ....                                *
*         10.00000               E_T_clu [GeV]            ETCLU       X1 *
*           .40000               R cone                   RCONE       X1 *
*                photon  isolation ....                                  *
*          5.00000               min. photon p_T          PTLMIN      X1 *
*          2.50000               max. photon eta          ETAMAX      X1 *
*           .10000               max R_gam-clust          RJE         X1 *
*           .40000               min R_isol               RISOLJ      X1 *
*           .20000               R for energy deposit     RDEP        X1 *
```

```
*         10.00000                max E_dep for isolat     EDMAX       X1 *
*                1                smearing on/off          KEYSME      X1 *
*                1                low/high lumi            KEYLUM      X1 *
*************************************************************************
*************************************************************************
*               **********************************                      *
*               *     *****************          *                      *
*               *     ***  MAKJET   ***          *                      *
*               *     *****************          *                      *
*               **********************************                      *
*                 clusters definition ....                                *
*            .40000               R cone                    RCONE      X1 *
*                 jets definition ....                                    *
*         15.00000                E_T_jets [GeV]            ETJET      X1 *
*          5.00000                eta coverage jets         ETAJET     X1 *
*************************************************************************
*************************************************************************
*               **********************************                      *
*               *     *****************          *                      *
*               *     ***   MAKBJE   ***         *                      *
*               *     *****************          *                      *
*               **********************************                      *
*                 jets definition ....                                    *
*         15.00000                E_T_jets [GeV]            ETJET      X1 *
*               b-jets..... ....                                          *
*          5.00000                min b-quark p_T           PTBMIN     X1 *
*          2.50000                max b-quark eta           ETBMAX     X1 *
*           .20000                max R_bj for b-jet        RJB        X1 *
*************************************************************************
*************************************************************************
*               **********************************                      *
*               *     *****************          *                      *
*               *     ***   MAKCJE   ***         *                      *
*               *     *****************          *                      *
*               **********************************                      *
*                 jets definition ....                                    *
*         15.00000                E_T_jets [GeV]            ETJET      X1 *
*               c-jets..... ....                                          *
*          5.00000                min c-quark p_T           PTCMIN     X1 *
*          2.50000                max c-quark eta           ETCMAX     X1 *
*           .20000                max R_cj for c-jet        RJC        X1 *
*************************************************************************
 ************************************************************************
*               **********************************                      *
*               *     *****************          *                      *
*               *     ***   MAKTAU   ***         *                      *
*               *     *****************          *                      *
*               **********************************                      *
*                 jets definition ....                                    *
*         15.00000                E_T_jets [GeV]            ETJET      X1 *
*             tau-jets..... ....                                          *
*         10.00000                min tau-had p_T           PTTAU      X1 *
*          2.50000                max tau-had eta           ETATAU     X1 *
*           .30000                max R_tauj for tau-j      RJTAU      X1 *
*           .90000                tau-had frac. of jet      PTFRAC     X1 *
 ************************************************************************
************************************************************************
*               **********************************                      *
*               *     *****************          *                      *
*               *     ***   MAKMIS   ***         *                      *
```

```
*               *     *****************         *                        *
*               ********************************                         *
*                    muon coverage     ....                               *
*          6.00000               min. muon p_T           PTMUMIN      X1 *
*          2.50000               max. muon eta            ETAMAX      X1 *
*                    unused cells     ....                                *
*                1                 smearing on/off          KEYSME      X1 *
*          0.00000                 cells threshold           ETCELL     X1 *
*                    SUSY particles     ....                              *
*               66                 KF code for LSP         KFLSP        X1 *
*********************************************************************
*********************************************************************
*********************************************************************
*               *********************************                        *
*               *     *****************         *                        *
*               *     ***   MAKTRA   ***         *                        *
*               *     *****************         *                        *
*               *********************************                        *
*                1                  track rec. on/off       KEYTRA      X1 *
*                1                  smearing on/off         KEYSME      X1 *
*               11                  detec. config.          KEYIDC      X1 *
*                2                  reconstr. cuts          KEYEFF      X1 *
*                     tracks definition ....                                *
*           .50000                 E_T_min track             ETTRA      X1 *
*          2.50000                 eta coverage track        ETATRA     X1 *
*********************************************************************
*********************************************************************
*********************************************************************
*               *********************************                        *
*               *     *****************         *                        *
*               *     ***   MAKMSC   ***         *                        *
*               *     *****************         *                        *
*               *********************************                        *
*********************************************************************
*********************************************************************
*               *********************************                        *
*               *     *****************         *                        *
*               *     ***   MAKTRG   ***         *                        *
*               *     *****************         *                        *
*               *********************************                        *
*               trigger electrons/photons                                 *
*           2.50000               eta coverage              ETAELE      X1 *
*          20.00000               pT for 1 electron         PTELE       X1 *
*          40.00000               pT for 1 photon           PTPHO       X1 *
*          15.00000               pT for 2 ele/pho          PTEM2       X1 *
*                 trigger muons                                            *
*           2.40000               eta coverage              ETAMUO      X1 *
*          20.00000               pT for 1     muon         PTMU1       X1 *
*           6.00000               pT for 2     muon         PTMU2       X1 *
*                 trigger electron/muons                                   *
*           2.50000               eta coverage electro      ETAEL1      X1 *
*           2.40000               eta coverage muon         ETAMU1      X1 *
*          15.00000               pT for electron           PTEMUE      X1 *
*           6.00000               pT for muon               PTEMUM      X1 *
*                 trigger jets                                             *
*           3.20000               eta coverage jets         ETAJET      X1 *
*         180.00000               pT for 1 jet              PTJET1      X1 *
*          75.00000               pT for 3 jets             PTJET3      X1 *
*          55.00000               pT for 4 jets             PTJET4      X1 *
*********************************************************************
```

Event listing (summary)

I	particle/jet	KS	KF	orig	p_x	p_y	p_z	E	m
1	!p+!	21	2212	0	.000	.000	7000.000	7000.000	.938
2	!p+!	21	2212	0	.000	.000	-7000.000	7000.000	.938
3	!u~!	21	-2	1	.254	-.028	24.568	24.569	.000
4	!s!	21	3	2	.167	.375	-425.051	425.051	.000
5	!u~!	21	-2	3	.254	-.028	24.568	24.569	.000
6	!s!	21	3	4	.167	.375	-425.051	425.051	.000
7	!H0!	21	25	0	-3.263	-42.532	-275.292	295.982	100.000
8	!W-!	21	-24	0	3.685	42.878	-125.191	153.638	77.974
9	!b!	21	5	7	-35.198	-33.809	-247.947	252.755	5.000
10	!b~!	21	-5	7	31.934	-8.723	-27.345	43.228	5.000
11	!e-!	21	11	8	-2.142	65.568	-94.036	114.658	.001
12	!nu_e~!	21	-12	8	5.827	-22.690	-31.155	38.980	.000
13	(H0)	11	25	7	-3.263	-42.532	-275.292	295.982	100.000
14	(W-)	11	-24	8	3.685	42.878	-125.191	153.638	77.974
15	e-	1	11	11	-2.142	65.568	-94.036	114.658	.001
16	nu_e~	1	-12	12	5.827	-22.690	-31.155	38.980	.000
17	p+	1	2212	1	-.088	.019	5615.946	5615.946	.938
18	K+	1	321	2	-.168	-.304	-705.130	705.130	.494
19	(b)	A 12	5	9	-33.083	-32.248	-232.046	236.653	5.000
20	(g)	I 12	21	9	-1.890	-1.379	-14.542	14.729	.000
21	(g)	I 12	21	10	.336	.024	-1.155	1.203	.000
22	(g)	I 12	21	10	.793	-1.140	-2.247	2.642	.000
23	(b~)	V 11	-5	10	30.580	-7.788	-25.303	40.756	5.000
24	(u)	A 12	2	1	-.167	.009	1359.485	1359.485	.006
25	(ud_0)	V 11	2101	2	.001	-.070	-5869.819	5869.819	.579
26	(string)	11	92	19	-3.263	-42.532	-275.292	295.982	100.000
27	(B*~0)	11	-513	26	-30.300	-28.840	-211.914	216.069	5.325
28	(pi0)	11	111	26	-1.346	-1.813	-12.838	13.035	.135
29	pi-	1	-211	26	.042	-.106	-.178	.254	.140
30	(rho+)	11	213	26	-1.382	-1.165	-8.407	8.640	.844
31	pi-	1	-211	26	-.705	-1.697	-7.361	7.588	.140
32	pi+	1	211	26	-.228	.385	-3.497	3.529	.140
33	(rho0)	11	113	26	-.158	-1.028	-3.224	3.468	.746
34	(rho0)	11	113	26	.559	-.026	-1.908	2.167	.859
35	(rho-)	11	-213	26	2.445	-1.209	-2.715	3.934	.813
36	(B+)	11	521	26	27.809	-7.033	-23.250	37.299	5.279
37	(string)	11	92	24	-.166	-.062	-4510.334	7229.305	5649.755
38	(rho+)	11	213	37	-.102	.167	174.607	174.609	.767
39	(Delta-)	11	1114	37	-.683	.115	1018.296	1018.297	1.234
40	(Delta~0)	11	-2114	37	.722	-.222	104.032	104.043	1.330
41	(rho0)	11	113	37	-.616	.225	34.551	34.567	.797
42	(rho+)	11	213	37	.415	-.330	7.614	7.683	.882
43	(Sigma-)	11	3112	37	.368	.104	13.708	13.766	1.197
44	(K*+)	11	323	37	-.570	.063	2.177	2.375	.758
45	p~-	1	-2212	37	.416	-.211	2.369	2.590	.938
46	K+	1	321	37	-.420	.260	1.383	1.549	.494
47	K-	1	-321	37	.098	-.056	-1.009	1.129	.494
48	pi+	1	211	37	-.410	-.056	-1.730	1.785	.140
49	(Delta0)	11	2114	37	.180	-.237	-3.372	3.621	1.286
50	(rho-)	11	-213	37	.272	.071	-.994	1.280	.756
51	(Delta~+)	11	-1114	37	-.011	.285	-18.630	18.674	1.259
52	pi-	1	-211	37	.070	.199	-27.740	27.741	.140
53	(rho+)	11	213	37	-.305	-.450	-2832.400	2832.400	.799
54	(eta)	11	221	37	.161	.081	-624.194	624.194	.548
55	n0	1	2112	37	.251	-.070	-2359.002	2359.002	.940
56	(B~0)	12	-511	27	-30.141	-28.684	-210.555	214.692	5.279

57	gamma	1	22	27	-.159	-.157	-1.359	1.377	.000
58	gamma	1	22	28	-.797	-.970	-6.978	7.090	.000
59	gamma	1	22	28	-.549	-.843	-5.859	5.945	.000
60	pi+	1	211	30	-1.410	-1.193	-7.734	7.953	.140
61	(pi0)	11	111	30	.029	.028	-.672	.687	.135
62	pi+	1	211	33	-.026	-.782	-1.331	1.550	.140
63	pi-	1	-211	33	-.132	-.246	-1.893	1.919	.140
64	pi+	1	211	34	.614	-.233	-1.728	1.854	.140
65	pi-	1	-211	34	-.055	.207	-.180	.313	.140
66	pi-	1	-211	35	2.219	-1.116	-2.672	3.651	.140
67	(pi0)	11	111	35	.226	-.094	-.043	.283	.135
68	(D*~0)	11	-423	36	10.249	-1.734	-9.030	13.915	2.007
69	(omega)	11	223	36	6.207	-1.326	-4.672	7.920	.784
70	pi+	1	211	36	1.330	-.553	-1.208	1.885	.140
71	(K0)	11	311	36	1.302	-.747	-1.258	2.021	.498
72	(K~0)	11	-311	36	8.721	-2.673	-7.083	11.559	.498
73	pi+	1	211	38	.281	-.050	87.841	87.842	.140
74	(pi0)	11	111	38	-.383	.217	86.766	86.767	.135
75	n0	1	2112	39	-.478	-.071	656.664	656.665	.940
76	pi-	1	-211	39	-.204	.186	361.631	361.631	.140
77	n~0	1	-2112	40	.660	-.301	64.676	64.687	.940
78	(pi0)	11	111	40	.062	.079	39.356	39.357	.135
79	pi-	1	-211	41	-.299	.083	29.336	29.337	.140
80	pi+	1	211	41	-.317	.143	5.216	5.229	.140
81	pi+	1	211	42	.267	-.390	7.225	7.242	.140
82	(pi0)	11	111	42	.147	.059	.389	.441	.135
83	n0	1	2112	43	.208	.090	12.619	12.656	.940
84	pi-	1	-211	43	.160	.014	1.089	1.110	.140
85	K+	1	321	44	-.599	-.039	1.829	1.987	.494
86	(pi0)	11	111	44	.029	.102	.348	.388	.135
87	n0	1	2112	49	.305	.009	-2.836	3.003	.940
88	(pi0)	11	111	49	-.125	-.247	-.536	.618	.135
89	pi-	1	-211	50	.130	-.198	-.050	.280	.140
90	(pi0)	11	111	50	.141	.269	-.943	1.000	.135
91	n~0	1	-2112	51	.155	.413	-14.773	14.810	.940
92	pi+	1	211	51	-.167	-.127	-3.857	3.865	.140
93	pi+	1	211	53	-.260	-.421	-2742.137	2742.137	.140
94	(pi0)	11	111	53	-.045	-.029	-90.262	90.262	.135
95	gamma	1	22	54	-.120	.097	-459.772	459.772	.000
96	gamma	1	22	54	.281	-.015	-164.422	164.422	.000
97	(D*-)	11	-413	56	-6.291	-7.402	-52.951	53.873	2.010
98	pi+	1	211	56	-1.227	-1.150	-8.292	8.462	.140
99	(omega)	11	223	56	-11.203	-10.016	-74.564	76.067	.781
100	pi-	1	-211	56	-10.094	-8.923	-66.050	67.410	.140
101	pi+	1	211	56	-1.327	-1.193	-8.699	8.881	.140
102	gamma	1	22	61	.070	-.021	-.427	.433	.000
103	gamma	1	22	61	-.041	.049	-.245	.254	.000
104	gamma	1	22	67	.165	-.003	.001	.165	.000
105	gamma	1	22	67	.062	-.091	-.044	.118	.000
106	(D~0)	11	-421	68	9.426	-1.555	-8.299	12.791	1.865
107	(pi0)	11	111	68	.824	-.179	-.731	1.124	.135
108	gamma	1	22	69	3.266	-.558	-1.996	3.868	.000
109	(pi0)	11	111	69	2.941	-.768	-2.676	4.052	.135
110	K_L0	1	130	71	1.302	-.747	-1.258	2.021	.498
111	K_L0	1	130	72	8.721	-2.673	-7.083	11.559	.498
112	gamma	1	22	74	-.109	.136	34.703	34.703	.000
113	gamma	1	22	74	-.273	.080	52.063	52.064	.000
114	gamma	1	22	78	.072	.045	37.023	37.024	.000
115	gamma	1	22	78	-.010	.034	2.333	2.333	.000
116	gamma	1	22	82	.126	-.013	.294	.320	.000

```
 117  gamma         1     22   82     .021     .072     .095     .121     .000
 118  gamma         1     22   86     .076     .094     .211     .243     .000
 119  gamma         1     22   86    -.047     .008     .137     .145     .000
 120  gamma         1     22   88    -.018    -.129    -.140     .191     .000
 121  gamma         1     22   88    -.107    -.117    -.396     .427     .000
 122  gamma         1     22   90     .154     .162    -.598     .639     .000
 123  gamma         1     22   90    -.013     .107    -.345     .361     .000
 124  gamma         1     22   94    -.090    -.020  -45.071   45.071     .000
 125  gamma         1     22   94     .045    -.009  -45.191   45.192     .000
 126  (D~0)        11   -421   97   -5.786   -6.758  -48.554   49.397    1.865
 127  pi-           1   -211   97    -.505    -.643   -4.398    4.475     .140
 128  pi-           1   -211   99   -2.332   -2.343  -16.023   16.361     .140
 129  pi+           1    211   99   -7.171   -6.353  -47.866   48.816     .140
 130  (pi0)        11    111   99   -1.701   -1.319  -10.674   10.890     .135
 131  K+            1    321  106    4.600   -1.413   -4.304    6.475     .494
 132  (rho-)       11   -213  106    4.825    -.142   -3.995    6.316     .791
 133  gamma         1     22  107     .332    -.140    -.313     .477     .000
 134  gamma         1     22  107     .492    -.039    -.418     .647     .000
 135  gamma         1     22  109     .674    -.149    -.542     .878     .000
 136  gamma         1     22  109    2.266    -.619   -2.134    3.174     .000
 137  K+            1    321  126   -1.488   -2.642  -19.440   19.681     .494
 138  pi-           1   -211  126   -4.298   -4.116  -29.114   29.716     .140
 139  gamma         1     22  130   -1.345    -.972   -8.182    8.349     .000
 140  gamma         1     22  130    -.356    -.347   -2.492    2.541     .000
 141  pi-           1   -211  132    2.368    -.434   -2.056    3.169     .140
 142  (pi0)        11    111  132    2.458     .293   -1.938    3.147     .135
 143  gamma         1     22  142     .845     .109    -.749    1.134     .000
 144  gamma         1     22  142    1.613     .184   -1.190    2.013     .000
================================================================================
                  sum:  2.00          .00      .00      .00 14000.00 14000.00
 ------------------------------------------------------------------------------
 ------------------------------    ATLFAST    ------------------------------
 ------------------------------------------------------------------------------
          K(I,1)  K(I,2)  K(I,3)  K(I,4)  K(I,5)   P(I,3)   P(I,4)   P(I,5)
 ------------------------------------------------------------------------------
  /ISOELE       1      11      15      11       1    -1.16     1.60    63.77
 ------------------------------------------------------------------------------
 ------------------------------------------------------------------------------
 ------------------------------------------------------------------------------
 ------------------------------------------------------------------------------
   /JET/       1       5      11      14       1    -2.25    -2.34    42.13
   /JET/       2      -5      10      11       1     -.72     -.20    26.44
 ------------------------------------------------------------------------------
 ------------------------------------------------------------------------------
 ------------------------------------------------------------------------------
 /PTMISS/     PXMISS    PYMISS      PXNU      PYNU
               4.918   -25.089     5.827   -22.690
 ------------------------------------------------------------------------------
 /TRIGER/  TRGALL      T
           TRGEM1 TRGPH1 TRGEM2 TRGMU1 TRGMU2 TRGEMU TRGJT1 TRGJT3 TRGJT4
                T      F      F      F      F      F      F      F      F
 ------------------------------------------------------------------------------
.......
  other events skipped
.......

............
  print out of histograms skipped
............
 ===> Directory : (HBOOK)
```

```
3333 (N)   ATLFAST
1101 (1)   MAKCLU: clusters multiplicity
1110 (1)   MAKCLU: B-field delta_phi vers p_T
1111 (1)   MAKCLU: B-field counters vers p_T
1112 (1)   MAKCLU: delta_phi jet-sum_particle
1113 (1)   MAKCLU: delta_eta jet-sum_particle
1114 (1)   MAKCLU: delta_r jet-sum_particle
1210 (1)   MAKMUO: muon multiplicity NOISOLATED
1211 (1)   MAKMUO: muon multiplicity ISOLATED
1221 (1)   MAKMUO: muon multiplicity HARD
1231 (1)   MAKMUO: muon multiplicity HARD+isol
1212 (1)   MAKMUO: (pT-pTcru) vers pT muon ISOLATED
1213 (1)   MAKMUO: (eta-etacru) vers pT muon ISOLATED
1214 (1)   MAKMUO: (phi-phicru) vers pT muon ISOLATED
1219 (1)   MAKMUO: counter vers pT muon ISOLATED
1215 (1)   MAKMUO: mumu mass
1216 (1)   MAKMUO: mumu mass width subtract
1217 (1)   MAKMUO: 4 mu mass
1311 (1)   MAKELE: electron multiplicity ISOLATED
1321 (1)   MAKELE: electron multiplicity HARD
1331 (1)   MAKELE: electron multiplicity HARD+isol
1312 (1)   MAKELE: (pT- pTcru) vers E electron ISOLATED
1313 (1)   MAKELE: (eta-etacru) vers E electron ISOLATED
1314 (1)   MAKELE: (phi-phicru) vers E electron ISOLATED
1319 (1)   MAKELE: counter vers E electron ISOLATED
1315 (1)   MAKELE: ee mass
1316 (1)   MAKELE: ee mass subtract width
1317 (1)   MAKELE: eeee mass
1411 (1)   MAKPHO: photon multiplicity ISOLATED
1421 (1)   MAKPHO: photon multiplicity HARD
1431 (1)   MAKPHO: photon multiplicity HARD+ISO
1412 (1)   MAKPHO: (E-Ecru)/Ecru  vers E photon ISOLATED
1413 (1)   MAKPHO: (theta-thetacru) vers E photon ISOLATED
1416 (1)   MAKPHO: counter vers E photon ISOLATED
1415 (1)   MAKPHO: pho-pho mass
1501 (1)   MAKJET: jets multiplicity
1505 (1)   MAKJET: jetjet mass
1502 (1)   MAKJET: energy resolution PT=40-50 GeV
1503 (1)   MAKJET: energy resolution PT=200-250 GeV
1611 (1)   MAKBJE: b-jets multiplicity
1621 (1)   MAKBJE: b-quarks HARD multiplicity
1612 (1)   MAKBJE: p_T b-jet/b-quark FSR
1622 (1)   MAKBJE: p_T b-jet/b-quark HARD
1613 (1)   MAKBJE: eta b-jet/b-quark FSR
1623 (1)   MAKBJE: eta b-jet/b-quark HARD
1614 (1)   MAKBJE: phi b-jet/b-quark FSR
1624 (1)   MAKBJE: phi b-jet/b-quark HARD
1616 (1)   MAKBJE: b-jets Mjbjb
1617 (1)   MAKBJE: b-quark Mbb (after FSR)
1618 (1)   MAKBJE: M_bb b-jets/b-quark
1620 (1)   MAKBJE: Rmin b-jet, b-quark HARD
1711 (1)   MAKCJE: c-jets multiplicity
1721 (1)   MAKCJE: c-quarks HARD multiplicity
1712 (1)   MAKCJE: p_T c-jet/c-quark FSR
1722 (1)   MAKCJE: p_T c-jet/c-quark HARD
1713 (1)   MAKCJE: eta c-jet/c-quark FSR
1723 (1)   MAKCJE: eta c-jet/c-quark HARD
1714 (1)   MAKCJE: phi c-jet/c-quark FSR
1724 (1)   MAKCJE: phi c-jet/c-quark HARD
1716 (1)   MAKCJE: c-jets Mjcjc
```

```
1717 (1)   MAKCJE: c-quark Mcc (after FSR)
1718 (1)   MAKCJE: M_cc c-jets/c-quark
1720 (1)   MAKCJE: Rmin c-jet, c-quark HARD
1551 (1)   MAKTAU: tau-jets multiplicity
1561 (1)   MAKTAU: taus  multiplicity
1812 (1)   MAKMIS: reconstructed p_T
1815 (1)   MAKMIS: reconstructed p_T +cells
1822 (1)   MAKMIS: p_T nu
1813 (1)   MAKMIS: reconstructed pX
1814 (1)   MAKMIS: reconstructed pY
1816 (1)   MAKMIS: reconstructed pX +cells
1817 (1)   MAKMIS: reconstructed pY +cells
1823 (1)   MAKMIS: pX nu
1824 (1)   MAKMIS: pY nu
1830 (1)   MAKMIS: resol missing pX (sumET=0-25)
1831 (1)   MAKMIS: resol missing pX (sumET=25-50)
1832 (1)   MAKMIS: resol missing pX (sumET=50-100)
1833 (1)   MAKMIS: resol missing pX (sumET=100-200)
1834 (1)   MAKMIS: resol missing pX (sumET=200-300)
1835 (1)   MAKMIS: resol missing pX (sumET=300-400)
1836 (1)   MAKMIS: resol missing pX
1842 (1)   MAKMIS: PTmiss/PTnu
1843 (1)   MAKMIS: PXmiss/PXnu
1844 (1)   MAKMIS: PYmiss/PYnu
1901 (1)   MAKTRG: trigger content
1902 (1)   MAKTRG: muon trig eff. for low and high pT threshold
1903 (1)   MAKTRG: muon trig eff. for high pT threshold
2001 (1)   MAKTRA: tracks multiplicity
2002 (1)   MAKTRA: muon tracks d0 resolution
2003 (1)   MAKTRA: muon tracks z0 resolution
2004 (1)   MAKTRA: muon tracks phi resolution
2005 (1)   MAKTRA: muon tracks cottheta resolution
2006 (1)   MAKTRA: muon tracks pTinv resolution
2007 (1)   MAKTRA: muon tracks efficency
2012 (1)   MAKTRA: electron tracks d0 resolution
2013 (1)   MAKTRA: electron tracks z0 resolution
2014 (1)   MAKTRA: electron tracks phi resolution
2015 (1)   MAKTRA: electron tracks cottheta resolution
2016 (1)   MAKTRA: electron tracks pTinv resolution
2017 (1)   MAKTRA: electron tracks efficency
2022 (1)   MAKTRA: pion tracks d0 resolution
2023 (1)   MAKTRA: pion tracks z0 resolution
2024 (1)   MAKTRA: pion tracks phi resolution
2025 (1)   MAKTRA: pion tracks cottheta resolution
2026 (1)   MAKTRA: pion tracks pTinv resolution
2027 (1)   MAKTRA: electron tracks efficency
2202 (1)   MAKMSC: circularity of event
2203 (1)   MAKMSC: thrust of  event
2204 (1)   MAKMSC: oblatness of event
```